

Opportunity for Long Duration Storage Technologies: Thermal and Compressed Air Energy Storage

By

Seiji H. Engelkemier

B.S. in Engineering as recommended by Department of Mechanical Engineering
Massachusetts Institute of Technology, 2019

Submitted to the Department of Mechanical Engineering
in partial fulfillment of the requirements for the degree of

Master of Science in Mechanical Engineering

at the

Massachusetts Institute of Technology

June 2023

©2023 Seiji H. Engelkemier. License: CC BY-SA 4.0.

The author hereby grants to MIT a nonexclusive, worldwide, irrevocable, royalty-free license to exercise any and all rights under copyright, including to reproduce, preserve, distribute and publicly display copies of the thesis, or release the thesis under an open-access license.

Authored by: Seiji H. Engelkemier
Department of Mechanical Engineering
May 12, 2023

Certified by: Robert C. Armstrong
Chevron Professor of Chemical Engineering and Director of MIT Energy Initiative,
Thesis Supervisor

Certified by: Asegun Henry
Professor of Mechanical Engineering, Thesis Reader

Accepted by: Nicolas G. Hadjiconstantinou
Professor of Mechanical Engineering, Graduate Officer

Opportunity for Long Duration Storage Technologies: Thermal and Compressed Air Energy Storage

By

Seiji H. Engelkemier

Submitted to the Department of Mechanical Engineering on May 12, 2023
in partial fulfillment of the requirements for the
Degree of Master of Science in Mechanical Engineering

ABSTRACT

To mitigate more severe consequences of climate change, rapid decarbonization is necessary. The electric power sector contributes about 25% of US and global emissions, and its decarbonization is critical as other sectors become increasingly electrified. Intermittent renewable energy sources, namely solar photovoltaics and wind turbines have reduced emissions in the power sector. A key part in achieving higher rates of renewables adoption is energy storage. Particularly, long duration energy storage (LDES) is needed, for which the key variables are capital cost of energy capacity and discharge efficiency. There are few economical options available today for LDES aside from pumped hydropower storage, which is limited by geography. Fortunately, new technologies are under development.

Thermal energy storage (TES) is a promising class of technologies because energy can be stored cheaply as heat. A TES system converts electricity to heat and converts it back to electricity when needed. TES systems can utilize cheap storage material, but they must address the challenges of low discharge efficiency and to a lesser extent, high capital cost of discharge power capacity. Existing studies have mostly focused on a specific subsystem, such as the power block or storage material, or a single TES system. Few studies have reported on how the needs of future power systems and TES technology options guide the design choices for a TES system. This thesis addresses the topic and presents the opportunity space for TES systems. Three common strategies for system design are identified that balance the coupled tradeoffs of cost, performance, and technical risk. The first strategy is retrofitting thermal power plants with TES to replace combustion processes and operate the plants as storage assets. The second is the development of higher efficiency power cycles, primarily closed Brayton cycles, for new storage plants operating with maximum temperatures generally under 1000°C. The third strategy utilizes storage materials and power cycles at temperatures significantly above 1000°C which requires considerable research and development prior to commercialization efforts.

Compressed air energy storage (CAES) is another type of storage technology that is cited as a candidate for LDES. Geologic and economic considerations are found to be limiting factors in large scale deployment of CAES systems rather than technology development. However, in certain situations, CAES may be a valuable storage option. Therefore, compared to the optimism found in literature, a more pragmatic outlook on CAES is recommended to focus efforts on critical questions and avoid wasted resources.

The levelized cost of storage (LCOS) is used to assess future, representative TES and CAES systems in LDES applications. A sensitivity analysis is performed on LCOS parameters to show the effect of design choices on system cost. From the technology and cost assessments, recommendations are made to guide TES and CAES development as options for LDES.

Thesis Supervisor: Robert C. Armstrong

Title: Chevron Professor of Chemical Engineering and Director of MIT Energy Initiative

Acknowledgements

I express my sincere appreciation to my advisor, Robert C. Armstrong, for his guidance, wisdom, and continuing support throughout my time working with him. His insights, mentorship, and dedication have been instrumental in shaping this thesis.

I am deeply grateful to Emre Gençer for his mentorship. He helped guide my curiosity to craft useful knowledge, connect technical details to the bigger picture, and ask better questions. Beyond my research, I appreciate the thoughtfulness that he presented as we worked remotely during the pandemic.

I would like to thank Asegun Henry for being my thesis reader and providing his insights on thermal energy storage.

I express my gratitude to the members of the Future of Energy Storage team for giving me the opportunity to learn about the energy system through a multi-disciplinary lens. My thanks extend to the study's advisory team and Charles Forsberg who offered valuable insights and feedback throughout the process. I am sincerely appreciative of the staff at the MIT Energy Initiative, without whom the study could not have been completed.

I would like to thank my friends and colleagues from the Energy Initiative and Mechanical Engineering for their support and good company.

I gratefully acknowledge the assistance that I received from Saana, Una, and Leslie at the Mechanical Engineering Graduate Office. In addition, I sincerely appreciate the assistance and resources provided by the staff at the MIT Libraries.

Last, but certainly not least, I would like to thank my family, especially my parents, for the support and motivation that they have provided me.

Table of Contents

Acknowledgements.....	5
List of Figures	8
List of Tables	10
1 - Introduction	11
2 - Thermal Energy Storage.....	14
2.1 Introduction	14
2.2 What Is Thermal Energy Storage?.....	15
2.3 Technology	15
2.3.1 Charging: Electricity to Heat	16
2.3.2 Storage	18
2.3.3 Discharging: Heat to Electricity	24
Solid.....	28
2.4 Systems	30
2.4.1 Reutilization of power plant infrastructure	31
2.4.2 Increased efficiency at medium temperatures.....	36
2.4.3 High-temperature systems	38
2.5: Thermal Energy Storage for Non-Electricity Storage	40
2.5.1 Flexibility for Thermal Power Plants	40
2.5.2 Heat End Use.....	40
2.6 Cost Estimates.....	41
2.6.1 Discharge power cost.....	43
2.6.2 Energy cost.....	45
2.6.3 All-in cost.....	45
2.7 Conclusion.....	46
3 - Compressed Air Energy Storage	48
3.1 An overview of compressed air energy storage	48
3.2 CAES development efforts to date.....	48
3.3 Outlook	51
3.4 Basic principles of adiabatic CAES.....	51
3.5 Mechanical and thermal storage requirements	52
3.5.1 Air storage and geological siting	52
3.5.2 Thermal energy storage capacity requirements.....	58

3.6 Cost estimates.....	59
3.7 Potential for CAES technology improvement	62
3.7.1 Bypass turbines.....	62
3.7.2 Reuse of gas turbines.....	62
3.7.2 Liquid air energy storage.....	63
3.7.3 Adiabatic CAES with resistively heated thermal storage	63
3.7.4 Diabatic CAES for grid decarbonization	64
3.8 Summary findings and recommendations related to compressed air energy storage	64
4 - Levelized Cost of Storage.....	66
4.1 Default values and sensitivities.....	66
4.2 LCOS of TES	67
4.2.1 Retrofits.....	67
4.2.2 Future technologies	70
4.3 LCOS of CAES.....	74
5 - Conclusions	77
Appendix	78
Data for Figure 5	78
Data for Figure 6	78
Discharge efficiency curves for Figure 7	79
References	80

List of Figures

Figure 1: Four energy storage technology categories shown with a few subcategories.....	12
Figure 2: Energy losses (in orange) for each step of a generic TES system. The heat loss during storage will depend on how the system is operated.....	15
Figure 3: Comparison of coefficient of performance (COP) values for electricity-to-heat technologies. The Carnot lines show the ideal case; the upper line is applicable if sub-ambient (cold) thermal energy is utilized. For heat pumps, the solid line indicates the approximate COP within the range of operating temperatures. The dashed section continues the trend to higher temperatures.	16
Figure 4: Categories of storage materials. Within latent heat materials, solid–liquid phase change materials (PCMs) are the practical choice. Listed materials (purple boxes) are indicative of the storage subtype; they do not represent an exhaustive list.	19
Figure 5: Comparing potential phase change materials by their melting temperature and latent heat of fusion.	21
Figure 6: Sensible heat materials (purple) are shown with fixed material cost and variable maximum operating temperature. Latent heat materials (teal) are shown at melting temperature with a range of material costs. The figure does not show cost estimates for materials that utilize both sensible and latent heat.....	22
Figure 7: Approximate efficiencies of heat-to-electricity technologies plotted against Carnot efficiency. “Turbine” is an estimate of realistic efficiency potential for technologies that involve heating up compressible fluids (Henry and Prasher 2014). See appendix for equations.....	24
Figure 8: Images of a few heat-to-power technologies. Clockwise from top left: steam turbine, gas turbine, thermionic converter, thermoelectric generator (Seetenky 2007; DOE 2006; Chao 2016; Gerardtv 2010). For scale, the gas turbine is several meters in length, and the thermoelectric generator is a few centimeters in length.....	29
Figure 9: Simplified diagram of how a thermal storage system can reuse equipment at a steam turbine power plant. In this example, two-tank molten salt is used; cheaper, alternative storage methods are available.	32
Figure 10: The upper graph shows age distribution of operational steam turbine capacity in the United States, including standalone turbines (coal, gas, nuclear, solar thermal, etc.) and turbines in combined cycle power plants. The lower graph projects available capacity for future years assuming a 50-year lifetime. Data is from EPA’s eGRID 2018 database, so plants brought online after 2018 are not counted.	33
Figure 11: Geographic distribution of steam turbine capacity in the United States that is expected to be available in 2050, using the same data source and assumptions as Fig. 10.....	34
Figure 12: Steam turbine capacity for plants that will be 50 years old or less in 2050 for top-ten countries and the rest of the world (RoW). The figure includes turbines that are attached to combined cycle gas plants. Calculated from S&P Global Platts database 2016.	35
Figure 13: Diagram of recuperated, closed Brayton power cycle commonly used for medium-temperatures TES systems (Turchi, Ma, and Dyreby 2012; McTigue et al. 2019). A heat pump (not pictured) could charge the hot (dark orange) and cold (dark blue) stores. Heat addition is shown with a two-tank liquid medium although other formats are possible. Heat rejection can be accomplished by air cooling instead of cold storage which would be favorable for resistively charged systems.....	37
Figure 14: A sample of high-temperature systems with different designs. Clockwise from top left: particle storage with combined cycle (NREL 2018); silicon PCM in container atop a heat exchanger with Brayton	

turbine (Chad Taylor et al. 2020); silicon PCM with TPV (Datas et al. 2016); liquid silicon with TPV (Amy et al. 2018).	38
Figure 15: Flowsheet of a conventional diabatic CAES system with two combustors, which describes the D-CAES plant at Huntorf, Germany (Figure: Future of Storage).	49
Figure 16: Flowsheet of a diabatic CAES system with a recuperator, which describes the D-CAES plant at McIntosh, Alabama (Figure: Future of Storage).	50
Figure 17: Typical ranges of energy density, on a logarithmic scale, for pumped storage hydropower systems with heads of approximately 50 to 1,400 meters, CAES, and Li-ion batteries.	53
Figure 18: Illustrations of underground formations to store compressed air (Figures used with permission from Geostock Sandia).	54
Figure 19: Map, which was originally commissioned for underground petroleum storage, showing regions of the United States that are favorable for CAES (Figure: Barnes and Levine 2011).	56
Figure 20: Surface reservoir provides pressure to enable air extraction at constant pressure. (Figure: Giramonti and Smith 1983).	58
Figure 21: LCOS of TES retrofit with steam turbine plants for high-cost estimate (top) and low-cost estimate (bottom). Different color scales are used between the two graphs to highlight the range of LCOS values. The upper and lower white dashed lines indicate capacity factors of 25% and 5%, respectively.	68
Figure 22: LCOS breakdown for steam turbine plant with TES using low-cost estimates. All three panels are at 10% capacity factor but with varying cycling frequency and discharge duration. The legend abbreviations are cost per power (CPP with subscripts "c" and "d" for charge and discharge), cost per energy (CPE), fixed and variable operations and maintenance (FOM and VOM).	69
Figure 23: LCOS versus lifetime for the low-cost estimate (blue) and the same estimate with doubled power capacity cost (red).	70
Figure 24: LCOS of (a) crushed rock & sCO ₂ and (b) liquid silicon & TPV systems based on mid-cost estimates. Note the color scaling is unique to each graph to maximize contrast, and the y-axis limits differ between the two plots. (c), (d) Self-discharge cost of the two technologies as a percentage of LCOS, which is calculated as the cost to recharge the lost heat.	71
Figure 25: LCOS of the crushed rock (top) and liquid silicon (bottom) at 10% capacity factor and varying cycling frequency.	72
Figure 26: LCOS sensitivity analysis for the future TES technologies: crushed rock & sCO ₂ and liquid silicon & TPV. The estimates are shown for a system operating at 10% capacity factor and 52 cycles per year. The red bars indicate increase in costs, while green bars indicate decreasing costs.	73
Figure 27: LCOS of CAES based on mid-cost estimate.	74
Figure 28: Contribution of cost categories to the LCOS of CAES at 10% capacity factor for varying cycling frequencies.	75
Figure 29: LCOS sensitivity analysis of CAES.	76

List of Tables

Table 1: Comparison of heat-to-electricity conversion methods 25
Table 2: Three near- and long-term strategies for TES..... 31
Table 3: TES System cost estimate..... 42
Table 4: Parameters to calculate all-in cost..... 45
Table 5: CAES System cost estimate 61
Table 6: Financial parameters..... 67

1 - Introduction

The electric power sector comprises about 25% of greenhouse gas emissions for both the United States (US) and the world (US EPA 2017; 2016). A leading cause of decarbonization is the deployment of variable renewable energy (VRE) generators, namely wind turbines and solar photovoltaics. The costs of both generators have drastically declined over the past decade, accelerating the rate of their deployment.

So far, thermal power generators such as combined cycle power plants, natural gas turbines, and coal fired power have provided significant flexibility to manage intermittency from VRE sources (Kasseris et al. 2020; IRENA 2019). To further decarbonize the power sector, energy storage is necessary to balance out the intermittency of VRE generation. The primary focus of this thesis is on grid-connected storage systems which use electricity as the only input and output.

A useful starting question is what level of decarbonization can be achieved with presently available technologies at current costs? Lithium-ion batteries (LIB) are getting cheaper and are already being deployed for grid-connected energy storage with durations of 2-4 hours. However, the cost of Li-ion batteries increases significantly for longer discharge duration. Pumped storage hydropower (PSH) has been used for decades, but it is dependent on geography and vulnerable to shifting climate patterns that affect water supply (Dowling et al. 2020).

Brown and Botterud address this question by modeling a simplified power system of the United States using only solar, wind, LIB, PSH, and transmission (2021). A key finding is that increased transmission capacity and regional interconnections reduce the energy storage capacity required and the system cost. The system cost is the amount invested to build storage and generation assets, and it can be leveled per unit electricity delivered. Even with increased transmission capacity, system costs rise rapidly when zero-carbon electricity accounts for more than roughly 90% of generation.

As the power sector moves to net-zero emissions, there will be a need for long(er) duration energy storage (LDES) to resolve intermittency and reduce reliance on fossil fuel power plants. Currently, there is no agreed upon definition for “long duration”. Long duration has been used to describe storage with at least 10 hours of electricity at rated capacity (California Energy Commission 2020), but some expect that hundreds of hours could be necessary (Albertus, Manser, and Litzelman 2020a). An important note is that duration is quoted at rated capacity; storage plants can discharge for longer duration at below their rated capacity.

In addition to Brown and Botterud, models from other studies find that when the share of generation from VRE sources surpasses 70 - 90% of the total, technologies like LDES reduce the total system cost by avoiding overbuilding VRE capacity (Albertus, Manser, and Litzelman 2020a; Cole et al. 2021). Without LDES, achieving power sector decarbonization is estimated to cost 10—50% more, depending on the relative cost of storage, renewables, and firm, zero-carbon resources such as nuclear or geothermal (Sepulveda et al. 2021).

There are a variety of energy storage technologies as shown in Figure 1, some of which could be used for LDES. Besides lithium-ion batteries, another electrochemical storage technology is flow batteries which are being researched for LDES applications. Another storage category is chemical storage, for which there

is much discussion about using hydrogen or its derivatives such as ammonia. Under the umbrella of mechanical energy storage, commonly discussed technologies are pumped hydropower, compressed air, and flywheels. Thermal energy storage (TES) is also an option although relatively understudied for electricity-to-electricity applications; TES has typically been discussed in the context of electricity-to-heat or concentrated solar power (Dowling et al. 2020).

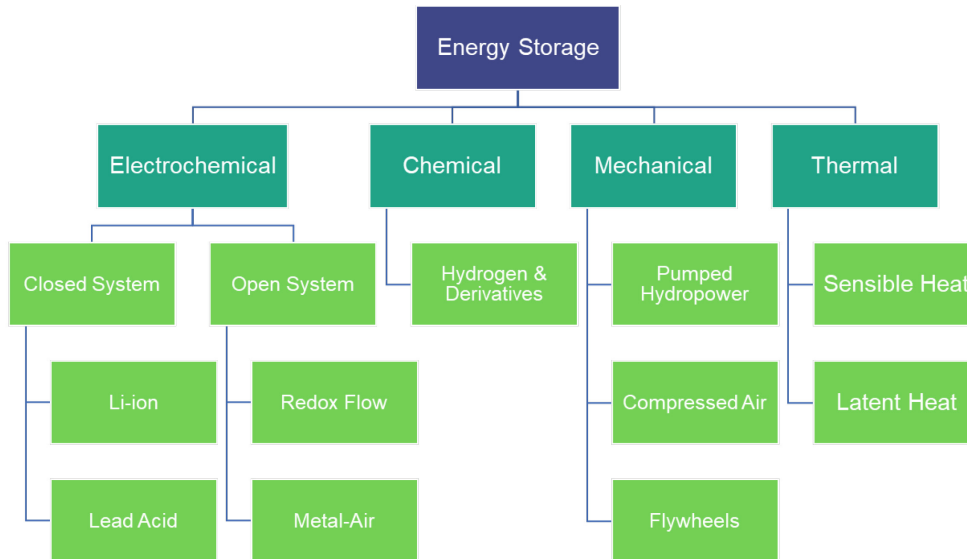


Figure 1: Four energy storage technology categories shown with a few subcategories.

With a variety of energy storage technologies, one question is what metrics should be used to compare technologies? Since electric power systems are usually designed to minimize cost while achieving goals such as high reliability and broad access, cost-focused metrics are useful. Additionally, cost-focused metrics can be used independently of the technology implementation although the values themselves are specific to a technology.

Sepulveda et al. explores the design space for LDES using five variables: the capital costs for charge power ($\$/kW_e$), discharge power ($\$/kW_e$), and energy capacity ($\$/kWh$) along with charge and discharge efficiencies (%) (Sepulveda et al. 2021). Energy storage costs are measured in the units of medium such as thermal ($\$/kWh_{th}$) or mechanical energy. Dividing the energy storage by the discharge efficiency yields units of $\$/kWh_e$. For some technologies, charge power, discharge power, and energy capacity can be sized independently, so variables for all three are required.

In addition to these five variables, several more are useful in considering the holistic cost of an energy storage system: the fixed operation and maintenance (FOM) costs for charge power ($\$/kW_e\text{-yr}$), discharge power ($\$/kW_e\text{-yr}$), and energy capacity¹ ($\$/kWh\text{-yr}$); variable operation and maintenance (VOM) with units

¹ FOM of energy storage components are also measured in units of the storage medium e.g. kWh_{th} .

of $\$/kWh_e$; capital recovery period (yrs); and the self-discharge rate (fraction/hr). Together, these 11 variables provide sufficient data to assess the cost of storage technologies.

Of course, technical factors are critical too such as feasibility, ramp rates, and degradation. For specific projects where one is deciding which technology to use, these factors should be considered. However, for systems level analysis, assessing these factors on a comparable basis is difficult given the sensitivity to plant-specific operating profiles.

The aim of Sepulveda et al. was to understand the importance of storage attributes, independent of technology implementation (2021). A parametric sweep of the five variables listed above was completed for a set of scenarios with different firm resources and varying load and weather conditions. Based on multivariate regression, the most important attributes to reduce the total system cost were reducing energy capacity cost and increasing discharge efficiency. Improvements in energy capacity cost and discharge efficiency are more than twice as effective at reducing system cost compared to improvements in discharge power cost, charge power cost, or charge efficiency.

Their study found that to achieve system cost reductions greater than 10%, energy capacity costs need to be below 20 $\$/kWh$. This cost target agrees with findings from other work (Albertus, Manser, and Litzelman 2020a; Ziegler et al. 2019a). Storage systems with discharge efficiencies in the range of 40–60% are found to reduce system costs 5–20% when energy capacity costs are 20 $\$/kWh_e$ even with power costs at 1000 $\$/kW_e$.

Given this background of important characteristics for LDES, this thesis examines how thermal and compressed air energy storage may be suited, or not, for LDES. For each storage type, the technology is first assessed by its major components and then at the system level before providing estimates for the key variables listed previously. Following that, those estimates are used to generate levelized cost of storage (LCOS) values which is a measure, albeit imperfect, of the economic competitiveness of a storage technology. LCOS values are calculated per technology under varying discharge duration and cycling frequency. For insight on connecting engineering decisions to economics, cost breakdowns by subsystem are completed and sensitivities to high-, mid-, and low-cost scenarios are examined.

2 - Thermal Energy Storage

2.1 Introduction

In 2017, about 75% of the world's electricity supply was generated by thermal power sources—that is, by plants where a fuel is combusted to heat steam, air, or another fluid that drives a turbine (IEA 2019). As the electricity sector decarbonizes, the heat sources used for thermal power generation will transition away from fossil fuels to relatively greater reliance on sources such as geothermal energy, hydrogen fuel, solar thermal energy, biomass, nuclear fission, and possibly nuclear fusion. Some of these plants will need to respond to variations in the availability of renewable energy sources; for these types of generators, thermal energy storage (TES) can provide flexibility.

Some concentrated solar power plants, which have been deployed to a significantly lesser extent than solar photovoltaics, already use TES with thermal oil or molten salt to shift generation from peak sunlight hours to match demand. Researchers have proposed TES for nuclear plants to decouple the power block from the reactor so that plant can provide both baseload and peaking capacity (C. Forsberg, Brick, and Haratyk 2018). In these roles, TES can improve efficiency, serve combined heat and power needs, and deliver other services. Together, these opportunities present interesting opportunities for TES technologies in the decarbonized grid of the future.

This thesis focuses on electricity-to-electricity storage, which is a significant but narrower opportunity for TES. The potential of electricity-to-electricity TES centers on the ability to use very low-cost storage materials such as crushed rock. To utilize such low-cost storage mediums, the key challenges to overcome are the low discharge efficiency and high capital cost of converting heat to electricity.

A combination of high power and low energy costs suggests that TES will be most interesting as a long-duration storage technology. Basic geographic constraints may be a factor, primarily the ability to deliver the several thousand tons of storage material needed for a gigawatt-hour-scale facility. A TES facility would have a similar areal footprint as a thermal power plant, which typically requires tens to hundreds of hectares on relatively flat land. Water demands for cooling will depend on the system design. Economies of scale generally disfavor electricity-heat-electricity TES in small-scale applications such as behind-the-meter electricity storage.

A review of the TES systems that have been proposed by commercial developers and researchers suggests three main strategies for overcoming the key challenges of heat-to-electricity efficiency and cost of power. In all strategies, TES utilizes low-cost storage materials. In the first strategy, TES is installed at existing thermal power plants, particularly coal plants, to replace heat from fuel combustion and to reuse the existing power generation equipment, which reduces the cost of power. The second strategy considers more efficient power cycles with peak temperatures slightly above the range of thermal storage technologies used presently. The third strategy relies on even higher temperature storage to increase efficiency, and, in some embodiments, requires research and development on newer power conversion technologies. These strategies provide several pathways for TES to support a decarbonized grid.

This chapter begins with a brief description of how thermal energy storage works, followed (in Section 2.3) by an overview of TES technologies grouped by function: charge, store, and discharge. With that

foundation, Section 2.4 describes systems that utilize each of the three strategies for overcoming TES’s key technical challenges. Section 2.5 provides cost estimates for two illustrative systems in 2050; Section 2.6 concludes.

2.2 What Is Thermal Energy Storage?

TES systems use electricity to heat up a material; the heated material is then insulated until the energy is needed, and finally the heat is converted back to electricity through a power conversion device. Figure 2.1 illustrates typical energy losses associated with each step for a generic TES system with 47% roundtrip efficiency (where “roundtrip efficiency” is defined as the fraction of electricity delivered back to the grid over the electricity drawn from the grid).

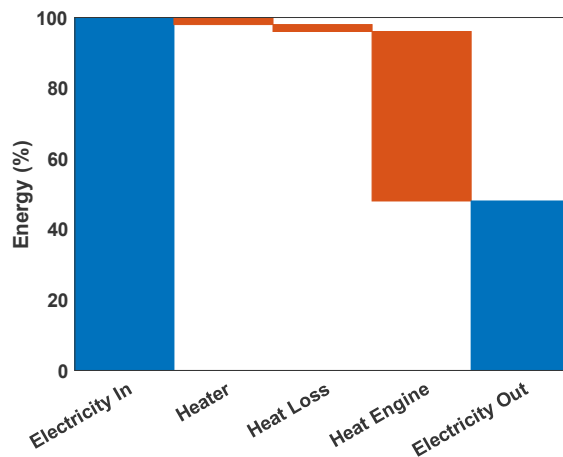


Figure 2: Energy losses (in orange) for each step of a generic TES system. The heat loss during storage will depend on how the system is operated.

The figure shows one of the key challenges of TES: the efficiency of the heat-to-electricity conversion step is the limiting factor for roundtrip efficiency. By contrast, the first step—converting electricity to heat—can be accomplished with minimal losses, and given sufficient insulation, losses to the ambient environment during heat storage (step two) can be limited to acceptable levels. More details are provided in Section 2.3.

2.3 Technology

The three main steps in TES are converting electricity to heat, storing heat, and converting heat back to electricity. While this basic description is true for storage technologies generally, it is worth examining the different technology options at each step before discussing entire systems. Certain synergies between these options are relevant for overall system design; these synergies are discussed in Section 2.4.

2.3.1 Charging: Electricity to Heat

Since this thesis focuses on TES systems that have only electrical energy as the input and output, other potential sources of heat are ignored although such sources can be utilized in real systems and can improve system performance. Those other sources include waste heat, nuclear, geothermal, combustion, and solar thermal.

Technology options for charging a TES system—that is, for converting electricity to heat—include a resistive heater, inductive heater, or heat pump. The figure of merit for converting electricity to heat is the coefficient of performance (COP) to distinguish it from thermal efficiency. Thermal efficiency is how much electricity is generated from a quantity of heat, and it cannot be higher than 100% and is often much lower. On the other hand, COP can be greater than 100%. For reference, a residential heat pump has a COP around 2 to 4 depending on ambient and desired temperatures. For relatively small temperature differences, the COP can be high, but as the temperature differences increase, COP falls, as seen in Figure 2.2. The figure shows a nominal case where low-temperature heat is supplied by ambient air at 25°C. Changes in heat pump design could improve the COP slightly and adjust the ratio of high and low temperature thermal energy. Higher capital and operating costs are drawbacks of heat pumps compared to resistive and inductive heaters. Exact values are unknown since high-temperature heat pumps are not commercially available yet.

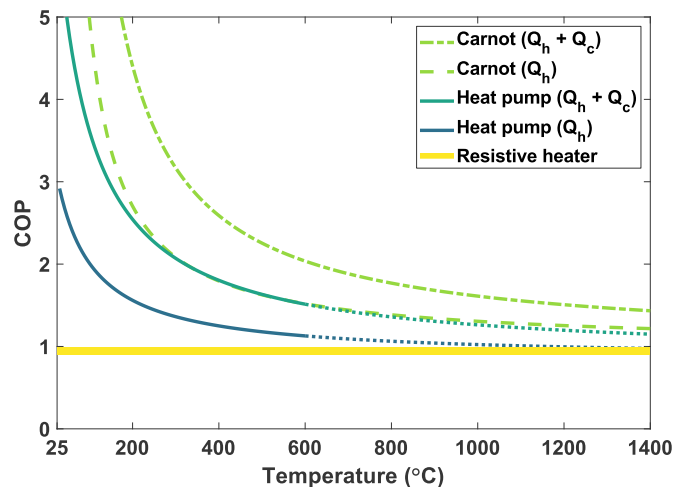


Figure 3: Comparison of coefficient of performance (COP) values for electricity-to-heat technologies. The Carnot lines show the ideal case; the upper line is applicable if sub-ambient (cold) thermal energy is utilized. For heat pumps, the solid line indicates the approximate COP within the range of operating temperatures. The dashed section continues the trend to higher temperatures.

For the heat pumps in the figure, the following equations and assumptions are used:

$$COP_{Q_h+Q_c} = \eta * \frac{\tau * \theta - 1}{\tau * \theta - \eta^2} * \frac{\tau + 1}{\tau - 1} \quad (1)$$

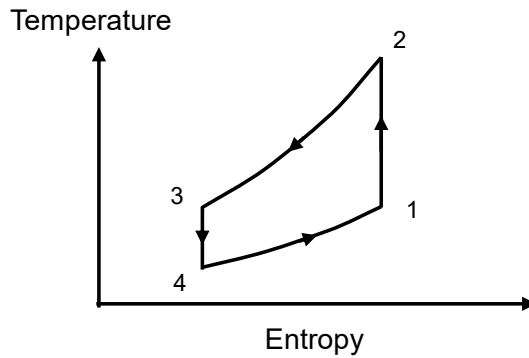
$$COP_{Q_h} = \eta * \frac{\tau * \theta - 1}{\tau * \theta - \eta^2} * \frac{\tau}{\tau - 1} \quad (2)$$

$$\tau = \frac{T_2}{T_1}$$

$$\theta = \frac{T_1}{T_3}$$

$$\eta = 0.85$$

$$T_1 = T_3 = 298K$$



Equation 1 is given by Olympios et al. (2021) to describe a case where thermal energy from both the high and low temperature steps are stored. Equation 2 is derived from the same reference for the case where only the high temperature thermal energy is stored. Temperature is expressed in Kelvin. The exact values for η , T_1 , and T_3 depend on system configuration. For the Carnot case, $\eta = 1$, and for the representative case, $\eta = 0.85$. For another thermodynamic analysis of pumped heat TES, see Laughlin (2017).

Resistive heaters can convert electricity to heat with a COP above 90%, but their COP cannot exceed 100% (Amy et al. 2018). Resistive heaters can be placed directly in the storage material, built into piping, or placed close to the container or pipes for indirect heating. Induction heating uses oscillating magnetic fields to generate heat within the storage material or an intermediate heat transfer fluid. Induction heating can overcome some heat transfer resistance compared to indirect resistive heating; however, inductive heating equipment is more expensive and not easily applied to all materials.

The maximum storage temperature will be a factor in choosing the heater. Current heat pump designs have practical limits around 550°C due to the properties of the materials available (at reasonable cost) for use in turbomachinery (Frate, Ferrari, and Desideri 2020; Laughlin 2017). Meanwhile, inductive heaters can heat materials to 3000°C, but ambient conditions and containment materials may set a lower limit (AZO Materials 2015; Inductotherm Corp. 2020). Resistive heaters made of metallic materials can reach 1400°C in oxidative environments (Kanthal 2018), and heaters made of ceramics or other materials can exceed 2000°C depending on the environment (Amy et al. 2018). Higher-temperature heaters tend to be more expensive.

In a power system with high shares of variable renewable generation, electricity prices are expected to be low for many hours of the year—as discussed in the literature (Sepulveda et al. 2021). Thus, it may be advantageous (though not necessarily so) to trade off higher COP in favor of lower charging power cost. Even so, charge efficiency and cost are found to be of secondary importance compared to other parameters.

Lower charging efficiency means more electricity will be used for the same amount of heat stored. This has no impact on the amount of storage capacity needed to meet a target discharge profile, which is determined by discharge efficiency and the rate of self-discharge. Resistive heaters will likely be the most common type of heating element used for TES systems given their simplicity and lower cost per unit of power.

2.3.2 Storage

As mentioned in the introduction to this chapter, the advantage of thermal energy storage compared to most other forms of storage is the ability to use low-cost storage materials. Long-duration storage, which TES systems are suited for, should aim for a capital cost below \$20 per kilowatt-hour of electrical energy (kWh_e) (Albertus, Manser, and Litzelman 2020b; Ziegler et al. 2019b).

To help understand the material selection process, the storage cost which is expressed in units of electricity ($\$/\text{kWh}_e$) can be separated into the discharge efficiency penalty and the thermal storage cost ($\$/\text{kWh}_{th}$). For a heat-to-electricity efficiency of 50%, the storage cost should be below \$10 per kWh_{th} . Efficiency values range from approximately 40% to 60%, as discussed in the next section on discharging technologies. Regardless of the exact efficiency, this cost target significantly constrains which materials can be used. The cost of some materials would itself exceed the target, even before accounting for containment, insulation, and construction which are costs associated with energy capacity.

As discussed in Section 2.3.3, which focuses on the discharging step in TES, higher storage temperatures can increase the thermal efficiency (converting stored heat back to electricity). Although the efficiency of this step will largely depend on the energy conversion system used, thermal inefficiencies act as a penalty on the capital cost of energy. Thus, high-temperature materials are desired because they enable higher efficiency (see discussion on Carnot efficiency in Section 2.3.3). However, costs for containment and insulation also increase with temperature. Different systems make different tradeoffs between energy cost, power cost, and heat-to-electricity efficiency, one of the key design challenges for TES.

The temperature–efficiency relationship generally rules out materials that cannot go above 400°C. These materials may still be useful for applications aside from power generation, such those described in Box 2.1.

Thus, considerations of materials-based energy cost can quickly filter out incompatible choices. Material cost per unit of thermal energy can be estimated with just a few variables. For sensible heat, the variables are cost per mass, specific heat capacity, and change in temperature.² For latent heat storage, the

² Trivially, cost per mass can be expressed as cost per volume and density.

variables are cost per mass and latent heat of fusion; latent heat of fusion is the energy associated with the phase transition between solid and liquid.

Besides cost, there are several ways to categorize storage materials. The broadest distinction is between storing thermal energy as sensible heat or latent heat. An object that increases in temperature as it is heated gains sensible heat, where the term “sensible” refers to the fact that the heat can be sensed through a change in temperature. By contrast, latent heat is the heat absorbed or released at a constant temperature or within a temperature range during a phase change.

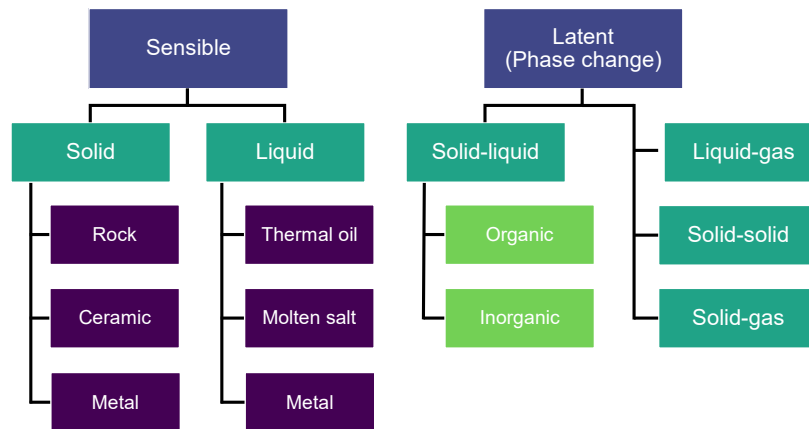


Figure 4: Categories of storage materials. Within latent heat materials, solid–liquid phase change materials (PCMs) are the practical choice. Listed materials (purple boxes) are indicative of the storage subtype; they do not represent an exhaustive list.

A benefit of latent heat storage compared to sensible heat storage is higher specific energy (energy per mass) and energy density (energy per volume). For latent heat, these values can be an order of magnitude larger than for sensible heat. However, for grid-scale storage, the space occupied by the plant is not a primary concern. Rather, the primary concern is cost—provided that the energy storage technology can meet the requirements of the specific application. For the heat storage applications described in Box 2.1, such as residential heating, higher energy density is favorable.

Sensible Heat Storage

Materials for sensible heat storage can be grouped by whether they are solid versus liquid. Liquids can be moved easily, which facilitates efficient heat transfer, but there is a risk that they will solidify, which could damage the system. In concentrated solar plants, this problem is solved by using electrical heat tracing in the pipes and cold storage tank. Downsides of this approach are increased capital cost and parasitic energy losses.

Molten salt is an example of a liquid storage material that has been used to provide over 13 GWh_e of storage in concentrated solar power plants.³ Most molten salts in use for storage today are nitrate salts with maximum service temperatures around 550°C (Laughlin 2017), but their cost exceeds the target of \$10/kWh_{th} (Glatzmaier 2011). There have been efforts to reduce the cost by increasing the temperature limit of molten salts with carbonate and chloride salts, but corrosion has been a major challenge (Liu et al. 2016). Other liquids such as molten glass and silicon have been proposed as candidate materials. Glass and silicon can reach temperatures of 1200°C and 2400°C respectively, but each introduces new challenges (Mohan, Venkataraman, and Coventry 2019; Amy et al. 2018; 2021).

Traditionally, liquids have been stored in two tanks, one for the hot liquid and one for the cold. This requires that the containment volume is double the storage material volume. An alternative design is a thermocline tank, which stores the hot and cold liquid in the same tank with a means to reduce internal heat transfer losses (Black & Veatch 2010). Such means include physical barriers and stratification. The capital cost savings of eliminating one tank must outweigh the operational costs of increased heat loss from the hot to the cold section.

One area of research involves filling thermocline tanks with cheaper solids while using a liquid to transfer heat in and out of the tank. This is better understood as a form of solid storage with immersion in the heat transfer fluid than as a form of liquid storage because the majority of heat capacity is supplied by the solids. Other forms of solid storage operate without constant immersion.

Solid storage has the potential to be less costly than liquid storage if earth-abundant materials are used. The challenge then becomes transferring heat to and from the solid. At larger storage volumes, both the heat transfer rate and amount of useful heat decrease if the process relies only on thermal conduction through the solid.

To avoid this, one option is to arrange the solid material so that fluids can flow through the interstices. Flow is easier to control for shaped materials like firebricks than for bulk materials like crushed rock (Soprani et al. 2019). The heat transfer fluid may make direct contact or flow in pipes for indirect heat transfer. As with thermocline tank systems, solid storage designs need to account for internal losses due to temperature gradients during charge or discharge. Additionally, solids can break down over time due to thermal cycling. This damage can be managed with controlled heat transfer rates and material selection. Thermal cycling can also cause settling of loose solids to the bottom of the container, placing stress on the container when it cools (Flueckiger, Yang, and Garimella 2013).

Another solid storage option uses particles stored in tanks along with particle-compatible heat exchangers (Ma, Zhang, and Sawaged 2017). Unlike solids in other forms, particles can be moved around readily, which makes it possible to separate the design of the heat storage component from the design of the heat transfer process. If the solid storage component is not required to do both, the heat exchanger can be sized independently of the system's energy storage capacity to reduce total system cost. Particles can be moved by conveyors or through fluidization. Fluidization involves blowing gas under the particles and

³ Calculated from "DOE Global Energy Storage Database" as of October 2020 ([link](#)).

lifting them such that they move like a fluid. Fluidization has been used for decades in some combustion and chemical processes. As with liquid storage, particles can be stored in two tanks or a single tank.

Latent Heat Storage

As already noted, latent heat storage utilizes a phase transition, hence the name phase change materials (PCMs). Most PCMs rely on solid–liquid transitions. Liquid–gas and solid–gas transitions are not practical because the large difference in volume creates significant engineering challenges and costs. Solid–solid transformations either occur at low temperatures or have relatively low latent heats—less than 25% of the latent heat of metal-based PCMs undergoing solid–liquid transitions (Nishioka et al. 2010; Fallahi et al. 2017). A PCM can store additional heat as sensible heat in its liquid and solid phases.

In the simplest case, a single material such as a metal alloy undergoes phase transition to absorb or release heat. A mixture of materials can also be used to reduce cost or lower the high melting point of a cheap material such as silicon. Reducing the melting temperature is desirable for lower temperature systems because it reduces costs associated with high-temperature tolerance. At a specific ratio of the constituent materials, a mixture is eutectic, which means that the mixture undergoes phase change at a single temperature. Non-eutectic mixtures undergo phase change over a temperature range within which solid and liquid phases co-occur. Figure 2.4 shows several options for PCMs and compares their melting temperature to energy density; data for this figure is available in the appendix.

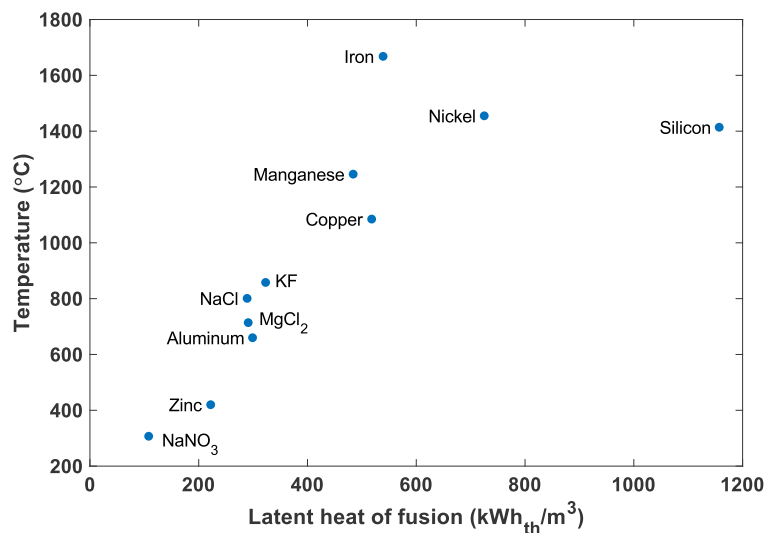


Figure 5: Comparing potential phase change materials by their melting temperature and latent heat of fusion.

Since PCMs solidify as they release heat, they cannot flow like the liquids used for sensible heat storage. For this reason, heat transfer for PCMs presents challenges similar to those for bulk solids used in sensible heat storage. There are several potential engineering solutions. Some designs embed heat exchangers

into the PCM and pump heat transfer fluids through the assembly. Filler materials with high thermal conductivity, such as metal fibers, can be added to the PCM to improve heat transfer rates (Lin et al. 2018). The PCM can be encapsulated so that a heat transfer fluid can flow over the PCM without mixing or reacting with it (Wickramaratne et al. 2018). An interesting variation on encapsulation involves the use of miscibility gap alloys, which embed a PCM inside a matrix of a different material instead of in individual capsules (Sugo, Kisi, and Cuskelly 2013). The bulk encapsulation process could be cheaper than individual encapsulation. For example, aluminum can be embedded in a graphite matrix and copper can be embedded in an iron matrix (Reed et al. 2019; Sugo, Kisi, and Cuskelly 2013).

Beyond heat transfer, other design concerns include cycle life, component segregation for multi-component materials, and undesired reactions with containment materials (Myers and Goswami 2016; Fernández et al. 2017). Another challenge in some systems is volume expansion during melting or solidification. This can introduce stresses that cause the containment vessel to fracture over time (Datas et al. 2016).

Figure 2.5 shows cost estimates for several sensible and latent heat storage options. The estimates are based only on direct material costs to provide a general comparison. Data used to generate this figure is available in appendix.

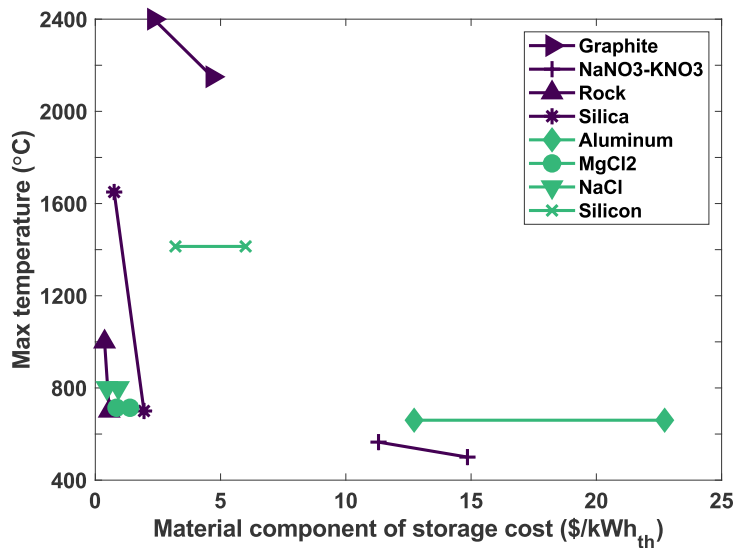


Figure 6: Sensible heat materials (purple) are shown with fixed material cost and variable maximum operating temperature. Latent heat materials (teal) are shown at melting temperature with a range of material costs. The figure does not show cost estimates for materials that utilize both sensible and latent heat.

In addition to grouping materials by the heat storage mechanism they use (i.e., sensible vs. latent heat), materials can be classified by their thermal and mechanical properties, and by other characteristics such

as toxicity and reactivity with container materials. While there is flexibility in selecting storage materials, this design choice involves tradeoffs that affect the rest of the system in terms of its ability to achieve low cost per unit of energy with acceptable efficiency and discharge power cost.

Containment and Insulation

Containment and insulation are integral parts of the storage system. Higher temperatures can increase the probability of containment failure through mechanisms such as corrosion and creep. Reliable containment is necessary so that the system can last hundreds or thousands of cycles over a plant's lifetime. Without reliable containment, leakage of storage materials or heat transfer fluids would lead to downtime and necessitate potentially challenging repairs for some designs. Compatibility between the storage and containment materials can be system specific.

Insulation is a key factor in setting the self-discharge rate. For reference, current molten salt tanks lose roughly 1% of stored heat per day (Sioshansi et al. 2009). Although this may seem high relative to other technologies, a constant heat loss rate of 1% per day leaves about 85% of total capacity after two weeks. Besides insulation, two other important factors are the ratio of the container's surface area to its volume and the temperature of the storage material. The larger the system, the smaller its surface area relative to its thermal mass. This results in lower rates of heat leakage and makes insulation more cost-effective.

In sensible heat storage systems, heat loss reduces the amount of energy stored and the temperature of the medium. Lower temperatures reduce discharge efficiency. In latent heat storage systems, energy capacity will be lower, but the temperature will stay constant provided that the PCM has not completely solidified. That may be beneficial for maintaining discharge efficiency, but the temperature difference to the ambient environment maintains a higher self-discharge rate. In both cases, the storage medium can be heated above the designed discharge temperature to offset predicted self-discharge losses, assuming the system can tolerate higher temperatures.

High-temperature insulation can be expensive—it is sometimes 10 or 100 times more costly than fiberglass insulation, which is typical for lower-temperature applications. Therefore, high-temperature insulation is usually limited to the hottest sections of the system. As the temperature decreases away from the inner layers, lower-cost materials such as aluminum silicate and mineral fiber can be utilized. Instead of air within the insulation, inert gases such as nitrogen and argon can be used to reduce oxidation, which can degrade insulation materials.

In high-temperature systems, radiative heat loss will also be a concern. One option that has been suggested involves low-emissivity coatings using metallic films (Robinson 2018). Low-pressure environments or vacuum-insulated panels have been suggested as a means to improve thermal insulation by reducing convective heat transfer (Robinson 2018). While such panels are used in buildings, reliability may be a challenge for hotter structures.

As a fraction of system cost, insulation costs can be quite significant. This can make high-temperature heat storage materials less attractive despite their low costs. According to some estimates from the literature, insulation costs can account for about half of the total energy capacity cost of TES systems (Amy et al.

2018; Ma, Davenport, and Zhang 2020). This suggests that lower-cost production methods or cheaper insulation alternatives are areas for future research.

2.3.3 Discharging: Heat to Electricity

In the heat-to-electricity conversion step, higher temperatures yield higher efficiencies as seen in Figure 2.6, although further efficiency gains become incremental at very high temperatures (beyond roughly 1200°C).

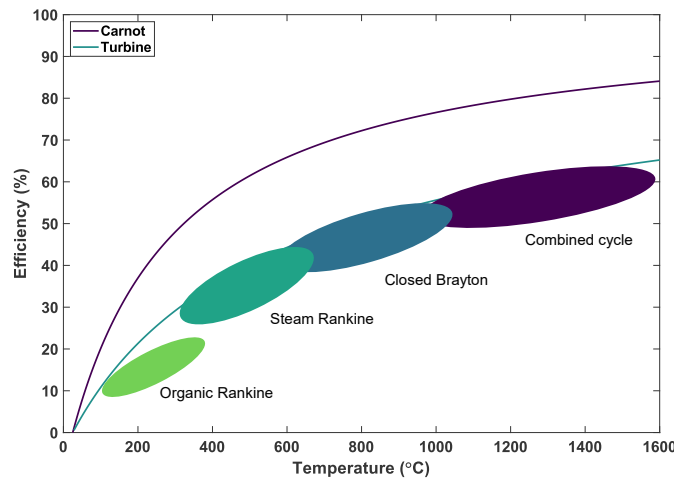


Figure 7: Approximate efficiencies of heat-to-electricity technologies plotted against Carnot efficiency. "Turbine" is an estimate of realistic efficiency potential for technologies that involve heating up compressible fluids (Henry and Prasher 2014). See appendix for equations.

Still, one reason to go to high temperatures is to enable higher rates of radiative heat transfer, which is crucial for some solid-state energy conversion devices. In addition to efficiency, key metrics are cost, flexibility, and technical readiness. Flexibility encompasses startup time and cost, ramp rates, minimum load, and part-load efficiency. For purposes of this thesis, it is assumed that future TES systems (2050 timeframe) will be sufficiently flexible to warrant excluding these considerations from the modeling analysis presented in Chapter 4. The value of flexibility depends on factors beyond the boundary of a storage plant. Table 2.1 compares currently dominant thermal power conversion technologies and alternative options that are at various stages of development.

Table 1: Comparison of heat-to-electricity conversion methods

Alternative technologies have the potential for reduced capital and operating costs, but they have not been demonstrated yet. [1] “Solid-state” encompasses several technologies: thermoelectric, thermophotovoltaic, and thermionic generators and electrochemical heat engines. [2] Value for supercritical CO₂; the exact value will depend on the gas and thermodynamic cycle used.

	Current			Alternative	
Power Block	Steam Turbine	Air Brayton Turbine	Combined Cycle	Closed Brayton	Solid-state ^[1]
Technology Maturity	Mature	Mature	Mature	Early commercial pilots, historical experience	Lab and small scale
Capital cost (relative)	High	Moderate to high	High	Moderate to high	Moderate to low
Operating cost (relative)	High	Medium	Medium	Medium	Low
Maximum temperature	600°C	1500°C	1500°C	800°C ^[2]	>1500°C
Efficiency	30-45%	30-45%	50-63%	45-55%	15-60%
Characteristics	Slow startup time (hours)	Fast response (mins)	Moderate response time (min - hours)	Fast response time (mins)	Fastest response time (sec); lacks rotational inertia

Steam Rankine Cycle

The steam Rankine cycle works by pumping and heating water, and then expanding the hot, pressurized steam over turbine blades. This turns a shaft which is connected to an electric generator. The steam is then condensed before repeating the cycle. Modifications to the basic steam Rankine cycle, such as superheat, reheat, and regeneration, are commonly used to increase efficiency. Additionally, plants can be designed to operate with subcritical, supercritical, or ultra-supercritical steam. A supercritical fluid exists in a range of temperature and pressures where it is not distinctly a gas or liquid. Supercritical fluids have useful properties such as higher density, which increases the power density of an electricity generation system. Higher pressures and temperatures require more expensive materials. Steam temperatures can be as high as 620°C and research is ongoing on systems that reach 700°C. For reference, the maximum operating temperature of nitrate molten salts currently used in concentrated solar power systems is about 550°C.

If the power plant has been shut off for a period, such that components have cooled down, components are heated gradually over several hours before generating power. This reduces thermal stress, which can shorten the lifetime of components. Electrical trace heaters and other measures can reduce the startup time (Shawn Flake 2016; IRENA 2019). Once running, steam plants can adjust power output faster, at a rate of around 2% of nameplate capacity per minute (IRENA 2019). Overall, steam Rankine cycles use mature technology and can achieve 30%–45% heat-to-electricity conversion efficiency (Beér 2007).

Open Brayton Cycle

In an open Brayton cycle, air is drawn from the atmosphere, compressed, heated (via combustion) to temperatures that are typically in the range of 1000°C–1500°C, and expanded before being exhausted back to the atmosphere. Although various open Brayton cycle designs are possible, the most common one involves axial compressors and expanders. In this case, the power from the expander is used to rotate the compressor and generator.

The Brayton cycle or slight variations of it underlie combustion turbines that have generated power for decades. Most gas turbines today combust natural gas directly in the working fluid to provide heat, although oil and other fuels can be used. “Gas turbine” here refers to the natural gas in a combustion turbine rather than to the gas that is the working fluid. Additionally, “turbine” can refer either to the entire gas turbine unit, which includes the compressor, combustor, and expander, or just to the expander. This thesis uses “turbine” to refer to the entire unit and “expander” to refer to the component.

Less common are indirectly fired open Brayton turbines, which use a heat exchanger to supply heat from coal, biomass, or other fuels with high ash content that would otherwise damage the equipment. Work is ongoing to adapt turbines for non-combustion applications, driven by interest from the nuclear and concentrated solar power communities .

Open Brayton turbines have much faster startup and response times compared to steam turbines given their lower thermal inertia; some can start up in less than 10 minutes and have ramp rates around 10% per minute (IRENA 2019).

Improvements in materials and blade cooling have allowed for higher peak temperatures in combustion turbines, which increases efficiency. The limitation for TES is building a heat exchanger that can withstand high pressure and temperature to deliver desired efficiencies. Demonstrations have been limited to around 1000°C (X. Zhang et al. 2018).

The exhaust from a turbine (or multiple turbines) can be hot enough to heat steam in a Rankine cycle; this configuration is called a combined cycle power plant. The high- and low-temperature cycles are commonly referred to as the topping and bottoming cycles. Compared to standalone natural gas turbines, which have efficiencies around 30%–40%, a combined cycle power plant can reach 50%–62% efficiency (Power Engineering 2018). However, startup time and overall flexibility are worse for a combined cycle plant than for a standalone turbine due to the constraints of the steam Rankine cycle.

Alternative technologies

Several alternative technologies are not necessarily new, but their lower performance to date or their early stage of development has limited their use for broad applications in power generation. With

additional research, development, and deployment, however, they may have the potential to become more cost-effective than or to be used with today's technologies.

Closed Brayton cycle

Although closed Brayton cycle turbines are uncommon today, they were initially preferred over open cycle gas turbines in the 1950s because the internal combustion of low-quality fuel would ruin turbines (McDonald 2012). In a closed Brayton cycle, the working fluid is reused—it is cooled down after the expander and then returned to the compressor. To increase efficiency, heat is transferred from the low-pressure expander exhaust to the high-pressure gas before external heat is supplied—this process, which is known as recuperation, reduces external heating requirements. Closed Brayton cycles allow for the use of working fluids other than air. Another advantage of these designs is that the background pressure—i.e., that of the low-pressure gas—can be increased to raise the gas density, which in turn increases the power density of the system and reduces costs.

Early designs used either air, nitrogen, or helium as the working fluid. Compared to using air, nitrogen reduces oxidation which extends the lifetime of components. Still, like open Brayton cycles, air and nitrogen require high temperatures (above 1000°C) for high efficiency.

Helium is attractive for its favorable heat transfer characteristics and inertness for potential coupling with nuclear reactors. However, there are challenges with helium systems such as leakage and unwanted vibrations that can cause damage. Historic experience with helium turbines and further details about the challenges of this technology are available from McDonald (2012). One concern with helium is long-term supply adequacy: the current supply is expected to last around 100 years, although new discoveries would extend that estimate (Bradshaw and Hamacher 2013; Glowacki, Nuttall, and Clarke 2013). Although a 100-year supply would extend beyond the 2050 timeframe of this study, most helium is co-produced with natural gas extraction, which is expected to decline, thus introducing uncertainty in current estimates. Given this concern, the benefits of helium may not outweigh its disadvantages when compared to other working fluids.

Currently, supercritical carbon dioxide (sCO₂) has been the focus of much research. There is potential to achieve thermal efficiencies of 50% or greater with peak temperatures around 700°C and work is ongoing to increase the temperature (ARPA-e 2019). There has been interest in developing this cycle from the nuclear community (for high-temperature reactors) and from the concentrated solar power community (for increased efficiency). There is also interest in using sCO₂ in fossil-fuel-based power plants, for which some designs have integrated carbon capture. The idea for a sCO₂ power cycle has been around since the mid-20th century; however, there have been challenges in developing materials and components that can withstand high temperature and pressure (DOE 2015). There is also a version where the sCO₂ becomes liquid for the compression stage of the power cycle, in which case it is a sCO₂ Rankine cycle.

Since work on developing sCO₂ technology is ongoing and there are few commercially operational facilities, current estimates of cost are uncertain. In its SunShot program, the U.S. Department of Energy (DOE) has set a cost target of \$900/kW_e with 50% heat-to-electricity efficiency and air cooling at 40°C (Mehos et al. 2016). Projects that use sCO₂ are being built beyond the benchtop scale. One company has delivered electricity to the grid from a 50-MW_{th} combustion-based sCO₂ demonstration plant in Texas

using a variation known as the Allam-Fetvedt cycle (Patel 2021). Another company offers an 8-MW sCO₂ Rankine system designed for waste heat recovery; this system has been factory tested and one unit is slated for commissioning in 2022 (Held 2014; Siemens Energy 2021). Although early applications of sCO₂ cycles may rely on combustion, much of the underlying knowledge and experience will be transferrable to TES and other non-combustion applications.

Solid-state energy converters

Unlike turbines, this class of devices avoids the need to simultaneously contend with large thermal fluxes and mechanical forces (Henry and Prasher 2014). This opens the door to a broader variety of materials.

Thermoelectric Generator

The Seebeck effect, which underlies thermoelectric generators, has been known for over two centuries. Thermoelectric generators have found use in applications including satellites and rovers, which use heat from nuclear material. This technology is well suited for applications that have volume constraints and require long lifetimes with minimal maintenance. However, efficiency has been limited to a range of 1%–15% due to tradeoffs inherent to these devices' material properties (Henry and Prasher 2014; Q. Zhang et al. 2017). Unless efficiency can be improved significantly, thermoelectric generators are unlikely to be a primary conversion method for TES.

Thermophotovoltaics

Thermophotovoltaics (TPV) are photovoltaic cells that are designed to convert photons from a thermal emitter, instead of the sun, into electricity. The thermal emitter is usually hotter than 1000°C and has a different wavelength distribution than the sun. Accordingly, TPV cells are designed differently than solar PV cells. Recent work has demonstrated efficiencies greater than 40% and pathways to greater than 50% efficiency (LaPotin et al. 2021; Omair et al. 2019). These pathways involve advances in multi-junction cells, spectrally selective emitters, and back-surface reflectors to increase efficiency as well as reusable substrates for lower cost manufacturing (Amy et al. 2018; D. Fan et al. 2020). Given the similarities to solar photovoltaics, existing research and fabrication methods can be leveraged for faster progress. A study from 2003 estimated TPV costs at around \$3 per watt (Palfinger et al. 2003) and projected future costs around 30 cents per watt. The latter projection is supported by similar estimates from newer studies (Seyf and Henry 2016).

Electrochemical Heat Engine

Electrochemical heat engines, often called thermally regenerative electrochemical systems, use temperature-driven changes in electrochemical potential to generate electricity. Some systems cycle a battery between two temperatures; however, these designs have achieved low performance to date (Lee et al. 2014; Linford et al. 2018). Others use a heat-driven pressure gradient to pass ions through an electrolyte (Limia et al. 2017). Recently, a new class of continuous electrochemical heat engines was introduced that could enable greater efficiency by decoupling thermal and electrical conduction pathways (Poletayev et al. 2018; Henry 2018). In one version, heat is supplied to a high-temperature electrolyzer that generates hydrogen, and a lower-temperature fuel cell converts the hydrogen into electricity. The devices can be assembled in a closed loop with heat exchange between the chemical products of both devices to increase efficiency. Some electricity from the fuel cell powers the electrolyzer. With a supply

of external heat to reduce the electrical demand of the electrolyzer, net electrical output is positive with efficiencies estimated around 10% (Poletayev et al. 2018). Different symmetric reactions can be used, so that devices can be designed for low- or high-temperature heat sources.

Thermionic Converter

Thermionic converters have a hot cathode and a cold anode. Heat is applied to the cathode which causes electrons to be emitted; the electrons then travel—either through a vacuum gap or through a vapor—to the anode. The electron balance is restored by electrically connecting the cathode and anode, which powers a load. Active research efforts during the latter half of the 20th century focused on using thermionic converters with nuclear power, particularly for space applications (Abdul Khalid, Leong, and Mohamed 2016). Renewed research on thermionics will need to address challenges around materials and fabrication before this technology can see use with TES (Go et al. 2017). Commercialization efforts, typically with fuels as the heat source, for applications such as remote or portable power and combined heat and power are ongoing (James Temple 2020).

Figure 8 shows what a few of these heat-to-electricity technologies look like as built.

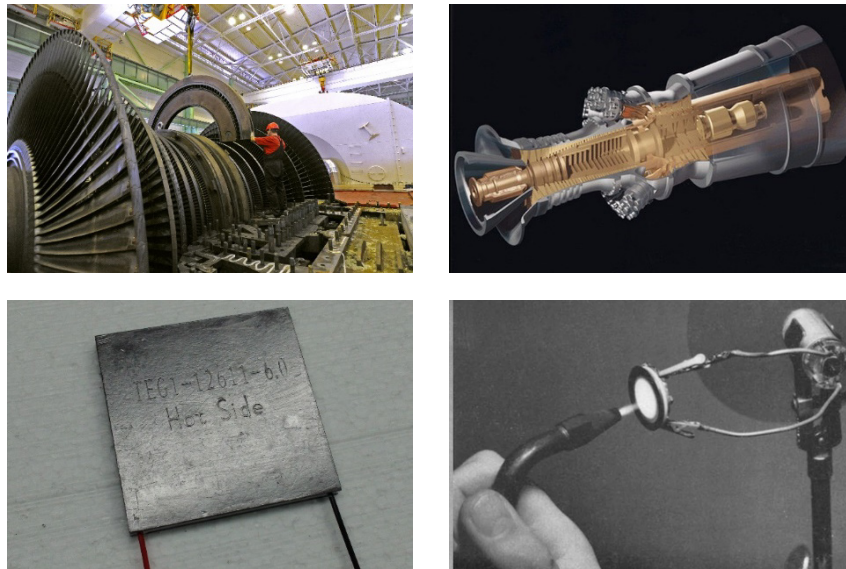


Figure 8: Images of a few heat-to-power technologies. Clockwise from top left: steam turbine, gas turbine, thermionic converter, thermoelectric generator (Seetenky 2007; DOE 2006; Chao 2016; Gerardtv 2010). For scale, the gas turbine is several meters in length, and the thermoelectric generator is a few centimeters in length.

Other technologies

Several other heat-to-electricity conversion technologies are in use commercially or are the subject of active research. At present, however, these technologies seem unlikely to be competitive with the options

described above as the primary conversion method in TES applications. Examples of technologies in the research phase are pyroelectrics and thermoacoustics (Pandya et al. 2019; Timmer, de Blok, and van der Meer 2018).

Systems that use an organic Rankine cycle are used commercially for waste heat recovery and geothermal applications. They are designed to generate power from low-temperature heat, so their efficiency is relatively low: typically 10%–20% (Quoilin et al. 2013). This precludes the use of an organic Rankine cycle as the primary discharge method in a TES system, though such systems can be used in conjunction with other technologies.

Stirling engines are technologically mature and have the potential to achieve high efficiency. This makes them attractive for small scale, distributed power generation. However, the cost per unit of power remains high compared to Brayton turbines or combined cycle plants of similar thermal efficiency.

2.4 Systems

The technologies discussed so far can be assembled in a variety of combinations to form a complete system. In weighing tradeoffs, some designs balance cost, performance, and feasibility better than others. A review of academic papers and commercial efforts to develop thermal energy storage shows that systems tend to follow one of three strategies:

- 1) Reutilization of power plant infrastructure
- 2) Increased efficiency at medium temperatures
- 3) High-temperature systems

These three strategies are listed in order of decreasing technical maturity. Technologies from each strategy will mature over time, providing a role for TES from the present day to beyond 2050.

Table 2: Three near- and long-term strategies for TES

Strategy	Retrofit	Increase efficiency at medium temperature	Ultra-high temperature
Readiness	Today	Low - moderate risk < 10 years	Moderate - high risk > 10 years
Power conversion	Steam turbine	Closed Brayton e.g. sCO ₂	Combined cycle, solid-state
Storage materials	Crushed rock, molten salt	PCM e.g. metal alloys	Silicon, silica, graphite
Max temperature	650 C	850 C	> 1200 C
Efficiency	30 - 45%	40 - 55%	50 - 60+ %
Response time	mins - hours	mins	sec - mins
Minimum load (% nameplate capacity)	10 - 50%	10 - 50%	~ 1 - 40%

2.4.1 Reutilization of power plant infrastructure

A number of power plants, particularly coal-fired ones, are being retired before the end of their expected lifetime because they can no longer run economically or meet environmental standards. This is happening today in industrialized regions like the United States and European Union. Early retirements are also likely in countries with younger power plant fleets, such as China and India, as they try to meet decarbonization targets.

There is an opportunity to reuse these power plants for thermal energy storage. As shown in Figure 2.8, thermal storage and a heat exchanger to generate steam would replace the combustion boiler. Resistive heaters or heat pumps would draw (low/zero-carbon) electricity from the grid to charge the system. The existing turbine, pumps, cooling tower, and other equipment would be reused to generate electricity without emissions.

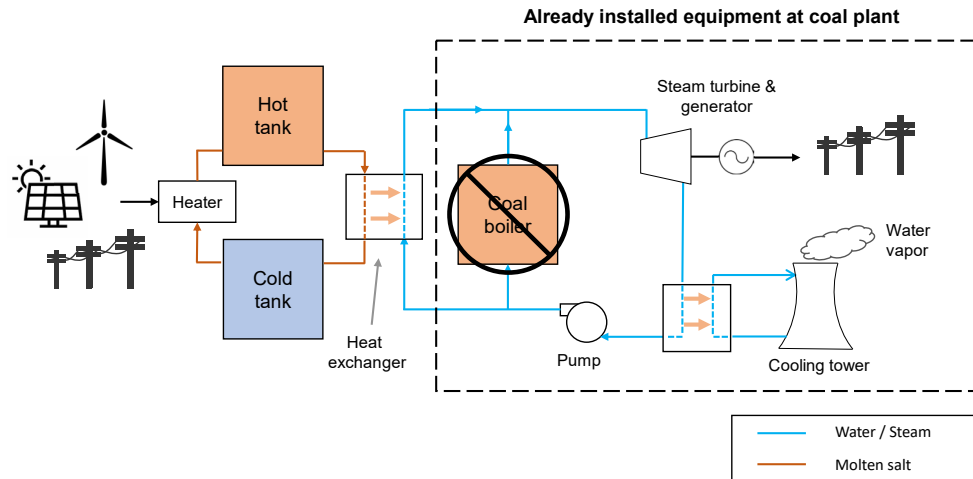


Figure 9: Simplified diagram of how a thermal storage system can reuse equipment at a steam turbine power plant. In this example, two-tank molten salt is used; cheaper, alternative storage methods are available.

At first glance, the efficiency of steam Rankine cycles seems too low to make the system economical. However, it might be possible to acquire existing plants at low cost if the alternative is early retirement. Retirement could have negative value to the plant owner due to decommissioning costs net scrap value. In addition, existing grid connections can be reused. Lastly, with peak temperatures around 600°C, a wide variety of cheap storage materials can be utilized, allowing for lower energy capital cost compared to current, two-tank molten salt storage systems. Together, these factors could allow for economical reuse of fossil fuel powered steam turbines in regions with high shares of renewable generation.

An important consideration is the remaining lifetime of the power plant being repurposed. On average, a steam turbine plant in the United States operates for 50 years (Grubert 2020). Although there is variation between plants based on equipment, operational history, and repairs, this is a useful approximation. Use of steam turbine plants for energy storage could extend or shorten the nominal 50-year lifetime through a combination of lower utilization but more cycling. The top chart of Figure 2.9 shows the age distribution of installed steam turbine capacity in the United States that is less than 50 years old. The bottom chart shows when that capacity is expected to retire based on a 50-year retirement date. The figure uses data from the U.S. Environmental Protection Agency's 2018 eGRID database and does not consider new capacity additions.

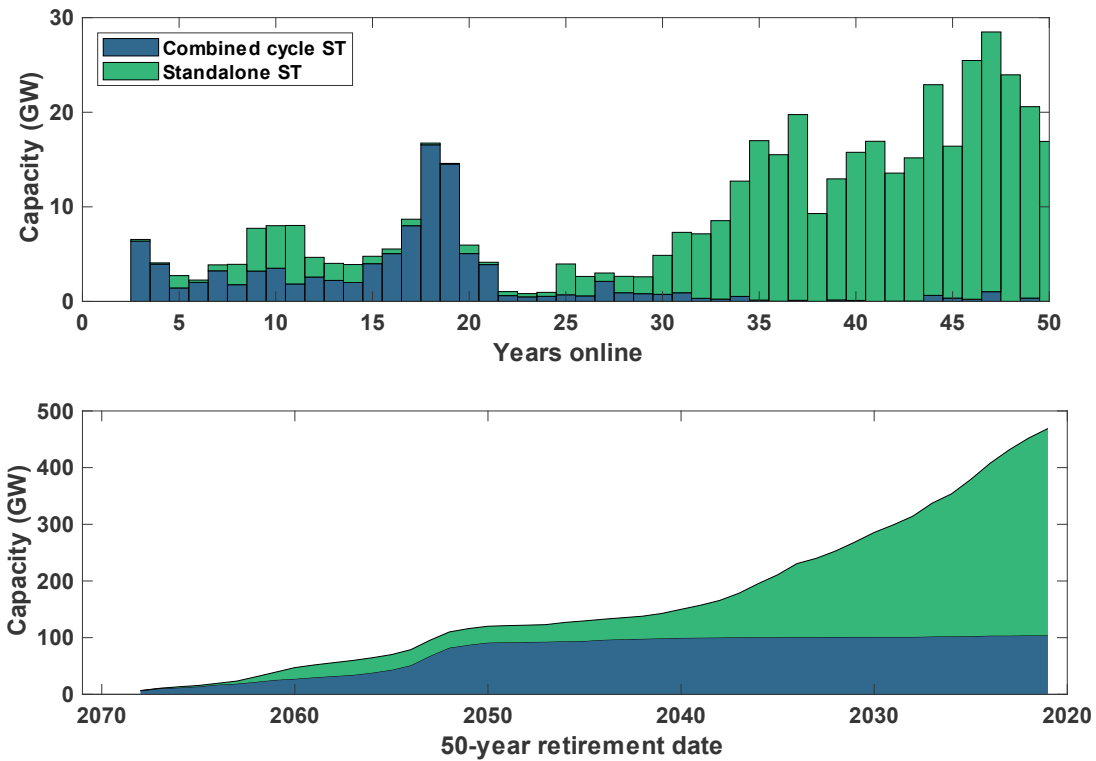


Figure 10: The upper graph shows age distribution of operational steam turbine capacity in the United States, including standalone turbines (coal, gas, nuclear, solar thermal, etc.) and turbines in combined cycle power plants. The lower graph projects available capacity for future years assuming a 50-year lifetime. Data is from EPA’s eGRID 2018 database, so plants brought online after 2018 are not counted.

Many U.S. coal plants will reach 50 years of operating life between now and 2040, limiting their potential lifetime as energy storage plants. Steam turbines attached to combined cycle plants could remain available longer since most were built after 2000. Although more detailed analysis is required, the lifetime of these plants, after they are retrofitted with TES, could be extended with targeted repairs.

As shown in Figure 2.10, existing power plants are distributed throughout the continental United States, so this strategy is not geographically limited. The window of time to utilize U.S. coal plants is short, given that retrofitted plants need to have sufficient remaining life to recover costs. Fortunately, the technologies required to implement this strategy are at a high level of technical readiness and could be deployed quickly with public and private coordination. Further, there is relevant experience to guide design from the construction of concentrated solar power plants and the repowering of coal plants into combined cycle power plants.

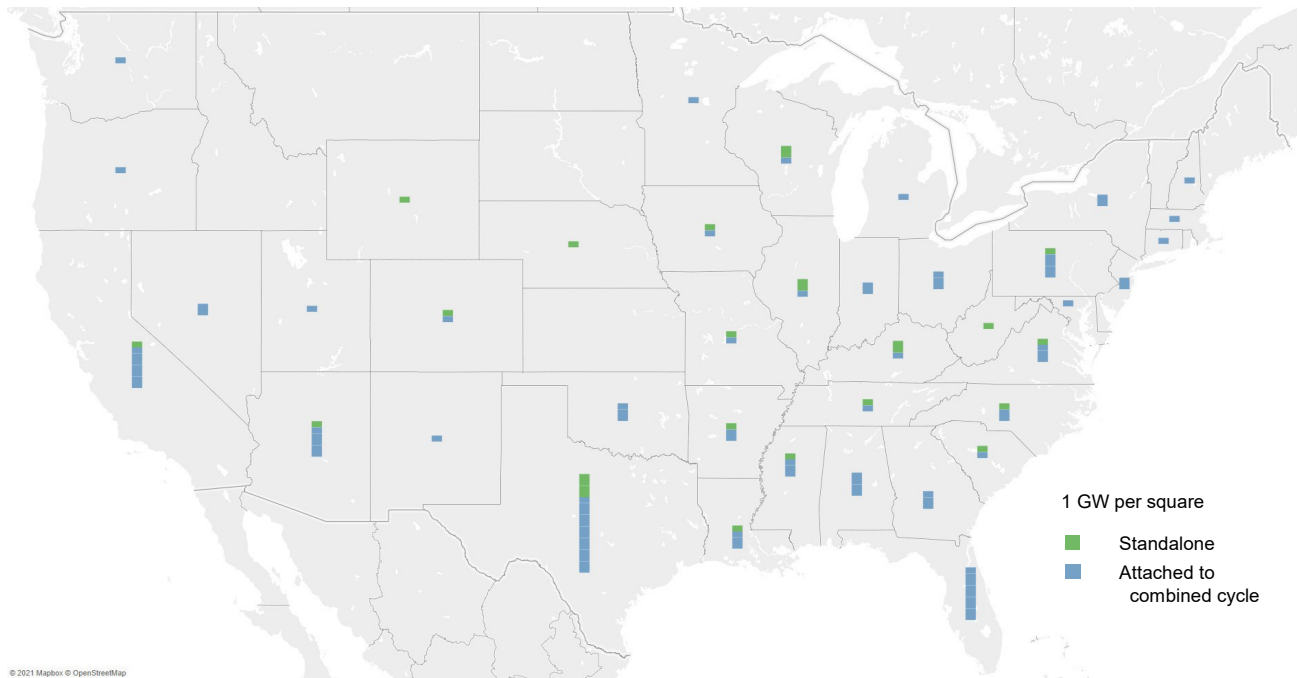


Figure 11: Geographic distribution of steam turbine capacity in the United States that is expected to be available in 2050, using the same data source and assumptions as Fig. Figure 10.

Internationally, there is a longer window of opportunity because coal plants have been built more recently and continue to be built, particularly in emerging market and developing economy countries. Plans to install new steam turbine capacity, mostly coal-fired, are generally being scaled back as countries reevaluate the economics and environmental impact of coal-fired electricity (CREA 2021). Figure 2.11 shows the steam turbine capacity that will be less than 50 years old in 2050 for the ten countries with the largest installed base of currently operating plants. The figure does not account for the construction of new plants. In China and India, which currently lead the world in new capacity additions, most new and recently built plants are either supercritical or ultra-supercritical and therefore have typical efficiencies above 40% (Hart, Bassett, and Johnson 2017).

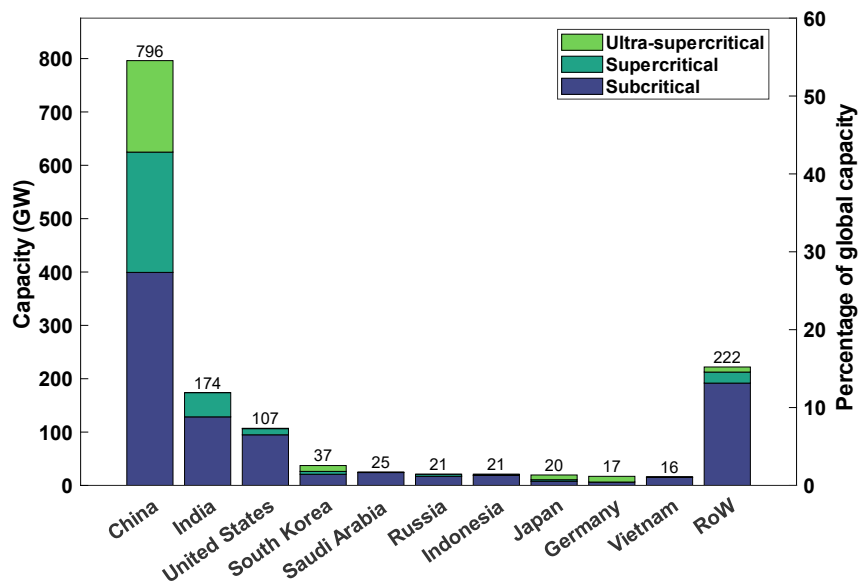


Figure 12: Steam turbine capacity for plants that will be 50 years old or less in 2050 for top-ten countries and the rest of the world (RoW). The figure includes turbines that are attached to combined cycle gas plants. Calculated from S&P Global Platts database 2016.

Researchers and commercial developers have recognized this opportunity. Designs have been proposed that use phase-change silicon, ceramic packed beds, or rocks to store heat cheaply (Meroueh and Chen 2019; Alumina Energy 2021; John Parnell 2020; GIZ 2020). One company started operating a pilot project in Germany during 2019 that has an energy capacity of 130 MWh_{th} and discharge capacity of 30 MW. The facility uses rocks, resistive heaters, and a steam turbine (Darrell Proctor 2019). While it did not repurpose an existing power plant, that is the intent for future projects (Collins 2021).

While some steam turbine retrofit concepts use resistive heating to charge the system, whereas others envision using a heat pump, a steam turbine would still be used to generate electricity. In the United States, the DOE has funded feasibility studies of this concept (Office of Fossil Energy 2020). In Germany, work towards a pilot project is underway (Jason Deign 2019). A heat pump for charging would improve roundtrip efficiency, and lower costs for discharge power would offset some of the increased cost for charging equipment.

Despite this potential, realistically, only some fraction of existing power plants will have sufficient efficiency and flexibility, and be in an appropriate location, to operate as TES plants. At this point in time, it is unclear how large that fraction is. As an example, one technical challenge will be to modify existing plants and design their thermal storage components such that the repurposed facilities can operate more flexibly than they were originally designed to for purposes of baseload power generation. Otherwise, frequent cycling will shorten plant lifetimes. Solutions can be leveraged from ongoing work to increase coal plant flexibility in response to intermittent renewable generation (IRENA 2019) and through strategies such as pairing batteries with TES (John 2017). Batteries could provide short-duration storage

to reduce cycling, and, when longer-duration storage is needed, batteries could provide time for the plant to warm up.

In the future, a strategy of reusing existing power plants may overlap with the third strategy: deploying high-temperature systems. A high-temperature topping cycle could repower a steam plant as a combined cycle plant or run in parallel to (and later replace) a natural gas combustion turbine at a combined cycle plant. Similarly, TES retrofits could function as intermediate storage options until it becomes economical to convert TES steam plants into combined cycle systems that use hydrogen or other carbon-neutral fuels. At that point, the thermal storage components could provide operational flexibility.

2.4.2 Increased efficiency at medium temperatures

Although the definition of “medium temperatures” is ambiguous in the literature, it is used here to refer to approximately 550°C–1000°C. Heat at these temperatures can drive alternative power cycles, such as closed Brayton cycles, to achieve roundtrip efficiencies in the range of 40%–55%. These cycles can be paired with sensible heat storage materials such as rocks, or with phase change materials like aluminum alloys.

Some proposed systems use sCO₂ Brayton or Rankine cycles for power generation. These cycles can increase efficiency with heat recuperation, as shown in Figure 2.12. With recuperation, less external heat is required, and the heat is supplied within a smaller temperature window near the peak cycle temperature. For this reason, latent heat storage is a more obvious match than sensible heat storage for sCO₂ and other systems with similar recuperation. The energy cost for sensible heat storage systems increases when these systems operate over a small temperature range, but sensible heat storage is still an option if the storage materials are cheap enough. For charging, resistive heaters are generally a better match since high-temperature heat pumps rely on sensible heat exchange rather than latent heat.

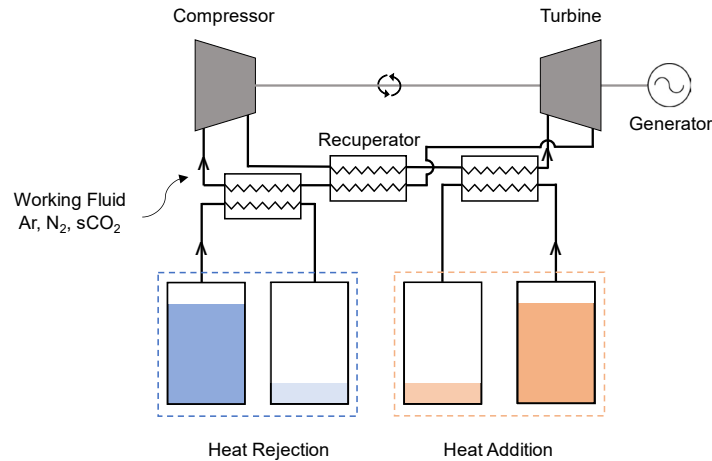


Figure 13: Diagram of recuperated, closed Brayton power cycle commonly used for medium-temperatures TES systems (Turchi, Ma, and Dyreby 2012; McTigue et al. 2019). A heat pump (not pictured) could charge the hot (dark orange) and cold (dark blue) stores. Heat addition is shown with a two-tank liquid medium although other formats are possible. Heat rejection can be accomplished by air cooling instead of cold storage which would be favorable for resistively charged systems.

Others have proposed using sCO₂ or non-supercritical fluids in a closed Brayton cycle to discharge the system, and a reverse Brayton cycle (i.e., a heat pump) to charge the system (Laughlin 2017; McTigue et al. 2019). This approach is commonly called pumped thermal energy storage or pumped heat storage. A heat pump would be similar to Figure 2.12 except the positions of the compressor and turbine would be switched as well as the flow direction. For non-supercritical fluids, research has concentrated on the use of inert gases such as helium, argon, and nitrogen for the working fluid. This approach increases the roundtrip efficiency by focusing on improvements to the charging efficiency, which can reduce the delivered cost of electricity. Heat recuperation can be used to increase charge and discharge efficiency. Even with recuperation, some versions of this power cycle can have a larger temperature range for external heat, making it amenable to latent and/or sensible heat storage.

As mentioned in Section 2.3.1, low electricity prices reduce the benefit of high charging efficiency relative to capital cost for charging power. Additionally, charging efficiency does not affect the amount of storage material needed.

A heat pump can be also used to store thermal energy at sub-ambient temperatures. Cold storage increases the discharge efficiency without requiring the hot storage to be at higher temperature. The downside to using a heat pump for charging is that it will require an additional set of turbomachinery equipment beyond the set used for discharging, which increases capital cost. This additional cost can be mitigated if reversible turbomachinery is developed (ARPA-e 2018).

Some versions of pumped thermal energy storage can use readily available equipment, which reduces commercialization risks. Current efforts to develop sCO₂ power systems range from projects that use lab-scale equipment at kW capacities to megawatt-scale demonstration plants. Since there is more

uncertainty about the power block than about the energy storage components of sCO₂ systems, the current rate of progress indicates that utility-scale deployments are likely to be possible before 2050.

2.4.3 High-temperature systems

This third strategy uses storage at high temperatures, ranging from 1000°C to 2400°C, or potentially higher. Temperatures in this range enable the use of combined cycles or solid-state energy converters that can achieve similarly high efficiencies of 50%–60%. Sensible or latent heat is possible with both technologies. Examples of each type are shown in Figure 14.

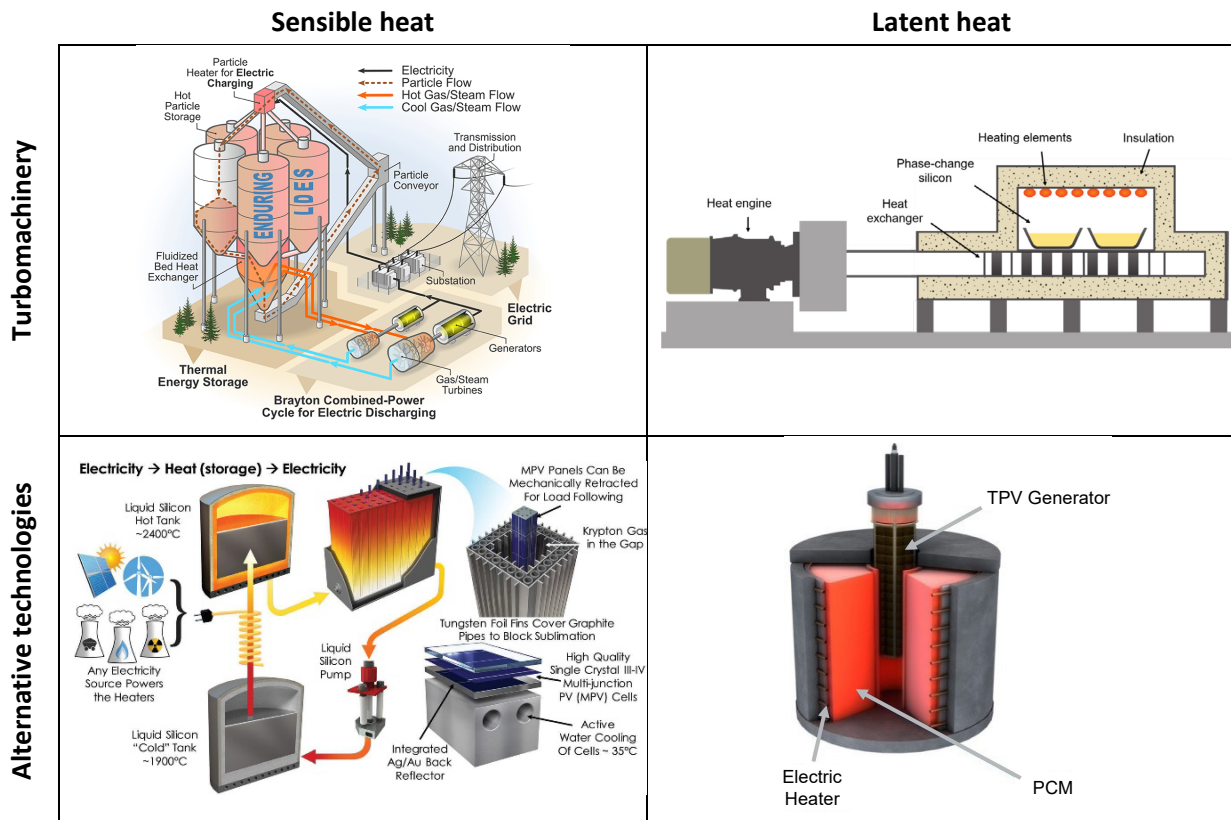


Figure 14: A sample of high-temperature systems with different designs. Clockwise from top left: particle storage with combined cycle (NREL 2018); silicon PCM in container atop a heat exchanger with Brayton turbine (Chad Taylor et al. 2020); silicon PCM with TPV (Datas et al. 2016); liquid silicon with TPV (Amy et al. 2018).

Turbomachinery-based designs generally limit technical risk to the heat exchanger that connects storage to the turbomachinery, and to the energy-related components, for either sensible or latent heat systems. However, technological improvements with respect to attributes such as startup time and ramp rate may be limited, particularly if a combined cycle system employs a steam Rankine bottoming cycle. By comparison, alternative energy converters, namely solid-state devices, still require R&D to achieve similar

efficiencies and cost per power, but they hold potential for better all-around performance. This includes high efficiency even at small scales.

At a systems level, these designs introduce risk in both the storage and discharge components. By comparison, the retrofit strategy can use established technologies for both storage and discharge. Most of the risk of the second strategy lies within the discharge components, although the use of latent heat storage introduces risks as well.

Figure 14 does not provide an exhaustive sampling of high-temperature systems. The variety of available designs suggests that, given the technical uncertainties, no dominant design has emerged yet. The system shown in the top left of the figure uses particle storage with a fluidized bed heat exchanger to power a combined cycle. The system at the top right uses the latent heat of silicon with an air Brayton turbine. A version of this system has been deployed for a commercial pilot project in Australia, the same one mentioned in Section 2.5. However, that project incorporates gas heating, so it does not represent a pure storage technology (Power Technology 2019). With further development, combined cycle configurations of this system are possible to boost efficiency. The system shown at the bottom right uses phase change silicon alloys with thermionic-enhanced thermophotovoltaic cells (Dadas et al. 2016). Its modular design may prove useful to overcome scaling challenges. The system at the bottom left uses sensible heat from liquid silicon at a peak temperature of 2400°C to power thermophotovoltaic cells.

High-temperature systems face several challenges. As one example, metallurgical-grade silicon is a common choice in high-temperature systems because it melts at high temperature (1414°C) and is inexpensive (Figure 2.5). Silicon expands as it freezes, however, which creates stresses in the container. Over time, these stresses can cause cracks and lead to containment failure (Jiao et al. 2019; Kevin Moriarty 2019). One solution is to alloy silicon to reduce this expansion; however, the alloy elements may be expensive even in small proportions (Jiao et al. 2019). Additionally, chemical reactions can occur between the container and the silicon or silicon alloys—for this reason, ensuring low reactivity has been a topic of research (Hoseinpur and Safarian 2020; Amy et al. 2021).

One design (not pictured) uses long, horizontal graphite blocks laid in parallel to store heat around 2000°C and generates electricity with TPV panels (Haley Gilbert 2021). Heat is transferred radiatively to the TPV panels as they slide between the blocks. Fewer moving parts and the use of sensible heat simplify the system design. As with all bulk solid storage systems, a tradeoff of this design is that, under partial discharge conditions, thermal gradients will develop within or between the blocks and cause some energy loss.

Another challenge arises from a phenomenon known as “creep,” which refers to the deformation of a material under stress even at levels of stress that are significantly below the material’s breaking strength. High temperature accelerates creep, leading to problems such as imperfect seals and changes in expected failure mode.

In the tradeoff between cost, performance, and technology readiness, the high-temperature strategy picks the first two. Achieving increased efficiency and flexibility while maintaining low storage cost requires high-temperature storage and/or new power conversion devices. On the structural side, more

research is needed to understand material performance at high temperatures and to ensure reliability for the intended lifetime of the plant.

2.5: Thermal Energy Storage for Non-Electricity Storage

Although this thesis focuses on energy storage using electricity as the only input and output, thermal energy storage can also be utilized in other applications. These uses are briefly addressed in this section.

2.5.1 Flexibility for Thermal Power Plants

Thermal storage can be used to store heat from a relatively inflexible heat source, such as a large coal or nuclear plant, and later use this heat to generate electricity on demand. This flexibility can help thermal power plants respond to variable renewable generation more efficiently. Steam accumulators, which store pressurized steam from a boiler or another heat source and later return steam directly to the system, represent an early form of thermal storage. They have been used in power plants and industrial facilities for decades (González-Roubaud, Pérez-Osorio, and Prieto 2017). For longer duration storage, it would be more economical to store heat in an unpressurized fashion because pressure vessels are expensive. There is interest in systems that incorporate thermal storage between a nuclear reactor and its power generation unit as a way to address ramping constraints on the reactor (C. Forsberg, Brick, and Haratyk 2018). Similarly, thermal storage could be used to provide flexibility in the operation of combined heat and power plants. Separately, an existing commercial TES project in Australia stores heat from either combusted biogas produced by a wastewater treatment plant or from grid charging. Heat from both sources is used to generate electricity (Power Technology 2019).

2.5.2 Heat End Use

As seen in Figure 2, converting heat back to electricity is the most inefficient step in TES systems. Therefore, TES can be valuable in applications where heat is the desired output, enabling greater demand-side flexibility. For example, instead of using electrical energy storage to power heating or cooling equipment, thermal storage can be used with materials such as wax or ice. This is an opportunity for TES given growing demand for cooling and electrification of heating, as discussed in Chapters 8 and 9.

There are companies that are already providing TES for space cooling and refrigeration in commercial buildings such as offices, warehouses, and data centers (Greentech Media 2020; Google 2021).

In countries like France and China, tariff structures support off-peak electric heating of hot-water tanks or firebricks (for space heating) to even out load profiles for baseload generators (C. W. Forsberg et al. 2017). Drake Landing is a planned residential community in Canada that stores heat seasonally from rooftop solar thermal collectors in boreholes (Mesquita et al. 2017). In the winter, a district heating system circulates warm fluid to the homes, which are equipped with heat pumps.

The industrial sector is characterized by diverse processes with a range of specific requirements for temperature, heat transfer rates, and process integration, among other constraints. For example, milk pasteurization and cement clinker production have notably different requirements. Thus, the applicability of thermal storage to industrial applications will vary (Friedmann, Fan, and Tang 2019; Thiel and Stark 2021).

2.6 Cost Estimates

Data from published papers and reports were used directly or as parameters to develop cost estimates. Although some demonstration plants have been built, no utility-scale TES facility has been built yet. At this early stage, significant uncertainties apply when projecting costs and performance to 2050. This study makes several assumptions, for example with respect to learning rates for power conversion devices. The values are provided in Table 3 for three representative TES systems, each corresponding to one of the systems described in Section 2.4. The remainder of this section describes the methodology to estimate specific variables.

Table 3: TES System cost estimate

Key metrics for three illustrative TES systems. FOM and VOM are fixed and variable operation and maintenance costs, respectively. The storage cost in $\$/kWh_e$ is calculated by the cost expressed as $\$/kWh_{th}$ divided by the discharge efficiency. The crushed rock system follows the strategy of increasing efficiency at medium temperatures. The liquid silicon system uses high temperatures to increase efficiency.

Technology		Steam turbine retrofitted with thermal storage			Crushed rock with sCO ₂			Liquid silicon with multi-junction TPV		
Cost Scenario		High	Mid	Low	High	Mid	Low	High	Mid	Low
Charging Capital Cost	$\$/kW_e$	3.3	3.3	3.3	3.3	3.3	3.3	24	24	24
Discharging Capital	$\$/kW_e$	290	258	225	1,226	736	494	880	498	362
Energy Capital Cost	$\$/kWh_{th}$	22	12	2.8	9.0	5.4	2.9	26	16	6.4
	$\$/kWh_e$	63	32	6.5	20	11	5.3	52	30	11
Efficiency up	%	97	97	97	99.5	99.5	99.5	99.5	99.5	99.5
Efficiency down	%	35	39	43	46	50	55	50	54	57
Capital Recovery	Yr	30	30	30	30	30	30	30	30	30
FOM discharge	$\$/kW_e\text{-yr}$	8.7	7.7	6.8	3.9	3.9	3.9	4	2	2
FOM charge	$\$/kW_e\text{-yr}$	0.1	0.1	0.1	0.08	0.08	0.08	0.58	0.58	0.58
FOM storage	$\$/kWh_{th}\text{-yr}$	0.66	0.75	0.84	0.05	0.03	0.02	0.15	0.09	0.04
VOM	$\$/kWh_e$	0	0	0	0	0	0	0	0	0
Self-discharge	% per hr	0.04	0.04	0.04	0.04	0.02	0.02	0.04	0.02	0.02

The cost values are provided in 2020 USD for all three systems. Steam turbines retrofitted with thermal storage assumes that a steam turbine plant can be acquired at zero cost. A resistive heater, thermal storage, and a steam-generation heat exchanger are required, and they constitute the power and energy costs. The thermal storage costs are based on molten salts for the high-cost estimate and crushed rock for the low-cost estimate. An average of the two are used for the mid-cost estimate. These costs are assumed to be achievable in the near term, approximately 2025.

Crushed rock storage with a closed Brayton sCO₂ power block is representative of systems that follow the strategy of increasing efficiency at medium temperatures. Liquid silicon storage with thermophotovoltaic (TPV) cells is representative of systems that follow the high-temperature strategy.

One of the differences between the systems is the tradeoff that they make between storage cost and efficiency. The liquid silicon system has higher storage cost due to higher temperatures, which enable slightly higher efficiency. On the other hand, the steam turbine retrofit has the lowest discharge efficiencies but can achieve low energy cost in the near term.

The estimates in Table 2.3 show that there is potential for TES to achieve a cost target of less than \$20 per kWh_e for long-duration storage technologies.

Lower discharge power costs are expected for a futuristic, TPV-based system, as compared to a turbomachinery-based system, because of TPV cells' modularity and manufacturing process (Kavлак, McNerney, and Trancik 2018).

2.6.1 Discharge power cost

The methods used to estimate power capacity cost for the two TES systems are similar to the ones in Schmidt et al. (2017). From a high level, a logistic curve models annual production rates of power components (GW/yr). The formula for a logistic curve is

$$f(x) = \frac{L}{1 + e^{-k(x-x_0)}}$$

where L is the maximum value, k is the growth rate, x is the number of years from 2020, x_0 is the midpoint.

Annual production rates are summed to calculate cumulative production. A single factor power law relates cumulative production to cost per power (\$/W) using a constant factor and an exponent based on learning rates. The formula for the power law is

$$g(y) = C_0 * y^{-b}$$

$$b = -\log_2(1 - LR)$$

where C_0 is a constant term, y is the cumulative capacity, and the exponent b is calculated from the learning rate, LR .

The logistic curve is modeled with a maximum value of 58 GW/yr. This results from an estimated 7000 GW of global power capacity installed for TES with power systems having a lifetime of 30 years for both technologies, and the two technologies each having 25% share of the 7000 GW ($7000 \text{ GW} / 30 \text{ years} * 25\% = 58 \text{ GW/yr}$). The value of 7000 GW is estimated from early modeling results of both Texas and New England. The power capacity necessary for the United States was estimated by scaling the values for each region by the ratio of the US's net generation to that of the region (EIA 2015). Using the ratio of net generation as a proxy for storage power capacity, a factor of 10, which is an order of magnitude estimate used by this report, is used to estimate the global energy storage capacity from US capacity in 2050. In 2020, global electricity generation was 6.3 times greater than the United States and on an increasing trend (BP 2021). Capacity built for non-storage applications of TPV and sCO₂ cycles was not included in the global capacity estimate but would be beneficial to reducing costs.

The inflection point of the logistic curve is set at 2045. The assumption of 25 years (from 2020, when costs were modeled) to reach the inflection point is an aggressive but plausible timeframe given that there has been progress on both technologies already (Gross et al. 2018). The logistic growth rate is calculated by assuming the production rate in 2020 is 1 MW/yr.

For the "Liquid silicon & Multi-junction TPV" system, the mid- and low-cost estimates are based on Amy et al. (2018). Values from the paper adjusted for overhead and interconnection costs as well as inflation. For the high-cost estimate, values from literature were used to calculate the constant factor in the power law formula. Essig et al. estimates \$0.84/W (2020\$, Supplementary Figure 3) as the cost for a multi-junction cell in a long term scenario for a plant with a production volume of 1 GW/yr (2017). The cell efficiency in Essig et al. is lower than in Table 2.3. It is assumed that more efficient cells can be produced from similar equipment and processes, so the cost per watt is adjusted for higher efficiency resulting in a lower cost. Assuming that a company with a single, large manufacturing plant has a maximum market share of 10% (Statista 2017), the constant in the power law is calculated using the corresponding cumulative capacity when global annual production is 10 GW/yr (such that $10 \text{ GW/yr} * 10\% \text{ market share} = 1 \text{ GW/yr plant}$). The learning rate is set at 15%, less than the historical rate for crystalline silicon PV cells (Kavlak, Mc Nerney, and Trancik 2018). Non-cell costs are applied from Amy et al. along with overhead costs (2018).

For the "Crushed rock & sCO₂" system, a similar approach is used. The average of three cost estimates for the main components of a sCO₂ cycle in Carlson et al. (2017) is adjusted for inflation and assumed to be achievable in 2022. From this, the constant factor in the power law is calculated for learning rates of 5%, 10%, and 15% which correspond to the high-, mid-, and low-cost estimates. Values for civil, electrical, and indirect costs from case 6 of Sargent & Lundy (2020) are added onto the cost of the components, for a subtotal of 221 \$/kW in 2020. These additional costs decline at the percentage rate given in NREL's Annual Technology Baseline (ATB) with 2020 as the baseline which results in a 14% reduction by 2050. Following this, overhead costs are applied.

2.6.2 Energy cost

The energy costs for the “Liquid silicon & Multi-junction TPV” system are based on Amy et al. (2018). The high- and low-cost scenarios use the high and low estimates from the paper adjusted for discharge efficiency and overhead costs. The mid-cost scenario is the average of the high- and low- cost scenarios.

The energy cost of the “Crushed rock & sCO₂” system was estimated using a bottom-up model of a rectangular trench filled with basalt (C. Forsberg and Aljefri 2020). Basalt was assumed to cost \$73 per ton (Alibaba 2021c; Strefler et al. 2018), insulation and containment cost approximately \$4200 per m² (Black & Veatch 2010), and excavation at \$130 per m³ (Specialty Grading 2020; “How Much Does Rock Excavation Cost?” 2018).

Early capacity expansion model runs that suggested roughly 100 hours of duration would be optimal for a system with similar values as the mid-cost case. Therefore, with a nominal power capacity of 1 GW_e and discharge efficiency of 50%, the energy cost was estimated for a capacity of 200 GWh_{th}. The high-, mid-, and low-cost values were calculated by varying the depth of the trench between 20–30 m and the temperature difference between roughly 200°C– 500°C. For a sense of scale, a trench with an energy capacity of 200 GWh_{th} would be about 20 m deep, 60 m wide, and 550 m in length although exact values depend on the assumptions used.

At smaller scales, the surface area to volume ratio increases, so the energy capacity cost increases as well (as described in Section 2.3.2) but generally by less than 10% even for a system with an energy capacity of 20 GWh_{th}.

The low temperature difference reflects a scenario using molten salt as a heat transfer fluid that comes into direct contact with the rock. At higher temperature differences (and correspondingly higher temperatures), molten salts may not be a viable heat transfer fluid, but other fluids could be used with indirect heat transfer. Other storage concepts may also be able to provide heat at the same temperatures with similarly low cost (Ma, Davenport, and Zhang 2020).

2.6.3 All-in cost

The following values were used to estimate the all-in cost. The overhead factor is multiplied to the direct and indirect costs for power and energy. The values are based on numbers from Sargent & Lundy (2020) and the MIT Energy Initiative’s Future of Storage study.

Table 4: Parameters to calculate all-in cost

Sales tax	7.5%	
EPC fee	20%	
Project contingency	10%	
Overhead (multiplier)	1.4	(1 + EPC fee + Sales tax) * (1 + Contingency)
Interconnection	30 \$/kW	

2.7 Conclusion

Thermal energy storage (TES) remains a promising option for long-duration energy storage because heat can be stored in cheap materials. The main challenge for this class of technologies is converting heat back into electricity efficiently and cost-effectively. This chapter describes three approaches that address this challenge.

The first strategy repurposes existing steam turbine power plants by replacing the fossil fuel and boiler used in those plants with thermal storage and a new steam generator. This approach can be implemented today since it relies on commercially de-risked technologies. Areas for improvement include reducing the cost of energy and creating engineering plans for optimal integration and operation. Experience with concentrated solar power is translatable to subcritical steam plants—and with more work, TES can be extended to supercritical and ultra-supercritical plants. The latter two types of plants will likely remain online longer given their higher efficiencies and deployment in countries with longer decarbonization timelines. In the interim, adding TES to supplement combustion would reduce emissions and provide flexibility in responding to intermittent output from solar and wind generators. Once this strategy is demonstrated, governments and owners of fossil-fuel power plants may find that TES offers an attractive opportunity for repurposing otherwise stranded assets.

The second approach uses alternative power cycles, namely closed Brayton cycles, that have higher increasing efficiency at medium temperatures (550°C–1000°C). In general, the thermodynamics are understood, whereas work remains to be done on component fabrication and testing. Although there are still technical challenges to resolve to enable higher temperatures and efficiencies, commercial demonstrations of these power cycles are underway in non-storage applications. As the demand for gas-fired open Brayton turbines declines, the gas turbine industry may find a significant opportunity in manufacturing and servicing these new turbines for low- or zero-carbon thermal power plants. Progress in non-storage applications will drive down power block costs, with benefits for systems that follow this second strategy.

The third strategy utilizes high-temperature materials and power conversion devices to reach high levels of efficiency and reduce power costs. Given the R&D required, grid-scale deployment is unlikely to be feasible in the 2030s but could be viable before 2050. A challenge for this approach is improving the lifetime performance of high-temperature materials to ensure they are reliable for the lifetime of the plant. This includes all the “auxiliary” components such as pipes, pumps, and sensors, which may need to be re-designed from their lower-temperature counterparts. If these engineering issues can be resolved, high-temperatures TES systems hold promise for low energy cost, relatively lower power cost, high efficiency, and favorable flexibility.

The following recommendations reflect the stage of development of different TES technologies and therefore track the three strategies closely. DOE has already funded studies on the integration of TES with coal plants. An analysis of national, retrofit-capable capacity combined with detailed studies of representative plants would provide a more accurate assessment of the potential for the retrofit strategy.

Support for first-of-a-kind projects through DOE's Loan Program Office, state energy innovation grants, or other programs could kickstart the industry. The second strategy would benefit from funding for scale-up programs and support for manufacturing. The third strategy would benefit from applied research to improve understanding and capabilities for high-temperature materials, engineering, and energy conversion systems.

Just as experience and price reductions for rechargeable batteries have been driven by larger volume markets like electric vehicles, TES would benefit from earlier adoption in applications for thermal power plant flexibility and heat-only storage. Learning in these areas would increase the industry's experience and the market's familiarity with this type of energy storage, paving the way for grid-scale TES. Meanwhile, the technology could support emissions reductions in the buildings and industrial sectors.

3 - Compressed Air Energy Storage

3.1 An overview of compressed air energy storage

Compressed air energy storage (CAES) is a mechanical energy storage technology that uses electricity to compress air; the compressed air is then stored and re-expanded at a later time to generate electricity. The compression of the air generates a considerable amount of thermal energy. CAES systems can be categorized by how this thermal energy is handled and where the compressed air is stored.

In diabatic CAES (D-CAES) systems, the heat of compression is transferred to the environment and restored by gas combustion on expansion. In adiabatic CAES (A-CAES) systems, the heat of compression is captured, stored separately from the compressed air, and returned during expansion.

CAES systems can also be distinguished based on whether they store compressed air above or below ground. In aboveground systems, the compressed air is stored in pressurized vessels made of materials such as steel or concrete. In underground systems, the compressed air is stored in existing geologic formations or in mined cavities.

In its simplest configuration, an A-CAES system consists of an air compressor, a storage chamber that holds the pressurized air, a thermal energy storage facility, and a turbine. In a D-CAES system, the thermal storage facility is replaced by a fuel combustion system.

In contrast to D-CAES, A-CAES is an energy storage technology. The efficiency of an A-CAES system is measured by dividing its electrical energy output by the electrical energy input. Studies of A-CAES systems have estimated efficiencies on the order of 55%–65% based on simulations (Hartmann et al. 2012; Barbour et al. 2021). The energy density of the aboveground thermal storage of A-CAES is comparable to that of thermal energy storage (without compressed air), making the aboveground footprint of an A-CAES facility similar to that of a thermal energy storage facility. Based on the values that have been reported for A-CAES systems regarding low energy cost, moderate efficiency, and low self-discharge rate—and assuming that these values can be achieved in practice—A-CAES technology could be suitable for long-duration storage and is therefore worth further study.

D-CAES systems are not emissions-free if they are fueled by natural gas, as is typically proposed. Although D-CAES does not qualify as an energy storage technology, these types of systems provide a mechanism for using cheap electricity to enhance the power generation efficiency and lower the CO₂ emissions of a gas turbine. For this reason, D-CAES is not discussed in detail in this thesis, though in a later section of this chapter (Section 3.7), it is noted that such systems may still merit investigation as an option for low-carbon electricity generation. Still, the volume of compressed air stored by the D-CAES system would limit the duration of any performance improvements achieved by adding D-CAES.

3.2 CAES development efforts to date

Storing energy by compressing air is an old idea that has been used in industrial settings since the 19th century. In industrial settings, compressed air was stored aboveground and was used to operate pneumatic equipment. Compressed air was first proposed as a grid-scale energy storage option in the

1940s (Gay 1948). It drew increased attention in the 1960s, prompted by interest in finding ways to store power from inflexible generators, such as large nuclear and coal-fired power plants, during periods of low demand (Budt et al. 2016; Donadei and Schneider 2016). D-CAES systems were the first options to be studied and two facilities of this type were commissioned: one in 1978 at Huntorf, Germany, and one in 1991 at McIntosh, Alabama.

The Huntorf plant, based on the flowsheet shown in Figure 3.5, has power and energy capacities of 321 MW and 640 MWh, respectively, and a discharge time of two hours. This plant stores compressed air in caverns with volume 310,000 m³ excavated in a salt dome and operates between minimum and maximum pressures of approximately 45 and 70 atmospheres (atm) respectively.

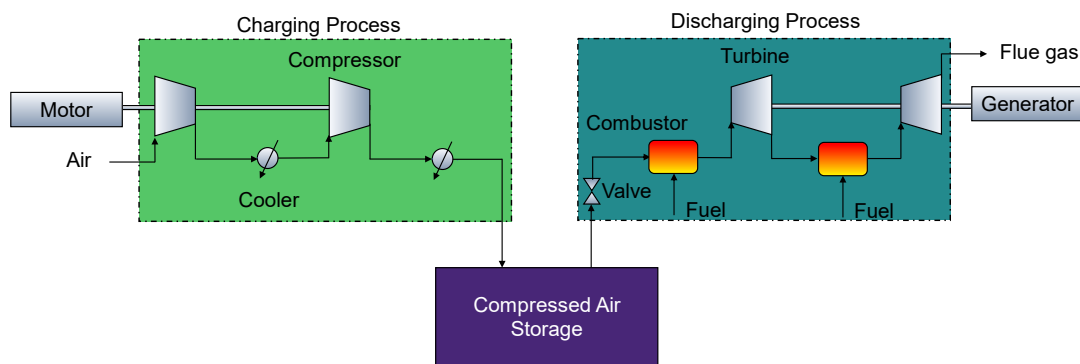


Figure 15: Flowsheet of a conventional diabatic CAES system with two combustors, which describes the D-CAES plant at Huntorf, Germany (Figure: Future of Storage).

The McIntosh facility is based on a more advanced design, using a recuperator as shown in Figure 3.2. It has a power capacity of 110 MW, which is smaller than Huntorf, but a higher energy capacity of 2.86 GWh and a maximum discharge time of 26 hours. The compressed air is stored in a 270,000 m³ salt cavern and the system operates between approximately the same maximum and minimum pressures as the Huntorf plant.

In both plants, natural gas combustion contributes significantly to energy capacity. At McIntosh, for example, for every unit of electrical energy generated, about 0.7 units of electrical energy (during charging) and 1.2 units of energy from natural gas are required (Donadei and Schneider 2016).

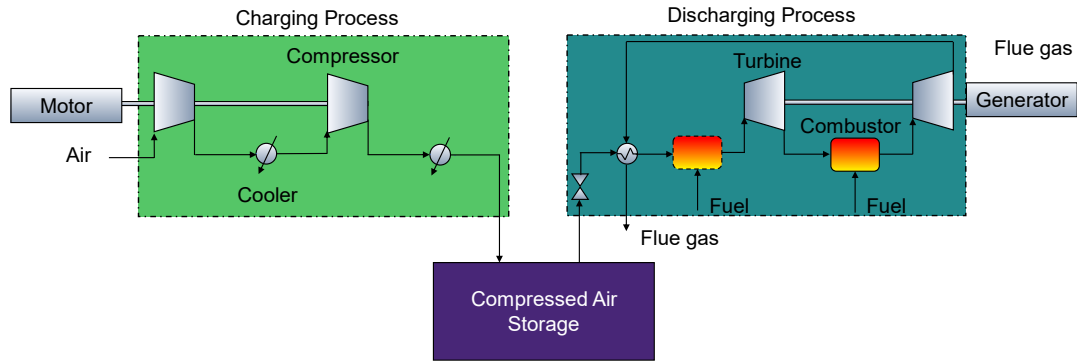


Figure 16: Flowsheet of a diabatic CAES system with a recuperator, which describes the D-CAES plant at McIntosh, Alabama (Figure: Future of Storage).

Though many D-CAES projects were proposed over the last three decades, all were subsequently abandoned; as a result, no D-CAES plants have been constructed since 1991. For a brief historical overview, the reader is recommended to Budt et al. (2016) and Donadei and Schneider (2016). In the United States, recently abandoned proposals include major projects sited in an abandoned limestone mine in Norton, Ohio and another sited in sandstone aquifers near Des Moines, Iowa. Apex-CAES is pursuing development of a 324-MW, 16-GWh D-CAES facility near Bethel, Texas, but there has not been publicly documented progress in recent years.

Some of the reasons for this lack of deployment activity are common to other storage technologies in looking at the evolution of the electric power sector over the past several decades. These reasons include lower than expected deployment of nuclear power, increased adoption of combined cycle power plants, and lower natural gas prices starting around 2009.

Other challenges are unique to grid-scale CAES including the need for large, typically geological, air-storage chambers with capacities on the order of tens of thousands to millions of cubic meters and the need to efficiently capture, store, and later return the large amounts of thermal energy that are generated when air is compressed.

At present, there are no active, grid-scale A-CAES facilities, though small-scale A-CAES facilities have been built. As with D-CAES, many projects have been proposed and then discontinued. This was the case for two highly visible recent initiatives: the Adele Advanced Adiabatic CAES project in Europe, which was proposed in 2012, and the Lightsail Energy project in the United States, which was launched in 2008. Both were cancelled within the past few years. On a more positive note, Hydrostor, a Canadian company, commissioned a 1.75 MW (discharge), 15 MWh commercial A-CAES facility in Goderich, Canada in 2019 ("Hydrostor" 2021). Hydrostor has also announced plans for several projects on the order of several hundred megawatts in California and outside the US, which, if completed, would represent the first grid-scale deployment of A-CAES. Hydrostor excavates caverns in hard rock to store the compressed air, which is maintained under constant pressure by means of a surface water reservoir. In addition, ALACAES, a Swiss company, successfully tested a 600-kW, 1-MWh A-CAES pilot plant using a mountain cavern in 2016

(“ALACAES” n.d.). At least two A-CAES test facilities are currently operational in China. The larger of the two uses aboveground storage and has a capacity of 10 MW and 40 MWh (Tong, Cheng, and Tong 2021). Other A-CAES and liquid air energy storage facilities for testing and commercial uses are reported to be under construction in China (Tong, Cheng, and Tong 2021).

The only geological formations used for large-scale CAES storage to date have been salt domes, but bedded salt, hard rock caverns, and saline aquifers have also been studied for compressed air storage. Design constraints include the ability to maintain pressures on the order of 100 atm for hours to days and sufficient internal permeability to allow rapid discharge of the compressed air.⁴

Besides diabatic and adiabatic CAES, there is a third form of compressed air energy storage known as “isothermal CAES.” In this method, heat is continuously removed from the air as it is compressed (versus after each compression stage), so that the air temperature remains constant. The process is reversed for expansion. Isothermal compression and expansion processes are in principle more efficient than diabatic or adiabatic CAES, but it is difficult to achieve efficient and cost-effective isothermal processes in practice. Isothermal CAES has been the subject of some research and commercial development efforts, but no large-scale system of this type has yet been built (Jeff St. John 2015). This is in part because isothermal CAES does not address the key barriers to CAES deployment.

3.3 Outlook

Despite the fact that no grid-scale CAES facility has been deployed recently, the technology continues to attract interest. This is partly because CAES, in contrast to some other long-duration energy storage concepts, does not face fundamental technical challenges aside from identifying suitable underground sites for storing compressed air. Nonetheless, given the lack of progress, the future for CAES is unclear. Remaining sections of this chapter discuss mechanical and thermal requirements, cost estimates, and promising areas for technology improvement that could be relevant in determining whether CAES has a role to play in achieving a decarbonized electrical grid by 2050.

3.4 Basic principles of adiabatic CAES

When air is compressed adiabatically —meaning that the air is insulated from the environment during the compression process—it heats up. Thus, for example, if air initially at room temperature and pressure were compressed to 75 atm (a typical pressure for a CAES system), and if all the heat of compression were retained in the air, its temperature would reach approximately 750°C. This air has the capacity to do work because it is both hot and under pressure.

However, storing hot, compressed air is impractical. One issue is that hot air occupies more volume than the same mass of air at room temperature, increasing the cost of storage. Air at 750°C, for example, occupies about 3.4 times the volume of the same amount of air at the same pressure at room

⁴ For further discussion, see Section 3.3.6.

temperature. Furthermore, insulating a large volume of hot, pressurized air is difficult and expensive. For these reasons, a CAES system must remove the heat of compression so that the compressed air is left at a temperature close to that of the ambient environment. In an A-CAES system, a heat exchanger transfers this thermal energy to a thermal energy storage (TES) system.

3.5 Mechanical and thermal storage requirements

Grid-scale deployment of CAES depends on the availability of suitable, large-scale, underground air storage. The locations of such sites might not overlap with the preferred locations for energy storage. Furthermore, air storage might need to compete at some sites against the storage of other gases such as carbon dioxide and hydrogen.

Thermal storage requirements for a given plant configuration depend on the design of the compression and expansion processes. In a system with single-stage compression, about half the electrical energy is converted to mechanical exergy, the other half is converted to thermal exergy (MIT Energy Initiative 2022). As the number of compression stages increases, the temperature of the TES system decreases. In isothermal CAES systems, thermal energy is removed continuously from the air as it is compressed and expelled to the environment at ambient temperature.

3.5.1 Air storage and geological siting

CAES with aboveground air storage

Given the need to store large volumes of air at high pressure, aboveground storage options such as tanks or pipelines are expensive for long-duration storage. Further, locating many pressurized tanks in close proximity introduces safety risks. One potentially feasible option for longer-duration, aboveground storage is liquid air energy storage, which is discussed separately in Section 3.7.

For shorter-duration applications, CAES would compete with electrochemical storage technologies, such as lithium-ion and flow batteries, and other grid-balancing strategies, such as demand management. A new-build CAES plant would have power costs about two to three times higher than lithium-ion batteries, which currently represent the leading short-duration storage technology (MIT Energy Initiative 2022). If CAES power costs can be reduced to comparable levels, potentially by re-purposing gas turbines as discussed later in this chapter, energy costs for CAES would need to be lower than for batteries (battery energy costs are about \$250/kWh_e). According to the literature on pressure vessels and aboveground D-CAES, air storage costs in the range of \$50–\$200 per kWh_e are achievable, although costs in this range have not yet been demonstrated in practice (Cárdenas et al. 2019; Thompson 2016). Additional costs are incurred for thermal storage.

Even if aboveground CAES systems can achieve power and energy costs that are competitive with other grid-balancing options, other considerations such as efficiency, siting flexibility, response time, and modularity would favor electrochemical storage technologies or demand management. In regard to siting flexibility, Figure 17 illustrates the typical range of energy densities for CAES systems (Budt et al. 2016; He et al. 2021); energy densities for pumped storage hydropower and lithium-ion batteries are shown for comparison. As an example, a 4-hour, 100-MW CAES system with an energy density of 10 kWh_e/m³ would

require air storage capacity of approximately 40,000 m³, about equivalent to the volume of 16 Olympic-sized swimming pools.⁵ An equivalent lithium-ion storage system would occupy 30 to 65 times less space.

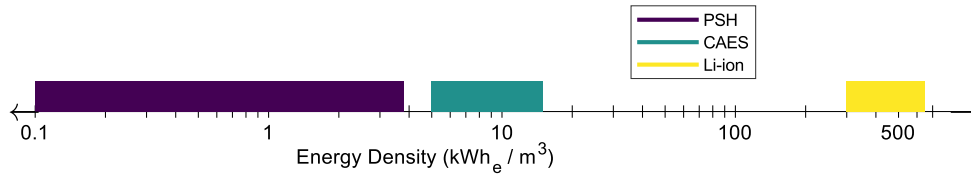


Figure 17: Typical ranges of energy density, on a logarithmic scale, for pumped storage hydropower systems with heads of approximately 50 to 1,400 meters, CAES, and Li-ion batteries.

For these reasons, CAES with aboveground air storage is generally not favorable for short- or long-duration storage. Aboveground liquid air storage, discussed later in this chapter (Section 3.7) may be an exception.

CAES with underground air storage

For underground storage, the commonly studied geological options are domal or bedded salt caverns, aquifers, depleted oil and gas wells, and hard rock mines. Figure 3.9 illustrates each option.

⁵ The volume of air storage is much greater than the volume of thermal storage. Therefore, air volume is the main factor in the energy density of CAES.

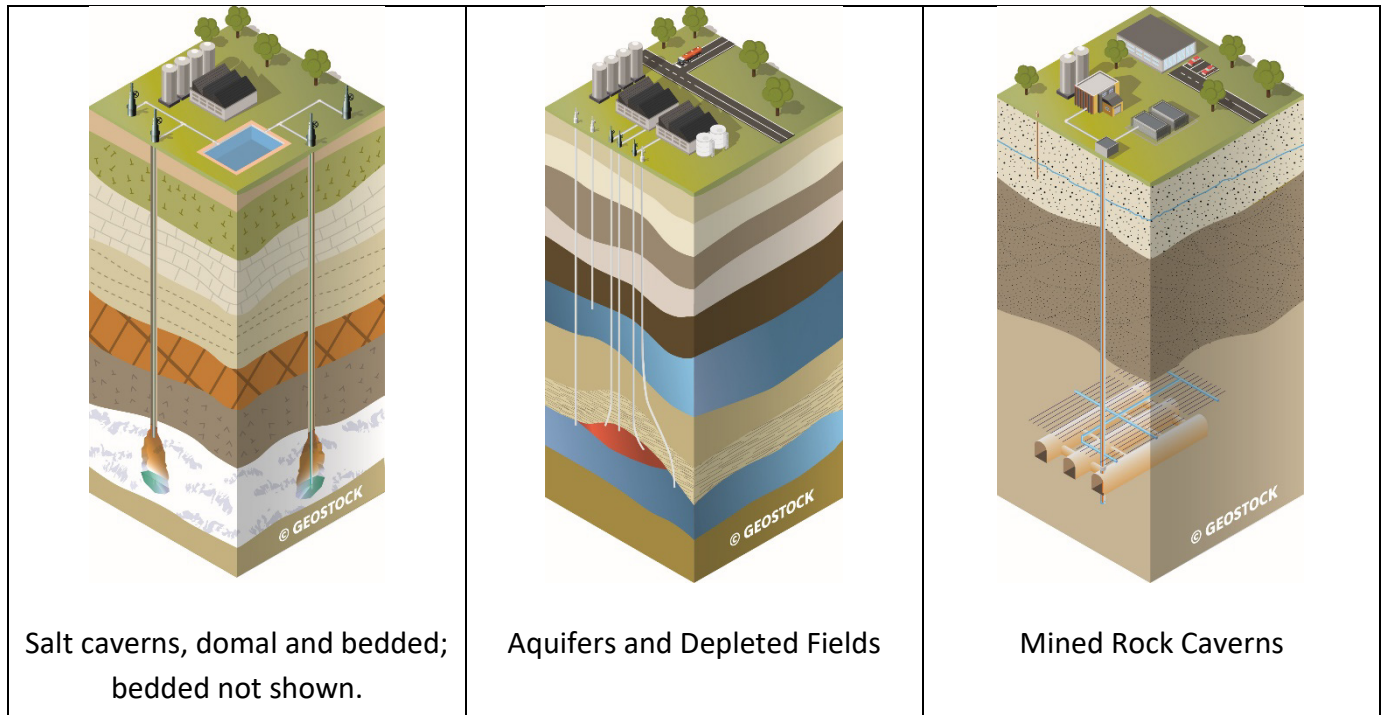


Figure 18: Illustrations of underground formations to store compressed air (Figures used with permission from Geostock Sandia).

Domal and bedded salt storage caverns are created using solution mining. This process starts with drilling a hole into the salt formation, then pumping water underground to dissolve the salt. The saturated brine is removed for waste disposal. The shape of the dome is controlled with a layer of oil to prevent dissolution of the cavern ceiling. Solution mining is a well-developed process that is used to create caverns for storing natural gas and waste. In the United States, suitable salt formations are concentrated around the Gulf Coast, the eastern half of the Great Lakes region, and in pockets of the Great Plains (Samir Succar and Robert H. Williams 2008).

Aquifers and depleted oil and gas wells are generally used “as found,” compared to other air storage options that involve mining operations. During first time setup at aquifers, air is injected to adjust the water level (Medeiros et al. 2018). For oil and gas wells, setup may involve flushing out residual hydrocarbon liquids and gases. Otherwise, residual hydrocarbons that are not removed before the well is used for CAES could mix into the stored air and be released when the air is extracted, contributing to greenhouse gas emissions.

Hard rock caverns left behind from mining operations can be suitable for air storage. In some cases, mine sections may have to be sealed off to prevent leakage. This type of geology is attractive for compressed air storage, but suitable sites are limited. New caverns can be created using standard mining methods, although the cost may be prohibitively high unless there is value in the mined material.

Note that salt and hard rock caverns can be sized to hold the volume of compressed air needed to deliver a specified energy capacity (via solution or rock mining). On the other hand, the maximum volume of

aquifers and depleted oil and gas wells is fixed by geology. If the desired energy capacity exceeds the available volume, adjacent formations must be identified and developed.

Several metrics are used to compare underground formations. The first one is the capital cost to evaluate and develop a site. This amount includes the cost to drill rock samples and test wells, apply for permits, conduct seismic testing, and test injections, among other steps. Most of the cost relates to energy capacity although some costs, such as the drilling of injection/extraction wells, relates to the rate of air flow and thus to the system's power capacity. Other metrics are the minimum and maximum pressures of the stored air. A minimum pressure is needed to maintain the structural integrity of the underground formation and to match the minimum turbine input pressure. The gas that maintains this pressure is called cushion gas, which is injected but never extracted. The minimum pressure is set either by considerations of structural integrity or by the designed inlet pressure of the first expander, whichever is greater. Maximum pressure is set by the physical properties of the underground formation.

Other metrics are porosity and permeability. Porosity is a measure of the empty space in a material. Permeability is a measure of how easily a fluid can flow through a material. A material can be porous without being permeable. Aquifers and depleted wells are filled with rocks of various shapes and sizes, leaving room for air in the voids between them and in the accessible pores of the rocks themselves. Low porosity means less volume for air. Low permeability means higher pressure losses when injecting or withdrawing air. The air-flow rate (and thus power) can be reduced to minimize pressure losses or additional injection/extraction wells can be added. Salt formations and hard rock caverns are almost entirely hollow, so losses are lower when injecting or extracting air.

Another consideration for injection and extraction rates is the structural integrity of the underground formation used to hold the air. This affects cycling frequency and thus can restrict the operational profile of a CAES plant.

The self-discharge rate of the storage site, which is air leakage through the surrounding earth, is also important. Often, the permeability of the overlying rock is distinct from the permeability of the geologic layer where the compressed air resides. For salt formations and hard rock caverns, leakage rates can be quite low. For other underground air storage options, leakage rates are site dependent. In any case, the primary factor in a plant's self-discharge rate will likely be the thermal storage.

The literature suggests that much of the United States has favorable geology for CAES, as seen in Figure 19. The literature also reports favorable geology in other countries (Aghahosseini and Breyer 2018; King et al. 2021). Regional analyses are often done at the macro scale, whereas technical and economic feasibility must be assessed at specific locations. Thus, the macro scale estimates are prone to overoptimistic estimates of air storage capacity.

The most favorable type of storage for compressed air is a salt cavern because salt caverns entail lower development risks, minimize internal pressure losses, and are compatible with frequent cycling. However, CAES will have to compete with other current and future uses for salt caverns: such caverns are used today to store natural gas and waste and could be used in the future to store hydrogen and possibly captured carbon dioxide. Hydrogen, in particular, presents storage challenges because it is a small

molecule that can diffuse easily through many materials and can be chemically and biologically reactive. Salt caverns have so far been the preferred choice for underground hydrogen storage, since other forms of storage are more susceptible to leakage and salt has low reactivity with hydrogen (Zivar, Kumar, and Foroozesh 2020). CAES has approximately ten times lower energy density than chemical energy storage, and chemical energy storage is not limited to electricity generation since hydrogen and other molecules can be used as feedstocks for chemical processes (Ozarslan 2012). Thus, if the supply of salt caverns available for storage applications is geologically limited, chemical energy (i.e. hydrogen) storage would be the higher-value and therefore preferred choice rather than CAES.

Porous geological media, which include aquifers and depleted wells, have also been used to store natural gas, but these facilities are cycled seasonally rather than daily or weekly as might be expected for CAES. Low cycling frequency for natural gas storage is economical because of the high energy density of chemical bonds. For CAES systems, which rely on mechanical exergy, more frequent cycling may be possible, depending on site conditions. Hydraulic fracturing for CAES might be used to improve permeability, but very little research has been published in this area.

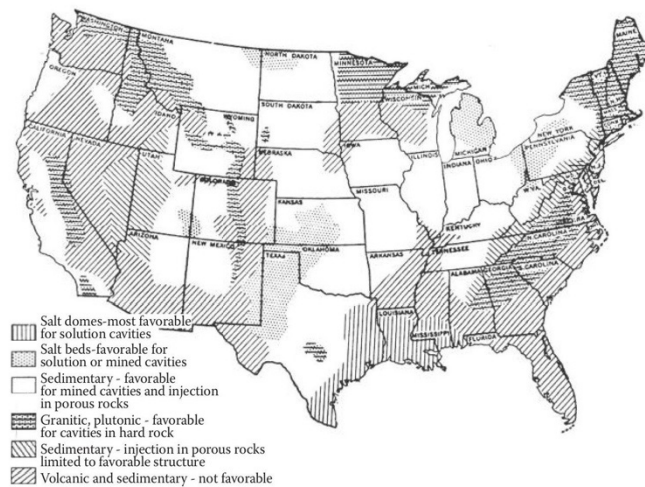


Figure 19: Map, which was originally commissioned for underground petroleum storage, showing regions of the United States that are favorable for CAES (Figure: Barnes and Levine 2011).

One example of the challenges of siting underground storage other than salt caverns is presented from an attempt made between 2009 and 2016 to develop an abandoned natural gas reservoir for a D-CAES project. The effort did not proceed beyond the request-for-proposals stage because the project proved economically uncompetitive with alternative storage bids. While A-CAES could mitigate some of the technical issues that made this project uncompetitive, removing residual methane from the reservoir without significant emissions would have been a remaining challenge.

A recent paper by Guo et al. provides a good review of CAES with aquifers (Guo et al. 2021). It discusses relevant analytical studies and summarizes results from an aquifer-based plant in Iowa that was proposed in 2003 and from field testing of an aquifer in Illinois during the early 1980s. Guo et al. conclude that a main challenge is the geological heterogeneity of aquifers and the need for better modeling and characterization methods to accurately assess a given aquifer's suitability for CAES. Under the right conditions, a porous medium could have cost and performance characteristics that could make it viable for underground air storage.

Unless information is available from prior studies, site-specific data must be collected for any underground storage option to determine feasibility. This requires hundreds of thousands to millions of dollars in upfront investment depending on the analyses required (Holst et al. 2012; Medeiros et al. 2018). While there is no guarantee of feasibility for any of the underground storage options, there will be greater uncertainty about the suitability of porous media storage sites.

Overall, the most favorable options for compressed air storage are salt caverns and abandoned hard rock mines. Both are in demand for competing uses, such as for chemical energy storage, and both are limited in supply. For porous media, suitability depends on site-specific conditions and on ensuring that resulting energy capacity costs and effects on efficiency are acceptable. Historically, some attempts to develop CAES projects in the United States have underestimated siting challenges. Looking ahead, more research on the challenge of identifying suitable underground storage sites would be needed to assess whether CAES could have a meaningful role in grid-scale energy storage.

Isochoric or isobaric compressed air storage

In isochoric storage, the volume of compressed air stays constant while the pressure changes. The McIntosh and Huntorf plants both use isochoric storage in salt caverns.

As mentioned in section 3.2, an alternative is isobaric storage. Isobaric systems use a fluid, such as water, to maintain the compressed air at a constant pressure. This fluid can be stored in a pool on the surface so that the hydrostatic pressure equals the pressure of the compressed air in the underground formation. On discharge, the fluid replaces the volume previously occupied by air, so a cushion gas is not required, although the minimum storage pressure is still constrained by the turbine's required input pressure. Because isobaric storage designs can maintain constant high pressure, they reduce the need for throttling. Thus, isobaric storage systems can achieve exergy densities two to three times greater than isochoric storage systems (Garvey and Pimm 2016; He et al. 2017).

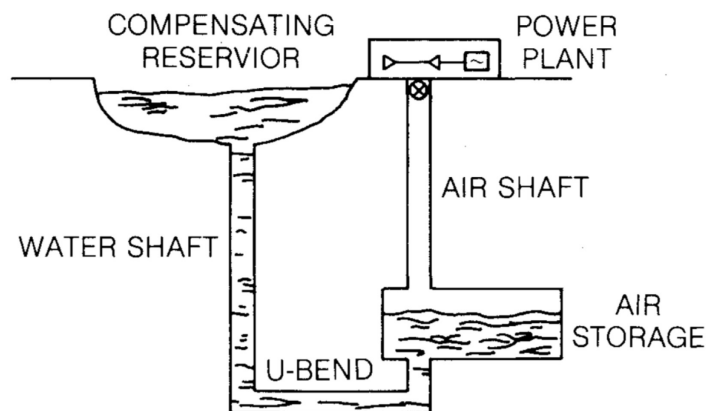


Figure 20: Surface reservoir provides pressure to enable air extraction at constant pressure. (Figure: Giramonti and Smith 1983)

While isobaric storage can provide higher exergy densities, the choice of pressure-compensating fluid has practical constraints. In a salt formation, salt would dissolve in the water, creating a saturated brine that would be corrosive to pipes and power equipment. Protective coatings could mitigate corrosion at additional cost. Another method of mitigation could be to use a thin layer of oil to reduce evaporation of brine into the compressed air (Giramonti and Smith 1983). Alternatively, fluids other than water could be used but they would have to be cheap and non-toxic since they would be needed in large quantities. For these reasons, isobaric storage is often suggested for proposed projects that use hard rock caverns.

3.5.2 Thermal energy storage capacity requirements

As described in Section 3.4, A-CAES systems require that the thermal energy generated in compression be stored and later restored during expansion of the compressed air. Given the high pressures and temperatures involved, using a pressurized vessel for thermal storage is impractical. As a result, heat exchange is necessary—potentially using an intermediate heat transfer fluid between the air and thermal storage. Temperatures of 300°C–400°C are typical of proposed A-CAES systems. These temperatures are lower than those encountered in the systems covered in section 2 on thermal energy storage. Still, the overall design process is the same, with flexibility to make different choices about thermal storage material, insulation, containment, heat exchanger, etc. The key difference is that lower temperatures allow for the use of cheaper materials—for storage and throughout the system—so that thermal energy storage costs (\$/kWh_{th}) can be lower.

Although there is some latent heat associated with water condensation due to ambient humidity, air intercooling is predominantly the removal of sensible heat from air.⁶ While thermal storage using latent heat or combined sensible and latent heat is possible, it is likely most cost-effective to use sensible heat storage to recover as much thermal energy as possible from compressed air. A maximum temperature of 400°C is comparable to the temperatures found in parabolic trough designs for concentrated solar power stations that use thermal oil. Although thermal oil may be a suitable heat transfer fluid, it would not be

⁶ Chapter 4 provides additional information on sensible and latent heat.

the cheapest option for energy storage. Other options are thermoclines or solid storage using materials such as recycled concrete or scrap metal (Geissbühler et al. 2018; J. Fan et al. 2018). Solid storage systems could use indirect or direct contact heat exchange with the heat transfer fluid, subject to the compatibility of the two materials.

3.6 Cost estimates

Since no large-scale A-CAES systems have been built, cost estimates must be developed from reports and academic literature. Many of these sources, however, provide estimates for D-CAES systems or do not specify whether the system is diabatic or adiabatic. A further issue is that among available papers and reports, several rely on the same few sources. As a result, older cost estimates have propagated to the more recent literature, often without clear justification. This introduces uncertainties as to the true versus reported costs of CAES.

Nonetheless, estimates for high, middle, and low costs can be developed from literature and compared against relevant benchmarks. For example, cost information for gas turbines and thermal energy storage systems can be used to estimate reference costs for CAES power and energy capacity, respectively. Because the aboveground power components of a CAES system, such as compressors, expanders, and heat exchangers, are technologically mature, their costs for a given plant design can be estimated by engineering firms. Costs for low- and medium-temperature thermal storage can be estimated with some accuracy using data from concentrated solar power applications. Costs for higher-temperature storage (above 600°C) are more uncertain; some estimates are available in Section 2.5. Most of the remaining uncertainty around CAES costs comes from uncertainty about the cost of air storage.

Five sources were identified that together provide a total of six cost estimates for A-CAES systems (Guerra et al. 2020; Huang et al. 2017; NYSERDA 2009; Gallo et al. 2016; IEA 2015). Gallo et al. (2016) provide high- and low-cost cases; both are included in this analysis. Another study by Guerra et al. (2020) presents minimum, baseline, and maximum costs—in that case only the baseline estimates were included because the underlying paper is focused on modeling the system effects of long-duration storage technologies and does not focus on CAES in particular.

Costs were adjusted for inflation from the year specified to 2020 using the consumer price index. If the year was not specified, the date of publication was used. In addition, some sources assumed roundtrip efficiencies higher than what is likely to be achievable in practice (e.g., 75% vs. 55%–65%) and did not disaggregate roundtrip efficiency into charge and discharge efficiencies (Yu, Engelkemier, and Gençer 2022). Based on a collaborator's simulation, charge and discharge efficiencies have similar values which can be expected in an ideal case. Therefore, as a simple estimate, the square root of the reported round trip efficiency was used to approximate charge and discharge efficiencies. To normalize cost estimates, the quoted energy cost was multiplied by the ratio of approximated discharge efficiency to the discharge efficiency from a colleague's simulations. Where reported efficiencies are higher than my estimates, this approach increases energy costs. Similarly, power costs were multiplied by the ratio of reported roundtrip efficiency to roundtrip efficiency from simulations (59%) (Yu, Engelkemier, and Gençer 2022). After

adjusting for inflation and efficiency, the average of the six estimates were taken to arrive at a single estimate for power and energy costs in 2020.

Most references report power costs as a single value, but the charge and discharge power components can be sized independently. Therefore, it was necessary to attribute some fraction of “total” power cost to charging and the remainder to discharging. For an ideal A-CAES system, the charging and discharging systems would be symmetric, so a 50/50 split would be expected. Of the five sources, two disaggregated power costs. One assumed a 40/60 split for charging and discharging; the other assumed a 55/45 split. In an actual system, the charging side is at a higher temperature and pressure, so charging power cost should be slightly higher. In this thesis, power costs are disaggregated using a 55/45 split.

The estimates of 2020 cost are used to project costs for 2050 by applying cost-reduction assumptions from references that provide cost estimates for the near-present and 2050. The fact that no A-CAES plant has been built creates additional uncertainty here. Based on a review of the literature, it is assumed that power costs could decline by 0%, 8%, and 24% from 2020 to 2050 in the high-, medium-, and low-cost scenarios, respectively. For context, the 2020 Annual Technology Baseline (ATB) published by the U.S. National Renewable Energy Laboratory projects that capital costs for gas turbines will decline by 14% between 2020 and 2050. Although the ATB does not explain the basis for these assumptions, design and manufacturing improvements to turbomachinery and other gas turbine components would generally be applicable to CAES as well. Likewise, values from the literature are used as the basis for the assumption that energy costs could decline by 0%, 11%, and 50% between 2020 and 2050 for high-, medium-, and low-cost scenarios, respectively. The low-energy-cost scenario reflects the potential for improvements in siting and developing air storage facilities, along with cost declines in thermal storage. Table 3.3 summarizes the estimates for 2020 and 2050 cost and efficiency values.

Table 5: CAES System cost estimate

Key metrics for A-CAES system. FOM and VOM are fixed and variable operation and maintenance costs, respectively.

Technology		2020	2050		
Cost Scenario		Reference	High	Mid	Low
Charging Capital Cost	\$/kW _e	452	452	418	344
Discharging Capital Cost	\$/kW _e	617	617	570	469
Energy Capital Cost	\$/kWh _e	53	53	47	27
Efficiency up	%	74	74	74	74
Efficiency down	%	79	79	79	79
Capital Recovery Period	Yr	30	30	30	30
FOM discharge	\$/kW _e -yr	3.5	3.5	3.5	3.5
FOM charge	\$/kW _e -yr	3.5	3.5	3.5	3.5
FOM storage	\$/kWh _{th} -yr	0.53	0.53	0.47	0.27
VOM	\$/kWh _e	0	0	0	0
Self-discharge	% per hr	0.04	0.04	0.02	0.02

Given limited cost data, some strong assumptions had to be made. Variable operations and maintenance (O&M) costs are set to zero, and those costs are considered to be captured by the fixed O&M costs. The fixed O&M estimate for power is based on a standalone gas turbine given similar components. The cost is split evenly between the charge and discharge (Sargent & Lundy 2020). The FOM for energy is an order-of-magnitude estimate of 1% of the energy capital cost (Oliver Schmidt et al. 2019). The self-discharge rate is set by the thermal storage losses. They are estimated to be 1% per day in the high-cost scenario and 0.5% per day in the mid- and low- cost scenarios.

3.7 Potential for CAES technology improvement

This section briefly describes a few technology concepts that could be used to improve CAES performance or cost. This discussion focuses primarily on concepts that could be relevant in situations where suitable underground storage sites can be identified. Only liquid air energy storage meaningfully addresses the problems with aboveground air storage. This section begins by discussing two concepts that could be applied to both adiabatic and diabatic CAES systems (i.e., bypass turbines and reuse of gas turbines); then liquid air storage is discussed before going on to other concepts that would be specific to either adiabatic or diabatic systems.

3.7.1 Bypass turbines

The requirement to throttle air down to the input pressure of the first turbine during discharge, as shown in Figure 3.3, significantly reduces the discharge efficiency of a CAES system. This efficiency loss can be reduced with a variable pressure throttle (Yu, Engelkemier, and Gençer 2022). During discharge, the throttle regulates the air to two pressure levels in sequence, and both turbines can be maintained at constant operating conditions. At the beginning of the discharging process, the compressed air is throttled to match the high-pressure turbine inlet; it then passes through both turbines in series. When the cavern pressure falls below the pressure required at the first turbine inlet, the compressed air bypasses the first turbine and is throttled to match the second turbine's inlet pressure. Reducing exergy losses through the throttling valve enhances the discharge efficiency of the system.

3.7.2 Reuse of gas turbines

One cost-cutting approach that has been proposed involves reusing stranded gas turbines to reduce the cost of CAES charge and discharge power (Nakhamkin 2010). To complete the CAES system, however, other components are still needed to perform functions such as heat exchange, thermal storage, and air storage.

Significant modifications are required to reuse existing gas turbines. These units contain integrated compressor and turbine stages. Some of the motive power generated during expansion drives the compression stage while the remaining motive power is used to generate electricity. This mode of operation requires compression and expansion to occur at the same time. For CAES operation, however, the compression (charge) and expansion (discharge) steps must be decoupled. One approach to deal with this design difference is to decouple the compressor and expander by adding a clutch mechanism to the gas turbine unit. Another approach is to use one half of the gas turbine by removing blades from the

compressor and adding a bypass to use just the expansion section, and vice versa. With this modification, two gas turbines are needed to create a compressor and expander pair.

An additional consideration is that gas turbines are designed to operate with specific pressure ratios and within a maximum pressure limit, so they could only be reused for the low-pressure compression and expansion stages. An additional challenge with this retrofit approach is that the location of existing turbines may not coincide with sites where underground air storage is available. Alternatively, there would be costs to relocating gas turbines. Given these issues, repurposing retired gas turbines seems unlikely to be an attractive option.

3.7.2 Liquid air energy storage

A liquid air energy storage (LAES) system charges by compressing air to high pressure, similar to an A-CAES system, but the air is then cooled before its pressure is reduced to near-ambient levels. The pressure reduction can cool air to temperatures around -196°C where some of the air becomes liquid. (Air is a mixture of gases; its dominant component is nitrogen, which liquefies at -195.8°C .) The air that does not become liquid remains as a cold gas at ambient pressure; this air goes through a heat exchanger to cool the high-pressure, ambient-temperature gas. To generate electricity, the liquid air can be pumped to high pressure, heated back to a gas, and then run through one or more turbines, using a simple Brayton cycle or a derivative. Other methods have been proposed that use a Rankine cycle. In either approach, the heat from compression is stored so that it can be used during discharge, as with A-CAES. The ability to recover cold thermal energy during discharge and use that energy for the next charging cycle is unique to LAES.

Charge and discharge power capacity for LAES systems can be sized independently, as in CAES. Unlike CAES, however, LAES offers siting flexibility since all components are above ground. Liquid air has an estimated energy density around 95 kWh/m^3 , which is about 10–20 times the energy density of CAES. This greatly reduces the challenges associated with aboveground storage (Guizzi et al. 2015). Energy storage capacity for LAES systems scales with the size of their cryogenic tanks and hot and cold thermal stores. Gas liquefaction, using either the Hampson-Linde cycle, the Claude cycle, or another cycle, is a mature process that is already in use for industrial gas supply, natural gas liquefaction, and other applications. Compared to other liquefaction processes, the novelty in a LAES system lies in recycling the hot and cold thermal energy, which is key to increasing roundtrip efficiencies of approximately 50%–60% (Borri et al. 2021). In non-LAES gas liquefaction plants, heat recovery from compression and expansion is not possible because the gas is typically exported. Integration with waste heat from a nearby source can further improve the efficiency of LAES systems.

For LAES, technological maturity is not the primary concern, although gas liquefaction facilities do require advanced industrial capabilities and skilled labor. The key questions center on cost and efficiency. Given limited development to date, reliable cost estimates are not currently available. Small-scale plants (300 kW/2.5 MWh and 5 MW/15 MWh) have been built, and plans for larger facilities have been announced (Borri et al. 2021).

3.7.3 Adiabatic CAES with resistively heated thermal storage

For a typical adiabatic system, the temperature of thermal storage depends on the pressure ratio of the compressors and on the decision to employ intercooling (or not). Resistive heating can be used to increase

the temperature of thermal storage. Higher temperatures increase discharge efficiency and energy capacity for a given volume of stored air. Additionally, higher temperatures increase design flexibility with respect to the compression stages.

Since resistive heating introduces additional energy beyond the energy used for compression, systems that have this feature are no longer adiabatic, by definition. They still qualify as a form of electricity storage because only electricity enters and leaves the plant. In the literature, these systems are described as “combined heat and compressed air energy storage” or “hybrid thermal-CAES” (Houssainy, Janbozorgi, and Kavehpour 2018).

A thermal storage system can be designed to meet the maximum allowable temperature for each expansion stage. For the high-pressure turbine, maximum temperature is constrained by material limits. For the final expansion stage, allowable turbine inlet temperatures can be as high as those for open Brayton turbines, which are around 1400°C, although materials in the heat exchanger could enforce a lower limit. With resistive heating, the thermal storage component for a CAES plant could resemble the thermal energy storage systems described in Chapter 4.

3.7.4 Diabatic CAES for grid decarbonization

Although D-CAES is not a focus of this chapter, there may be a role for the technology when looking at the bigger challenge of decarbonizing the overall power system. As literature shows, dispatchable generation resources such as gas turbines with carbon capture and sequestration (at an approximately 90% carbon capture rate) are deployed even in highly carbon constrained scenarios (MIT Energy Initiative 2022). D-CAES systems paired with carbon capture and sequestration (CCS) can be viewed as analogous to gas turbines with CCS. The difference is that D-CAES systems can use low-carbon electricity to compress air ahead of time, increasing fuel efficiency during discharge. When the stored air is depleted, a D-CAES plant can switch modes to operate the compressor and expansion train simultaneously, like a gas turbine (Thomas McCafferty 1980, 1). Alternatively, hydrogen can be used instead of natural gas to eliminate the need for on-site CCS. For more technical detail and an example of a D-CAES system suited for CCS, see Zeynalian et al. (2020).

3.8 Summary findings and recommendations related to compressed air energy storage

Despite decades-long interest in adiabatic CAES and experience from two operational D-CAES plants, this energy storage technology has not found recent success. Aboveground CAES has been the subject of some research, but it is impractical for grid-scale electricity storage. CAES with underground air storage does not present major technical challenges with respect to its aboveground components—rather the challenge is finding and developing suitable underground sites to store compressed air.

Caverns in salt domes, bedded salt, and hard rock are attractive options for underground air storage. However, chemical energy (e.g., hydrogen) storage is a competing use for these geological features that may be more economical given its higher energy density. Studies indicate that porous media, such as aquifers and depleted oil and gas wells, are usable for CAES, but these options have not been demonstrated yet.

A-CAES is generally suited for long-duration storage, where low energy cost is a key metric. Key cost drivers for these systems are the siting process, the development of air storage facilities, and thermal storage equipment. Although cost estimates for CAES are subject to multiple uncertainties, estimates of energy cost for this technology are generally higher than estimates for other energy storage technologies that are expected to be available in the future. Power costs for CAES are not expected to decline significantly.

Potential opportunities to increase efficiency and lower power costs include incorporating a bypass turbine, reusing existing gas turbines, and applying resistive heating to the thermal storage component. However, none of these options addresses the critical issue of developing adequate underground air storage. Liquid air storage does solve the air storage problem, so it may offer a promising path forward. Given the early stage of development of liquid air systems, however, more data on performance and cost are needed to assess whether liquid air could be a competitive storage technology.

Ultimately, deployment of A-CAES with underground storage seems viable, and in some regions with favorable geological resources it may play a non-trivial role in the future. However, geological constraints and limited cost reduction potential would appear to make CAES less competitive over time as other long-duration storage technologies mature. Unless liquid air energy storage proves a major exception, CAES is unlikely to play a significant role in grid-scale storage—in the United States or globally.

4 - Levelized Cost of Storage

Levelized cost of storage (LCOS) is a useful metric to compare the holistic cost of technologies that are serving similar roles such as long duration storage. However, comparing the LCOS of technologies serving different functions, for example, long duration storage to frequency regulation, would be misleading.

Another limitation of LCOS is that calculation methods generally ignore details such as ramp rates which would be a relevant factor in operation. Furthermore, one of the main limitations of LCOS as a metric is that it measures the cost of a storage system, not its value. The difference between cost and value is nominally the profit which would drive investment decisions.

To measure value, capacity expansion models (CEM) or other simulations, which account for other resources on the grid, are required. However, CEMs require extensive datasets and expert users. CEMs require data on the cost of generators, fuel, storage, transmission, load profiles, renewable resource data (e.g. wind and solar data), and existing resource capacities among other information. The results are also dependent on simplifications used for model tractability and what policy scenarios are implemented. For further discussion on this topic, the reader is referred to the Future of Energy Storage (2022) by the MIT Energy Initiative.

While waiting for models which are validated and easy to use to become publicly available, LCOS is a useful metric for technology assessment since it can be calculated from handful of variables and provides insight on ways to lower the system cost. Estimates reported here are for nth-of-a-kind systems.

4.1 Default values and sensitivities

In a system with high shares of VRE generation, studies have noted that for many hours of the year, prices will be low for many hours of the year due to the low marginal cost of VRE generators (Sepulveda et al. 2021; MIT Energy Initiative 2022). For a small percentage of time, the price will be high when storage or other backup resources are utilized. Grid-scale storage systems would have access to wholesale prices. Current wholesale prices are around 40 \$/MWh but that varies greatly by location and time. For the LCOS calculations, the price of electricity to charge a storage system is set at 10 \$/MWh. This lower price reflects a future where abundant VRE generation causes low wholesale prices for significant fractions of the year and is when energy storage plants would charge (Sepulveda et al. 2021; MIT Energy Initiative 2022). The change in LCOS for other wholesale charging prices can be quickly estimated by the reader by adding the difference in the wholesale price and the penalty from roundtrip efficiency. Technologies with lower roundtrip efficiency are more sensitive to electricity prices, but at low prices, the penalty is small relative to the capital and operating expenses.

According to current expectations on the relative costs of VRE generation and energy storage, long duration storage is expected to have low capacity factors. While long duration storage is not expected to operate in simplified charge-discharge cycles (Schmalensee, Junge, and Mallapragada 2020), it is useful to see how LCOS changes for different cycling frequencies and discharge durations.

Financial assumptions used to calculate LCOS are listed in Table 5. The values are based the MIT Energy Initiative’s Future of Energy Storage report which was in part based on NREL’s ATB for 2020.

Table 6: Financial parameters

Debt fraction	40%
Inflation rate	3%
Interest rate	3%
Rate of return on equity	8%
Tax rate (Federal and state)	26%

Unless otherwise stated, LCOS values are shown for the mid-cost estimates provided in Tables 2 and 3, and the charge-to-discharge power ratios are set to unity.

4.2 LCOS of TES

4.2.1 Retrofits

The LCOS for a steam turbine plant retrofitted with TES under various cycling frequencies and discharge duration is shown in Figure 21. The high- and low-cost estimates refer to the values in Table 3.

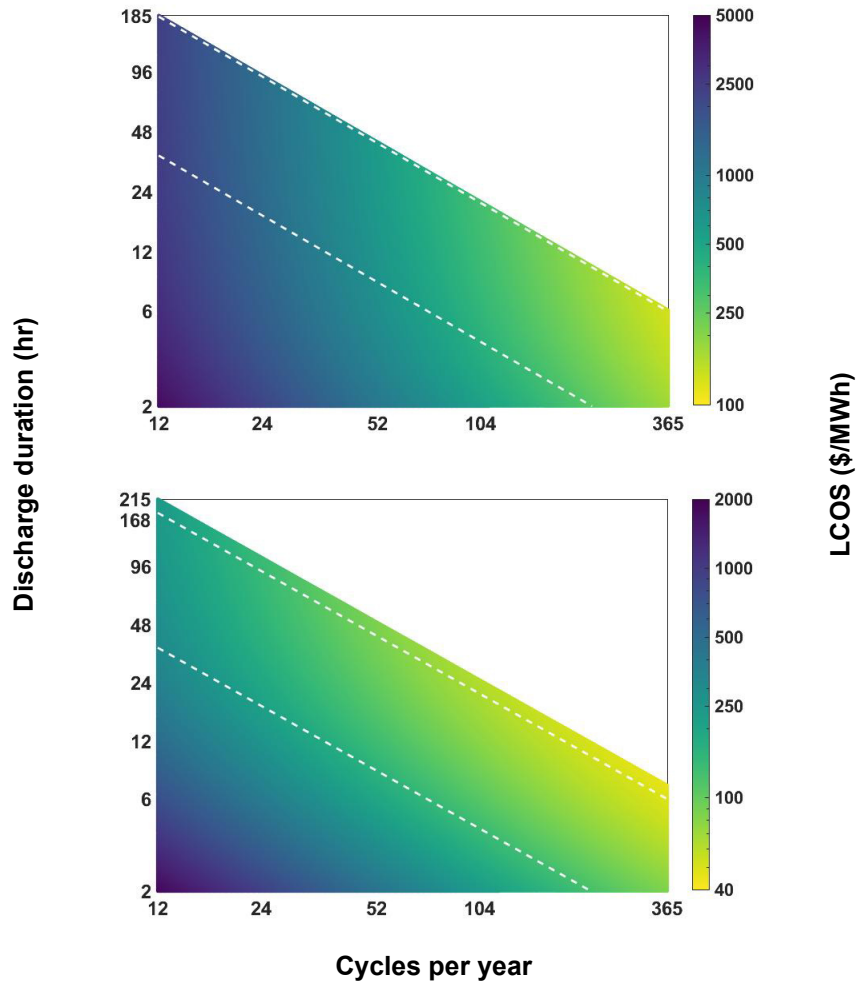


Figure 21: LCOS of TES retrofit with steam turbine plants for high-cost estimate (top) and low-cost estimate (bottom). Different color scales are used between the two graphs to highlight the range of LCOS values. The upper and lower white dashed lines indicate capacity factors of 25% and 5%, respectively.

For the high-cost TES retrofit estimate at the top of the figure, the LCOS increases quickly as cycling frequency decreases. The low-cost estimate has lower LCOS values and remains relatively low over a wider range of operating conditions. For example, at 10% capacity factor, the LCOS for the high-cost scenario is \$361/MWh for twice-weekly discharge (104 cycles per year) and \$1266/MWh for twice-monthly discharge (24 cycles per year). For the low-cost scenario, the values are \$94/MWh and \$175/MWh. Since the LCOS of the high-cost estimate is significantly higher than typical wholesale power prices, a high-cost system is unlikely to be built. On the other hand, a low-cost system is potentially attractive; therefore, the remainder of the analysis will focus on the low-cost system.

To understand where the difference in LCOS values arises, Figure 22 illustrates the cost contributions of each variable to the levelized cost for the low-cost scenario.

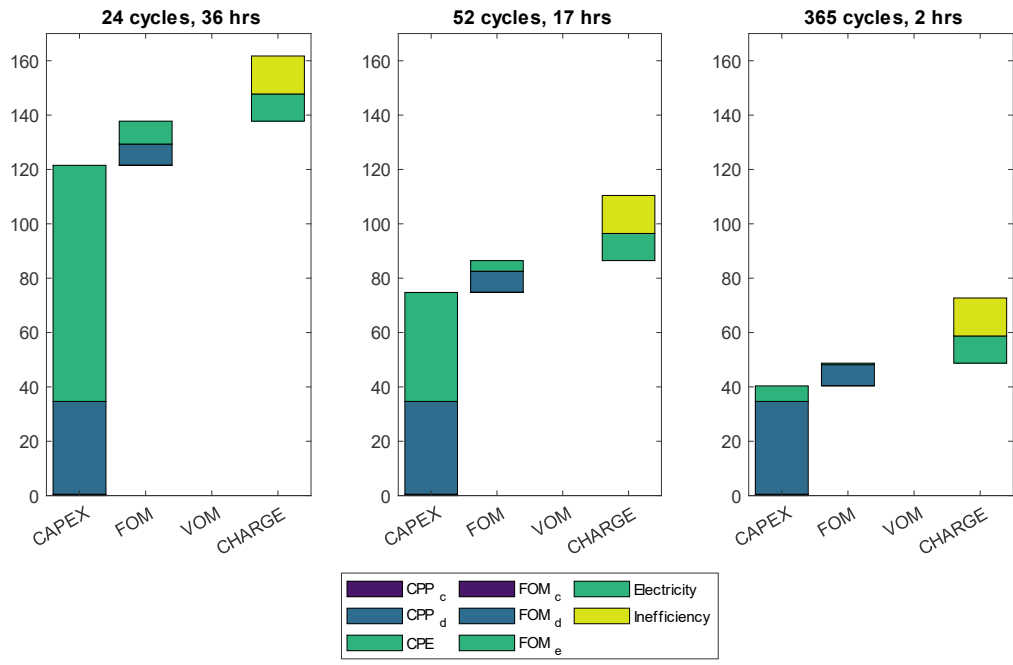


Figure 22: LCOS breakdown for steam turbine plant with TES using low-cost estimates. All three panels are at 10% capacity factor but with varying cycling frequency and discharge duration. The legend abbreviations are cost per power (CPP with subscripts “c” and “d” for charge and discharge), cost per energy (CPE), fixed and variable operations and maintenance (FOM and VOM).

While a low LCOS can be achieved for daily cycling, thermal transients could make daily cycling for only a few hours impractical for steam turbines. As the discharge duration increases, the contribution of the energy cost increases as expected. Thus, it is critical to reduce capital cost of energy capacity by a factor of 10 from by switching from molten salts to a cheaper medium. Although this system is characterized by relatively low roundtrip efficiencies (35%–45%), which incurs a penalty of around \$15/MWh on a levelized basis, aggressively reducing the energy capacity cost enables low-cost, long duration energy storage.

So far, the values shown have been for systems with a lifetime of 10 years which may be indicative for systems reusing coal plants in the United States and other industrialized nations as discussed in Section 2.4.1. It may be advantageous to invest in repairs to extend the lifetime of these plants. Since the repairs and costs would be specific to each plant, a rough estimate is made by doubling the power capacity cost of the low-cost estimate. Repairs would be associated with the existing steam turbine plant and therefore scale with power capacity. The LCOS of the low-cost scenario and the adjusted one are shown in Figure 23 with varying lifetimes.

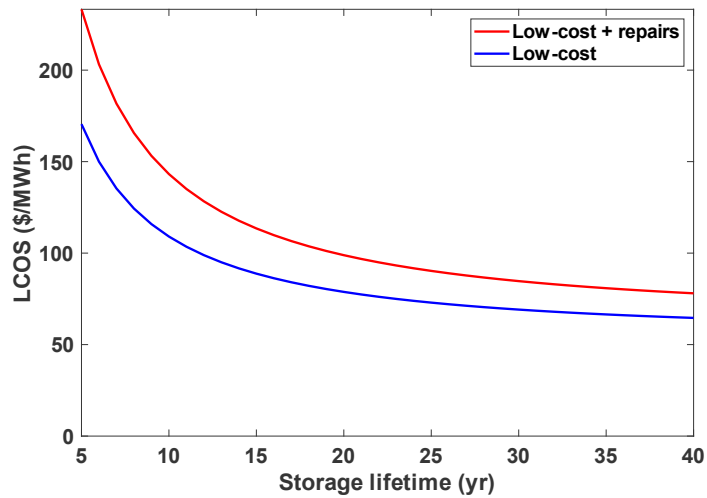


Figure 23: LCOS versus lifetime for the low-cost estimate (blue) and the same estimate with doubled power capacity cost (red).

For a system with an original lifetime of 10 years, repairs would pay for themselves if an additional 6 years of operation could be earned under the hypothetical repair costs. Although it becomes less cost-effective to repair plants with remaining lifetimes of 15 years or greater, it could be an option to build and maintain LDES resources until more cost-effective technologies are available. Beyond the United States and in regions with newer coal fleets, power plants repurposed for TES could have 20 years of lifetime remaining. At 20 years, most of the cost reductions due to increased lifetime are realized. While fewer repairs may be needed, there could be costs associated with converting the plant from baseload to flexible operation.

Despite uncertainties with the cost assumptions and potential engineering challenges, cost and performance estimates based on presently available technologies highlight the attractive potential to reuse steam turbine power plants as near term, cost-effective LDES globally.

4.2.2 Future technologies

Future TES technologies have potential to provide similarly low levelized cost as the retrofit option but with the flexibility to build anywhere since newer technologies would not rely on existing on-site infrastructure. Figure 24 shows the LCOS for a crushed rock & sCO₂ system and a liquid silicon & TPV system using the mid-cost estimates from Table 3.

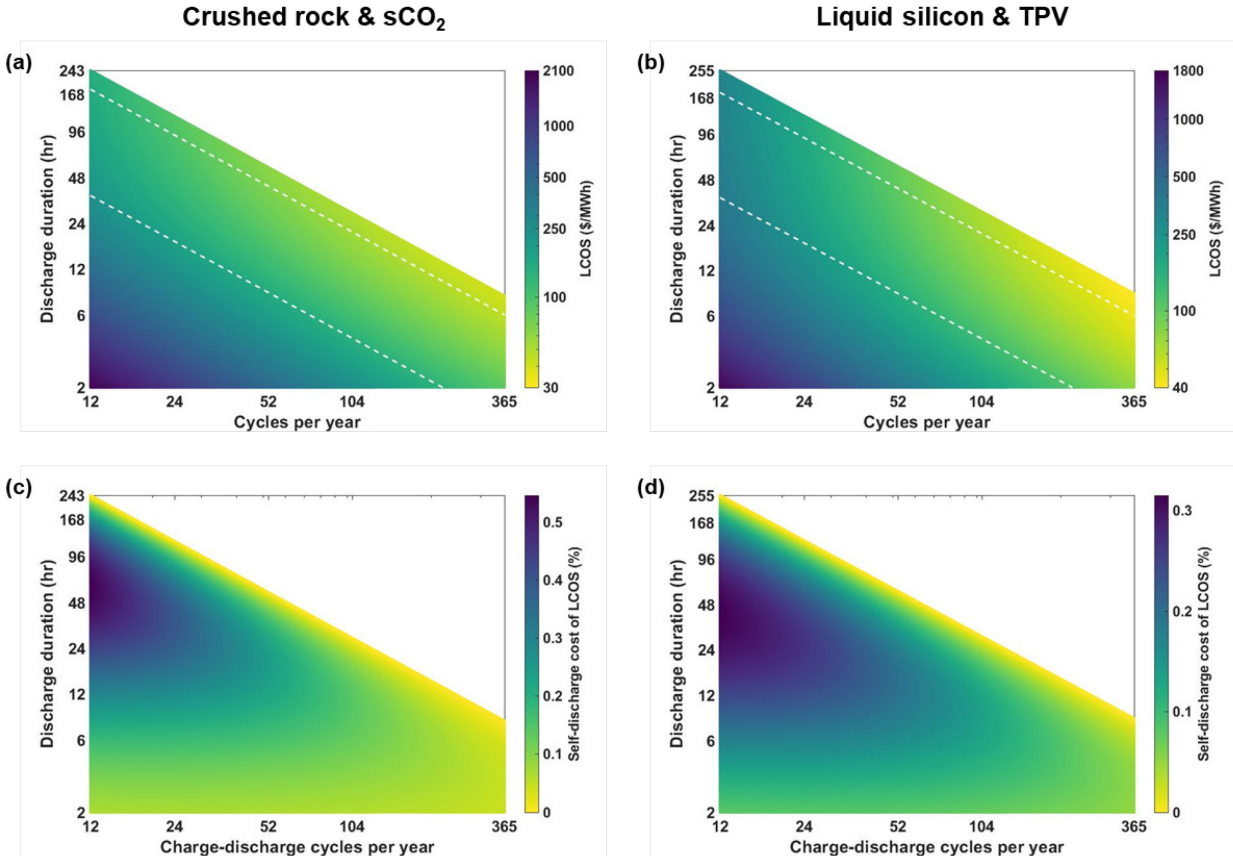


Figure 24: LCOS of (a) crushed rock & sCO₂ and (b) liquid silicon & TPV systems based on mid-cost estimates. Note the color scaling is unique to each graph to maximize contrast, and the y-axis limits differ between the two plots. (c), (d) Self-discharge cost of the two technologies as a percentage of LCOS, which is calculated as the cost to recharge the lost heat.

With the mid-cost estimates, crushed rock has lower energy cost ($\$/kWh_{th} * \eta_d$), so the LCOS is slightly lower than the liquid silicon system in the low cycling regime. Otherwise, the two technologies have similar LCOS values over a range of cycling frequencies and discharge durations. This is a result of both having similar discharge efficiency and energy capacity cost ($\$/kWh_{th}$) despite using two different strategies for TES and thus having drastically different thermal designs. For further detail, the cost contributions of each cost category are illustrated in **Error! Reference source not found.**

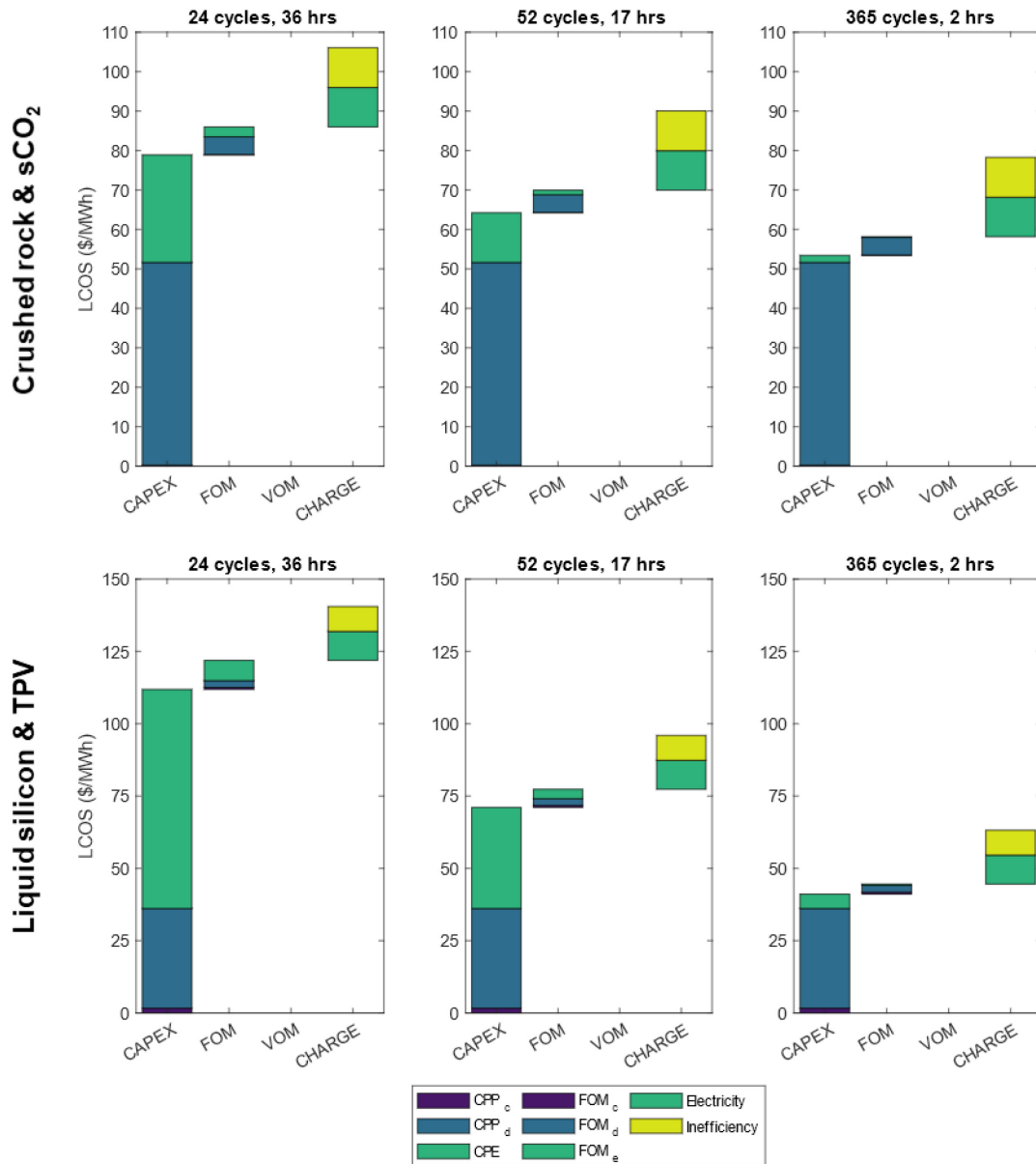


Figure 25: LCOS of the crushed rock (top) and liquid silicon (bottom) at 10% capacity factor and varying cycling frequency.

Between the two technologies, the main differentiator is the energy cost. The difference becomes more pronounced with longer discharge duration. Other costs such as charge and discharge power, FOM, VOM, and the charging cost are similar between the two technologies.

Sensitivity analyses between the three cost scenarios for each of the two technologies are shown in Figure 26. Sensitivities are shown for variables adjusted one-at-a-time.

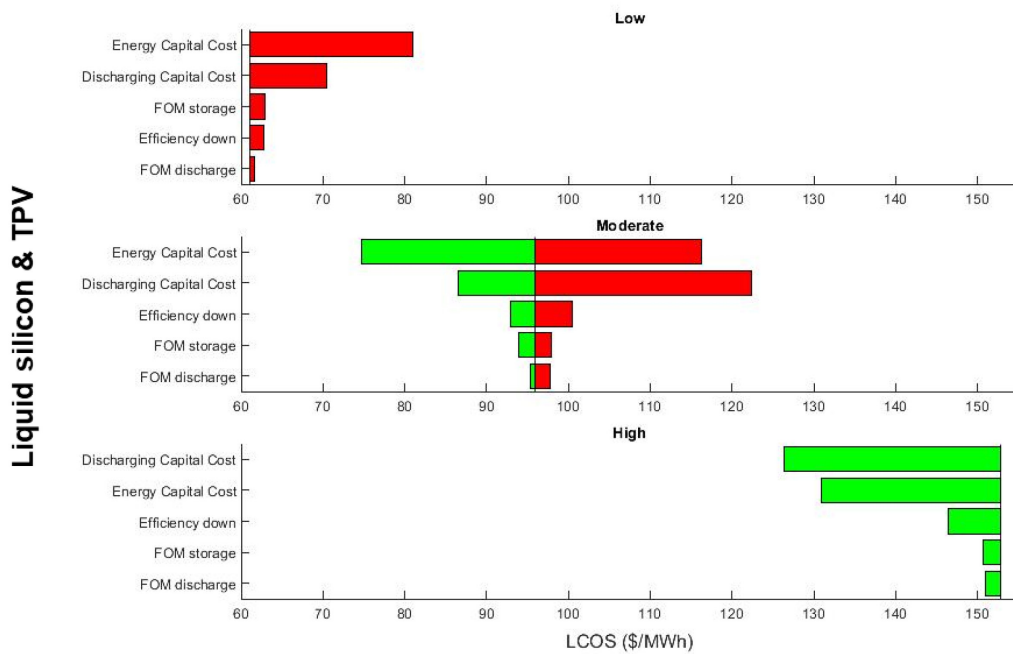
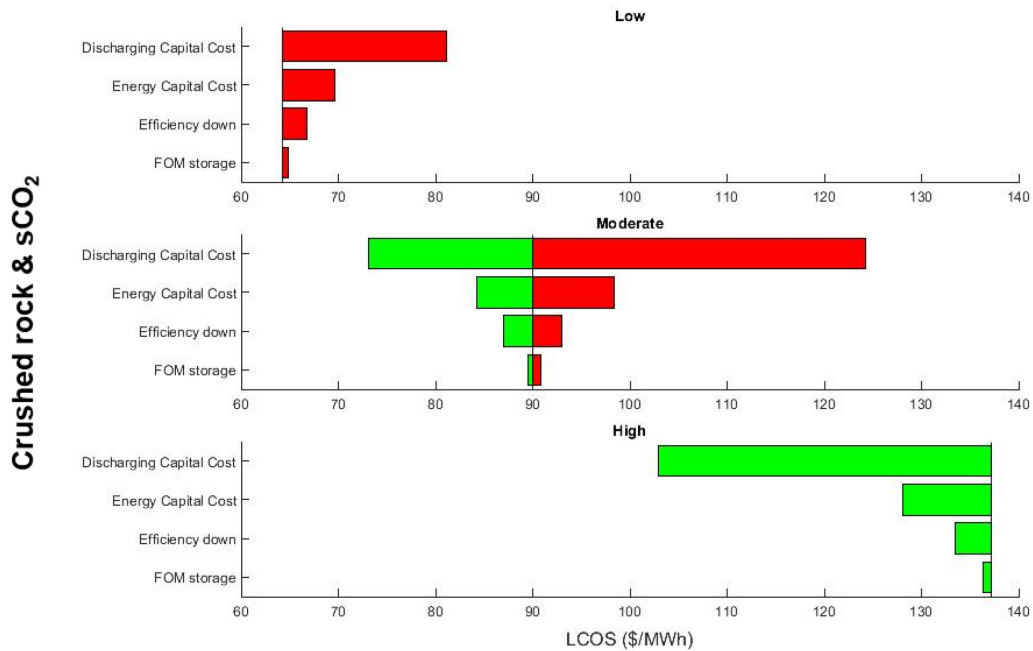


Figure 26: LCOS sensitivity analysis for the future TES technologies: crushed rock & sCO₂ and liquid silicon & TPV. The estimates are shown for a system operating at 10% capacity factor and 52 cycles per year. The red bars indicate increase in costs, while green bars indicate decreasing costs.

The horizontal bars originate from the LCOS calculated from the default values for the corresponding cost scenario. The green bars show the change in LCOS if that single variable is adjusted to the value in the low-cost scenario. Likewise, the red bar shows the change in LCOS using the high-cost estimate. Variables

that remained constant between scenarios are not plotted. Across both technologies and all three cost scenarios, discharge power and energy costs were the variables that had the greatest effect on LCOS. This may seem partly contradictory to the literature which finds discharge efficiency and energy cost to be the important variables. However, they are not contradictory because first, the sensitivity analysis uses a wide range of estimates for some variables rather than a fixed percentage difference across all variables. For example, the high and low discharge power costs are +69% and -34% of the mid-cost estimates whereas discharge efficiencies vary -8% and +10% respectively. The second reason is that the sensitivity analysis assesses LCOS of a single technology, not the interactions at a systems level as a capacity expansion model would.

While there are characteristics of the two technologies not captured by their LCOS that could have meaningful impact, such as ramp rates, TES has potential for low LCOS through multiple technology pathways.

4.3 LCOS of CAES

Although CAES will have challenges with identifying suitable underground storage sites, it could be feasible in some locations, so the potential range of LCOS is calculated. As listed in Table 5, energy costs for CAES are higher than TES even though CAES has higher discharge efficiencies. As such, Figure 27 shows the LCOS of CAES is higher than TES for the same cycling frequency and discharge duration.

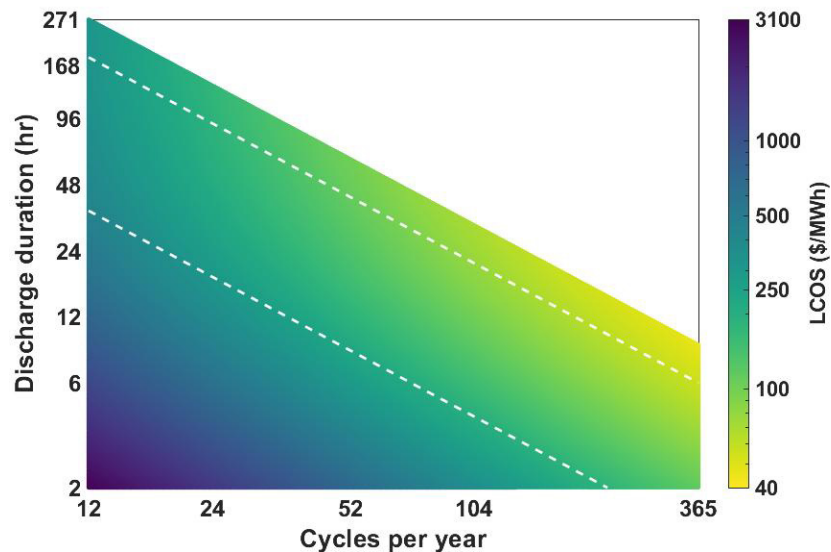


Figure 27: LCOS of CAES based on mid-cost estimate.

Figure 28 shows the breakdown of the levelized cost by category.

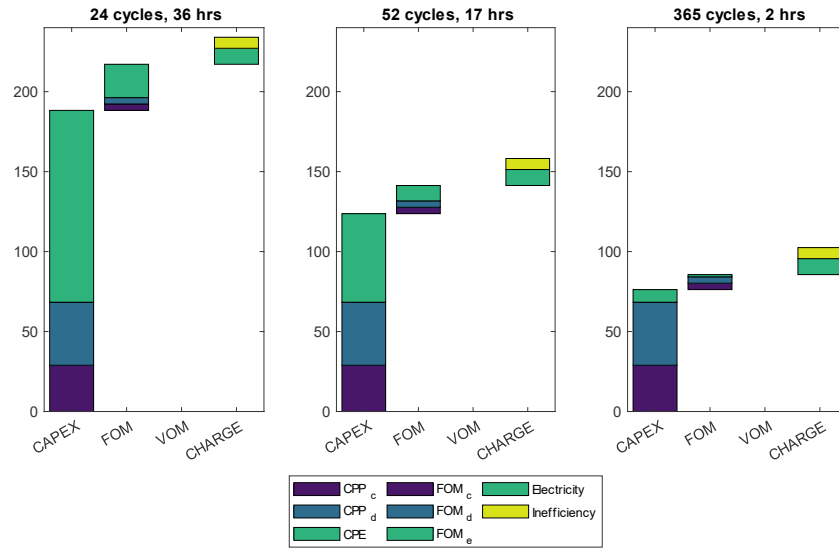


Figure 28: Contribution of cost categories to the LCOS of CAES at 10% capacity factor for varying cycling frequencies.

With CAES, the levelized costs of charge and discharge power capacity are similar, unlike TES where the charge power cost is a small percentage. The higher roundtrip efficiency of CAES reduces the cost penalty from the electricity needed to charge the system.

Like Figure 26, Figure 29 Figure 27 illustrates the range of LCOS values across the low-, mid-, and high-cost scenarios with one-at-a-time sensitivity analysis.

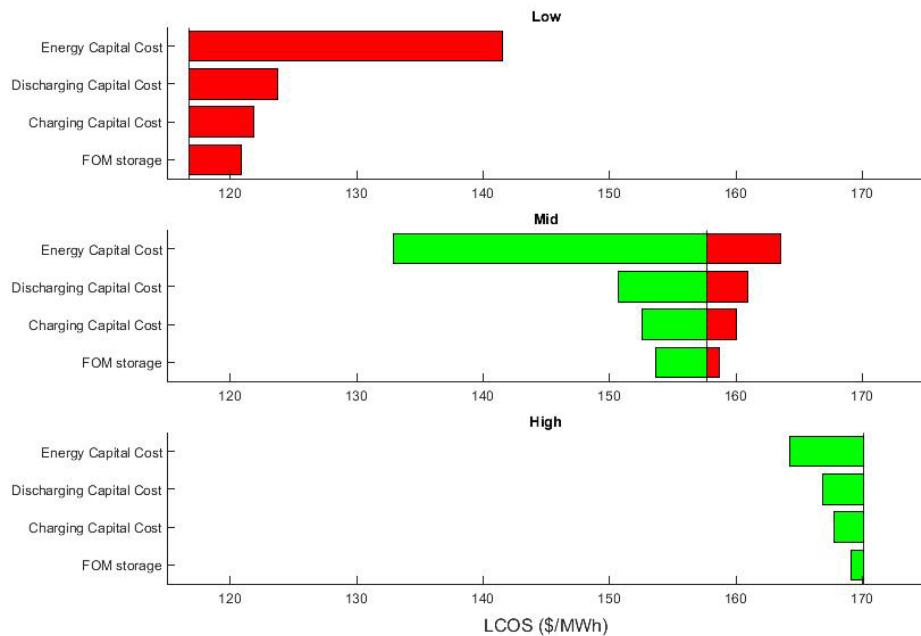


Figure 29: LCOS sensitivity analysis of CAES.

Charge and discharge efficiency were held constant across the three scenarios, so the two variables are not shown. Energy and discharge capital costs decline significantly between the low- and mid-cost scenarios which in turn causes the largest changes in LCOS.

While the LCOS values for CAES may seem promising, the underlying cost assumptions have uncertainties as described earlier. Additionally, the cost assumptions do not capture the key challenges associated with deploying CAES at grid-scale which include finding suitable underground air storage sites.

5 - Conclusions

Decarbonization of the electric power sector through high shares of renewable energy generation is critical to decarbonizing the global economy. As the share of VRE generation grows, longer duration energy storage (LDES) will be essential to minimizing the cost of this energy transition. The most important factors for LDES are reducing energy capacity cost and increasing discharge efficiency. Among a variety of technology options, thermal energy storage (TES) and compressed air energy storage (CAES) were assessed for their potential as LDES technologies.

Although CAES has a decades-long history and low technical risk with above-ground components, the identification of suitable geological sites for underground air storage is a critical challenge for grid-scale deployment. In the most favorable sites, such as salt domes and hard rock mines, CAES will be competing with chemical energy storage which has approximately ten times greater energy density. Other underground resources such as aquifers and depleted oil and gas fields may work, but site-specific data will need to be collected to determine viability. Aboveground CAES with pressurized tanks is uncompetitive for short or long duration energy storage. On the other hand, liquid air energy storage (LAES) may solve the energy density issue of aboveground CAES and the siting challenges of underground CAES. Unfortunately, representative performance data and costs for LAES are not available yet. Despite the uncertainties with CAES, this thesis provides guidance to people researching technologies for CAES and those considering CAES for commercial development.

Thermal energy storage (TES) is a worthwhile technology to consider given the multiple strategies to achieve low energy cost and increase discharge efficiency, the key variables for LDES. This thesis identified three strategies that TES technologies generally utilize. For the first strategy, TES using materials with peak temperatures around 600°C can be installed with existing steam turbines; they would be charged by low-carbon electricity to replace or supplement heat from fossil fuel combustion. This strategy uses commercially available technology, so it could be deployed within the decade. In the second strategy, systems can utilize more efficient power cycles, namely closed Brayton cycles, paired with slightly higher temperature thermal storage. Although R&D challenges remain, some closed Brayton cycle equipment is undergoing validation, pointing the way to deployment between 2030 and 2050. The third strategy is to use much higher temperature storage, 1000°C or greater, with a combined cycle or solid-state energy converters to reach even higher discharge efficiencies. Additional research is required for the third strategy, so grid-scale projects are expected to be deployed closer to 2050.

This thesis brings together context on the energy storage needs of a deeply decarbonized grid with the technical aspects of thermal as well as compressed air energy storage to find promising paths to lower cost energy storage. The hope is that with better alignment between R&D and the modeled requirements for a decarbonized grid, we can get there faster and cheaper.

Appendix

Data for Figure 5

Material	Type	T_{melt}	Density	Enthalpy	Enthalpy (volumetric)
-	-	$^{\circ}\text{C}$	kg/m^3	kJ/kg	$\text{kWh}_{\text{th}}/\text{m}^3$
Silicon	Metalloid	1414	2330	1787	1157
Iron	Metal	1668	7850	247.3	539
Nickel	Metal	1455	8902	293	725
Manganese	Metal	1246	7260	240	484
Copper	Metal	1085	8940	208.7	518
Aluminum	Metal	660	2712	396.9	299
Zinc	Metal	420	7135	112	222
KF	Salt	858	2480	468	323
NaCl	Salt	801	2160	482	289
MgCl_2	Salt	714	2320	452	291
NaNO_3	Salt	307	2260	172	108

Data for Figure 6

Material	Type	Cost_{low}	$\text{Cost}_{\text{high}}$	$T_{\text{h,low}}$	$T_{\text{h,high}}$	T_{c}	c_p	h_{sf}	
-	-	$\$/\text{kg}$	$\$/\text{kg}$	$^{\circ}\text{C}$	$^{\circ}\text{C}$	$^{\circ}\text{C}$	$\text{J}/(\text{kg}\cdot\text{K})$	kJ/kg	
Graphite	Sensible	0.70		2150	2400	1900	2000		[1]
NaNO_3 - KNO_3	Sensible	1.23		500	565	293	1386		[2]
Rock	Sensible	0.10		700	1000	100	1100		[3]
Silica	Sensible	0.35		700	1650	100	1128		[4]
Aluminum	Latent	1.40	2.50		660			396	[5]
MgCl_2	Latent	0.11	0.18		714			453	[6]
NaCl	Latent	0.06	0.12		801			482	[7]
Silicon	Latent	1.60	3.00		1414			1800	[8]

Sources for material costs:

[1] Kelsall, Buznitsky, and Henry 2021; Statista 2019

[2] Glatzmaier 2011

[3] Alibaba 2021c

[4] Ma, Davenport, and Zhang 2020

[5] Robinson 2018; Trading Economics 2021

[6] Alibaba 2021b; Dave Gibson 2011; Anita Balakrishnan 2015

[7] Dave Gibson 2011; Alibaba 2021a; U.S. Geological Survey 2021

[8] Amy et al. 2018; U.S. Geological Survey 2021

Discharge efficiency curves for Figure 7

The first equation is the formula for Carnot cycle efficiency. The Carnot cycle takes place between low- and high-temperature thermal reservoirs at T_C and T_H in units of Kelvin. The second equation is a formula for thermal efficiency of a cycle using a compressible fluid heated from T_C to T_H in units of Kelvin (Henry and Prasher 2014). The second formula is descriptive of Rankine and Brayton cycles.

$$\eta = 1 - \frac{T_C}{T_H}$$
$$\eta = 1 - \frac{T_C}{T_H - T_C} \ln\left(\frac{T_H}{T_C}\right)$$

References

- Abdul Khalid, Kamarul Aizat, Thye Jien Leong, and Khairudin Mohamed. 2016. "Review on Thermionic Energy Converters." *IEEE Transactions on Electron Devices* 63 (6): 2231–41. <https://doi.org/10.1109/TED.2016.2556751>.
- Aghahosseini, Arman, and Christian Breyer. 2018. "Assessment of Geological Resource Potential for Compressed Air Energy Storage in Global Electricity Supply." *Energy Conversion and Management* 169 (August): 161–73. <https://doi.org/10.1016/j.enconman.2018.05.058>.
- "ALACAES." n.d. Accessed June 27, 2021. <https://alacaes.com/>.
- Albertus, Paul, Joseph S. Manser, and Scott Litzelman. 2020a. "Long-Duration Electricity Storage Applications, Economics, and Technologies." *Joule* 4 (1): 21–32. <https://doi.org/10.1016/j.joule.2019.11.009>.
- . 2020b. "Long-Duration Electricity Storage Applications, Economics, and Technologies." *Joule* 4 (1): 21–32. <https://doi.org/10.1016/j.joule.2019.11.009>.
- Alibaba. 2021a. "99.5% NaCl Pool Salt Refined Industrial Salt." 2021. https://web.archive.org/web/20210827145841/https://sgdinghao.en.alibaba.com/product/1600056895051-821750555/99_5_NaCl_Pool_Salt_Refined_Industrial_Salt.html.
- . 2021b. "MgCl₂ Price per Ton." 2021. <https://web.archive.org/web/20210827144939/https://www.alibaba.com/showroom/mgcl2-price-per-ton.html>.
- . 2021c. "Natural Black Basalt Price Ton Stones For Construction - Alibaba.Com." 2021. <https://web.archive.org/web/20210827143705/https://www.alibaba.com/showroom/basalt-price-ton.html>.
- Alumina Energy. 2021. "Our Technology." Alumina Energy. 2021. <https://www.aluminaenergy.com/technology>.
- Amy, Caleb, Mehdi Pishahang, Colin C. Kelsall, Alina LaPotin, and Asegun Henry. 2021. "High-Temperature Pumping of Silicon for Thermal Energy Grid Storage." *Energy* 233 (October): 121105. <https://doi.org/10.1016/j.energy.2021.121105>.
- Amy, Caleb, Hamid Reza Seyf, Myles A. Steiner, Daniel J. Friedman, and Asegun Henry. 2018. "Thermal Energy Grid Storage Using Multi-Junction Photovoltaics." *Energy & Environmental Science* 12 (1): 334–43. <https://doi.org/10.1039/C8EE02341G>.
- Anita Balakrishnan. 2015. "Road Salt: Winter's \$2.3 Billion Game Changer." NBC News. February 18, 2015. <https://www.nbcnews.com/business/economy/road-salt-winters-2-3-billion-game-changer-n308416>.
- ARPA-e. 2018. "Duration Addition to Electricity Storage (DAYS) Overview." ARPA-e. https://arpa-e.energy.gov/sites/default/files/documents/files/DAYS_ProgramOverview_FINAL.pdf.
- . 2019. "HITEMMP Project Descriptions." ARPA-e. https://arpa-e.energy.gov/sites/default/files/documents/files/HITEMMP%20project%20descriptions_FINAL.pdf.
- AZO Materials. 2015. "What Is Induction Heating and How Do Induction Coils Work?" AZoM.Com. January 20, 2015. <https://www.azom.com/article.aspx?ArticleID=11659>.
- Barbour, Edward R., Daniel L. Pottie, and Philip Eames. 2021. "Why Is Adiabatic Compressed Air Energy Storage yet to Become a Viable Energy Storage Option?" *IScience* 24 (5): 102440. <https://doi.org/10.1016/j.isci.2021.102440>.
- Barnes, Frank S., and Jonah G. Levine, eds. 2011. *Large Energy Storage Systems Handbook*. 0 ed. CRC Press. <https://doi.org/10.1201/b10778>.
- Beér, János M. 2007. "High Efficiency Electric Power Generation: The Environmental Role." *Progress in Energy and Combustion Science* 33 (2): 107–34. <https://doi.org/10.1016/j.pecs.2006.08.002>.

- Black & Veatch. 2010. "Solar Thermocline Storage Systems: Preliminary Design Study." EPRI.
- Borri, Emiliano, Alessio Tafone, Alessandro Romagnoli, and Gabriele Comodi. 2021. "A Review on Liquid Air Energy Storage: History, State of the Art and Recent Developments." *Renewable and Sustainable Energy Reviews* 137 (March): 110572. <https://doi.org/10.1016/j.rser.2020.110572>.
- BP. 2021. "Bp's Statistical Review of World Energy 2021." 2021. <https://www.bp.com/en/global/corporate/energy-economics/statistical-review-of-world-energy.html>.
- Bradshaw, A. M., and T. Hamacher. 2013. "Nuclear Fusion and the Helium Supply Problem." *Fusion Engineering and Design*, Proceedings of the 27th Symposium On Fusion Technology (SOFT-27); Liège, Belgium, September 24-28, 2012, 88 (9): 2694–97. <https://doi.org/10.1016/j.fusengdes.2013.01.059>.
- Budt, Marcus, Daniel Wolf, Roland Span, and Jinyue Yan. 2016. "A Review on Compressed Air Energy Storage: Basic Principles, Past Milestones and Recent Developments." *Applied Energy* 170 (May): 250–68. <https://doi.org/10.1016/j.apenergy.2016.02.108>.
- California Energy Commission. 2020. "GFO-19-308 - Assessing Long-Duration Energy Storage Deployment Scenarios to Meet California's Energy Goals." California Energy Commission. California Energy Commission. January 31, 2020. <https://www.energy.ca.gov/solicitations/2020-01/gfo-19-308-assessing-long-duration-energy-storage-deployment-scenarios-meet>.
- Cárdenas, Bruno, Adam Hoskin, James Rouse, and Seamus D. Garvey. 2019. "Wire-Wound Pressure Vessels for Small Scale CAES." *Journal of Energy Storage* 26 (December): 100909. <https://doi.org/10.1016/j.est.2019.100909>.
- Carlson, Matthew D., Bobby M. Middleton, and Clifford K. Ho. 2017. "Techno-Economic Comparison of Solar-Driven SCO₂ Brayton Cycles Using Component Cost Models Baselined With Vendor Data and Estimates." In *ASME 2017 11th International Conference on Energy Sustainability*, V001T05A009. Charlotte, North Carolina, USA: American Society of Mechanical Engineers. <https://doi.org/10.1115/ES2017-3590>.
- Chad Taylor, Matthew Johnson, Nathan Levinson, and Jonathan Whalley. 2020. Energy Storage and Retrieval System. US20200018557A1, issued 2020. <https://patentimages.storage.googleapis.com/ff/25/79/4acf6215acbf2e/US20200018557A1.pdf>.
- Chao, Julie. 2016. "Scientists Look to Thermionic Energy Conversion for Clean and Efficient Power Generation." March 2016. <https://phys.org/news/2016-03-scientists-thermionic-energy-conversion-efficient.html>.
- Cole, Wesley J., Danny Greer, Paul Denholm, A. Will Frazier, Scott Machen, Trieu Mai, Nina Vincent, and Samuel F. Baldwin. 2021. "Quantifying the Challenge of Reaching a 100% Renewable Energy Power System for the United States." *Joule* 5 (7): 1732–48. <https://doi.org/10.1016/j.joule.2021.05.011>.
- Collins, Leigh. 2021. "Siemens Gamesa: Utilities Are Lining up for Our €40-50/MWh Long-Duration Thermal Energy Storage | Recharge." Recharge | Latest Renewable Energy News. February 26, 2021. <https://www.rechargenews.com/technology/siemens-gamesa-utilities-are-lining-up-for-our-40-50-mwh-long-duration-thermal-energy-storage/2-1-969626>.
- CREA. 2021. "Overseas Coal Briefing." Centre for Research on Energy and Clean Air. <https://energyandcleanair.org/wp/wp-content/uploads/2021/06/CH-Overseas-Coal-Briefing.pdf>.
- Darrell Proctor. 2019. "Volcanic Rock Offers New Take on Energy Storage." POWER Magazine. August 1, 2019. <https://www.powermag.com/volcanic-rock-offers-new-take-on-energy-storage/?printmode=1>.

- Datas, Alejandro, Alba Ramos, Antonio Martí, Carlos del Cañizo, and Antonio Luque. 2016. "Ultra High Temperature Latent Heat Energy Storage and Thermophotovoltaic Energy Conversion." *Energy* 107 (July): 542–49. <https://doi.org/10.1016/j.energy.2016.04.048>.
- Dave Gibson. 2011. "Common Road Salt Is Toxic." *The Adirondack Almanack*. January 12, 2011. <https://www.adirondackalmanack.com/2011/01/dave-gibson-common-road-salt-is-toxic-to-the-adirondacks.html>.
- DOE. 2006. *English: A GE H Series Stationary Gas Turbine Used for Electrical Power Generation*. <http://www.netl.doe.gov/scng/projects/end-use/at/images/at31176>. https://commons.wikimedia.org/wiki/File:GE_H_series_Gas_Turbine.jpg.
- . 2015. "Quadrennial Technology Review 2015. Chapter 4: Advancing Clean Electric Power Technologies. Technology Assessments: Supercritical Carbon Dioxide Brayton Cycle." *Quadrennial Technology Review 2015*. Department of Energy. <https://www.energy.gov/sites/prod/files/2016/06/f32/QTR2015-4R-Supercritical-Carbon-Dioxide-Brayton%20Cycle.pdf>.
- Donadei, Sabine, and Gregor-Sönke Schneider. 2016. "Chapter 6 - Compressed Air Energy Storage in Underground Formations." In *Storing Energy*, 113–33. Oxford: Elsevier. <https://doi.org/10.1016/B978-0-12-803440-8.00006-3>.
- Dowling, Jacqueline A., Katherine Z. Rinaldi, Tyler H. Ruggles, Steven J. Davis, Mengyao Yuan, Fan Tong, Nathan S. Lewis, and Ken Caldeira. 2020. "Role of Long-Duration Energy Storage in Variable Renewable Electricity Systems." *Joule* 4 (9): 1907–28. <https://doi.org/10.1016/j.joule.2020.07.007>.
- EIA. 2015. "State Electricity Profiles: Data for 2013." 2015. <https://www.eia.gov/electricity/state/archive/2013/>.
- Essig, Stephanie, Christophe Allebé, Timothy Remo, John F. Geisz, Myles A. Steiner, Kelsey Horowitz, Loris Barraud, et al. 2017. "Raising the One-Sun Conversion Efficiency of III–V/Si Solar Cells to 32.8% for Two Junctions and 35.9% for Three Junctions." *Nature Energy* 2 (9): 1–9. <https://doi.org/10.1038/nenergy.2017.144>.
- Fallahi, Ali, Gert Guldentops, Mingjiang Tao, Sergio Granados-Focil, and Steven Van Dessel. 2017. "Review on Solid-Solid Phase Change Materials for Thermal Energy Storage: Molecular Structure and Thermal Properties." *Applied Thermal Engineering* 127 (December): 1427–41. <https://doi.org/10.1016/j.applthermaleng.2017.08.161>.
- Fan, Dejiu, Tobias Burger, Sean McSherry, Byungjun Lee, Andrej Lenert, and Stephen R. Forrest. 2020. "Near-Perfect Photon Utilization in an Air-Bridge Thermophotovoltaic Cell." *Nature* 586 (7828): 237–41. <https://doi.org/10.1038/s41586-020-2717-7>.
- Fan, Jinyang, Wei Liu, Deyi Jiang, Junchao Chen, William Ngaha Tiedeu, Jie Chen, and Deaman Jjk. 2018. "Thermodynamic and Applicability Analysis of a Hybrid CAES System Using Abandoned Coal Mine in China." *Energy* 157 (August): 31–44. <https://doi.org/10.1016/j.energy.2018.05.107>.
- Fernández, A. Inés, Camila Barreneche, Martin Belusko, Mercè Segarra, Frank Bruno, and Luisa F. Cabeza. 2017. "Considerations for the Use of Metal Alloys as Phase Change Materials for High Temperature Applications." *Solar Energy Materials and Solar Cells* 171 (November): 275–81. <https://doi.org/10.1016/j.solmat.2017.06.054>.
- Flueckiger, Scott M., Zhen Yang, and Suresh V. Garimella. 2013. "Review of Molten-Salt Thermocline Tank Modeling for Solar Thermal Energy Storage." *Heat Transfer Engineering* 34 (10): 787–800. <https://doi.org/10.1080/01457632.2012.746152>.
- Forsberg, Charles, and Ali S Aljefri. 2020. "100-Gigawatt-Hour Crushed-Rock Heat Storage for CSP and Nuclear," 8.

- Forsberg, Charles, Stephen Brick, and Geoffrey Haratyk. 2018. "Coupling Heat Storage to Nuclear Reactors for Variable Electricity Output with Baseload Reactor Operation." *The Electricity Journal* 31 (3): 23–31. <https://doi.org/10.1016/j.tej.2018.03.008>.
- Forsberg, Charles W., Daniel C. Stack, Daniel Curtis, Geoffrey Haratyk, and Nestor Andres Sepulveda. 2017. "Converting Excess Low-Price Electricity into High-Temperature Stored Heat for Industry and High-Value Electricity Production." *The Electricity Journal* 30 (6): 42–52. <https://doi.org/10.1016/j.tej.2017.06.009>.
- Frate, Guido Francesco, Lorenzo Ferrari, and Umberto Desideri. 2020. "Multi-Criteria Economic Analysis of a Pumped Thermal Electricity Storage (PTES) With Thermal Integration." *Frontiers in Energy Research* 8 (April): 53. <https://doi.org/10.3389/fenrg.2020.00053>.
- Friedmann, S Julio, Zhiyuan Fan, and Ke Tang. 2019. "LOW-CARBON HEAT SOLUTIONS FOR HEAVY INDUSTRY: SOURCES, OPTIONS, AND COSTS TODAY."
- Gallo, A. B., J. R. Simões-Moreira, H. K. M. Costa, M. M. Santos, and E. Moutinho dos Santos. 2016. "Energy Storage in the Energy Transition Context: A Technology Review." *Renewable and Sustainable Energy Reviews* 65 (November): 800–822. <https://doi.org/10.1016/j.rser.2016.07.028>.
- Garvey, Seamus D., and Andrew Pimm. 2016. "Chapter 5 - Compressed Air Energy Storage." In *Storing Energy*, edited by Trevor M. Letcher, 87–111. Oxford: Elsevier. <https://doi.org/10.1016/B978-0-12-803440-8.00005-1>.
- Gay, Frazer W. 1948. Means for storing fluids for power generation. United States US2433896A, filed April 16, 1943, and issued January 6, 1948. <https://patents.google.com/patent/US2433896A/en>.
- Geissbühler, L., V. Becattini, G. Zanganeh, S. Zavattoni, M. Barbato, A. Haselbacher, and A. Steinfeld. 2018. "Pilot-Scale Demonstration of Advanced Adiabatic Compressed Air Energy Storage, Part 1: Plant Description and Tests with Sensible Thermal-Energy Storage." *Journal of Energy Storage* 17 (June): 129–39. <https://doi.org/10.1016/j.est.2018.02.004>.
- Gerardtv. 2010. *English: Picture of a Thermoelectric Seebeck Module (w:En:Thermoelectric Generator), Apparently Manufactured by TECTEG MFR..* Picture of our product taken 2010 Previously published: 2010-10-15 on our website. https://commons.wikimedia.org/wiki/File:Thermoelectric_Seebeck_power_module.jpg.
- Giramonti, A. J., and E. B. Smith. 1983. "Analytical Simulation of the Champagne Effect in CAES Power Plants." *Journal of Energy* 7 (6): 570–74. <https://doi.org/10.2514/3.62700>.
- GIZ. 2020. "Repurposing of Existing Coal-Fired Power Plants into Thermal Storage Plants for Renewable Power in Chile." Deutsche Gesellschaft für Internationale Zusammenarbeit. <https://4echile-datastore.s3.eu-central-1.amazonaws.com/wp-content/uploads/2020/09/01031505/200928-GIZ-Chile-ExecSummary-v6-English-corrected.pdf>.
- Glatzmaier, G. 2011. "Developing a Cost Model and Methodology to Estimate Capital Costs for Thermal Energy Storage." NREL/TP-5500-53066, 1031953. <https://doi.org/10.2172/1031953>.
- Glowacki, Bartek A., William J. Nuttall, and Richard H. Clarke. 2013. "Beyond the Helium Conundrum." *IEEE Transactions on Applied Superconductivity* 23 (3): 0500113–0500113. <https://doi.org/10.1109/TASC.2013.2244633>.
- Go, David B., John R. Haase, Jeffrey George, Jochen Mannhart, Robin Wanke, Alireza Nojeh, and Robert Nemanich. 2017. "Thermionic Energy Conversion in the Twenty-First Century: Advances and Opportunities for Space and Terrestrial Applications." *Frontiers in Mechanical Engineering* 3 (November): 13. <https://doi.org/10.3389/fmech.2017.00013>.
- González-Roubaud, Edouard, David Pérez-Osorio, and Cristina Prieto. 2017. "Review of Commercial Thermal Energy Storage in Concentrated Solar Power Plants: Steam vs. Molten Salts." *Renewable and Sustainable Energy Reviews* 80 (December): 133–48. <https://doi.org/10.1016/j.rser.2017.05.084>.

- Google. 2021. "Changhua County, Taiwan – Data Centers – Google." Google Data Centers. 2021. <https://www.google.com/about/datacenters/locations/changhua-county/>.
- Greentech Media. 2020. "Storing Energy in the Freezer: Long-Duration Thermal Storage Comes of Age." July 2020. <https://www.greentechmedia.com/articles/read/storing-energy-in-the-freezer-long-duration-thermal-storage-comes-of-age>.
- Gross, Robert, Richard Hanna, Ajay Gambhir, Philip Heptonstall, and Jamie Speirs. 2018. "How Long Does Innovation and Commercialisation in the Energy Sectors Take? Historical Case Studies of the Timescale from Invention to Widespread Commercialisation in Energy Supply and End Use Technology." *Energy Policy* 123 (December): 682–99. <https://doi.org/10.1016/j.enpol.2018.08.061>.
- Grubert, Emily. 2020. "Fossil Electricity Retirement Deadlines for a Just Transition," 4. <https://doi.org/10.1126/science.abe0375>.
- Guerra, Omar J., Jiazi Zhang, Joshua Eichman, Paul Denholm, Jennifer Kurtz, and Bri-Mathias Hodge. 2020. "The Value of Seasonal Energy Storage Technologies for the Integration of Wind and Solar Power." *Energy & Environmental Science*, 10.1039.D0EE00771D. <https://doi.org/10.1039/D0EE00771D>.
- Guizzi, Giuseppe Leo, Michele Manno, Ludovica Maria Tolomei, and Ruggero Maria Vitali. 2015. "Thermodynamic Analysis of a Liquid Air Energy Storage System." *Energy* 93 (December): 1639–47. <https://doi.org/10.1016/j.energy.2015.10.030>.
- Guo, Chaobin, Cai Li, Keni Zhang, Zuansi Cai, Tianran Ma, Federico Maggi, Yixiang Gan, Abbas El-Zein, Zhejun Pan, and Luming Shen. 2021. "The Promise and Challenges of Utility-Scale Compressed Air Energy Storage in Aquifers." *Applied Energy* 286 (March): 116513. <https://doi.org/10.1016/j.apenergy.2021.116513>.
- Haley Gilbert. 2021. "Antora Energy | Afwerx Energy Challenge Virtual Showcase." 2021. <https://reimagining.afwerx.com/exhibitor/antora-energy-11675>.
- Hart, Melanie, Luke Bassett, and Blaine Johnson. 2017. "Everything You Think You Know About Coal in China Is Wrong." Center for American Progress. May 2017. <https://www.americanprogress.org/issues/green/reports/2017/05/15/432141/everything-think-know-coal-china-wrong/>.
- Hartmann, Niklas, O. Vöhringer, C. Kruck, and L. Eltrop. 2012. "Simulation and Analysis of Different Adiabatic Compressed Air Energy Storage Plant Configurations." *Applied Energy* 93 (May): 541–48. <https://doi.org/10.1016/j.apenergy.2011.12.007>.
- He, Wei, Mark Dooner, Marcus King, Dacheng Li, Songshan Guo, and Jihong Wang. 2021. "Techno-Economic Analysis of Bulk-Scale Compressed Air Energy Storage in Power System Decarbonisation." *Applied Energy* 282 (January): 116097. <https://doi.org/10.1016/j.apenergy.2020.116097>.
- He, Wei, Xing Luo, David Evans, Jonathan Busby, Seamus Garvey, Daniel Parkes, and Jihong Wang. 2017. "Exergy Storage of Compressed Air in Cavern and Cavern Volume Estimation of the Large-Scale Compressed Air Energy Storage System." *Applied Energy* 208 (December): 745–57. <https://doi.org/10.1016/j.apenergy.2017.09.074>.
- Held, Timothy J. 2014. "Initial Test Results of a Megawatt-Class Supercritical CO₂ Heat Engine." In , 12. Pittsburgh, Pennsylvania. https://www.echogen.com/_CE/pagecontent/Documents/Papers/initial-test-results-of-a-megawatt-class-supercritical-co2-heat-engine-held.pdf.
- Henry, Asegun. 2018. "A New Take on Electrochemical Heat Engines." *Joule* 2 (9): 1660–61. <https://doi.org/10.1016/j.joule.2018.08.007>.

- Henry, Asegun, and Ravi Prasher. 2014. "The Prospect of High Temperature Solid State Energy Conversion to Reduce the Cost of Concentrated Solar Power." *Energy & Environmental Science* 7 (6): 1819–28. <https://doi.org/10.1039/C4EE00288A>.
- Holst, Kent, Georgianne Huff, Robert H. Schulte, and Nicholas Critelli. 2012. "Lessons from Iowa : Development of a 270 Megawatt Compressed Air Energy Storage Project in Midwest Independent System Operator : A Study for the DOE Energy Storage Systems Program." SAND2012-0388, 1035330. <https://doi.org/10.2172/1035330>.
- Hoseinpur, Arman, and Jafar Safarian. 2020. "Mechanisms of Graphite Crucible Degradation in Contact with Si–Al Melts at High Temperatures and Vacuum Conditions." *Vacuum* 171 (January): 108993. <https://doi.org/10.1016/j.vacuum.2019.108993>.
- Houssainy, Sammy, Mohammad Janbozorgi, and Pirouz Kavehpour. 2018. "Thermodynamic Performance and Cost Optimization of a Novel Hybrid Thermal-Compressed Air Energy Storage System Design." *Journal of Energy Storage* 18 (August): 206–17. <https://doi.org/10.1016/j.est.2018.05.004>.
- "How Much Does Rock Excavation Cost?" 2018. *Howmuchisit* (blog). 2018. <https://www.howmuchisit.org/rock-excavation-cost/>.
- Huang, Y., H.S. Chen, X.J. Zhang, P. Keatley, M.J. Huang, I. Vorushylo, Y.D. Wang, and N.J. Hewitt. 2017. "Techno-Economic Modelling of Large Scale Compressed Air Energy Storage Systems." *Energy Procedia* 105 (May): 4034–39. <https://doi.org/10.1016/j.egypro.2017.03.851>.
- "Hydrostor." 2021. 2021. <https://www.hydrostor.ca/>.
- IEA. 2015. "Technology Roadmap Hydrogen and Fuel Cells." International Energy Agency.
- . 2019. "Electricity Information 2019." International Energy Agency.
- Inductotherm Corp. 2020. "FAQs: General." *Inductotherm Corp.* (blog). 2020. <https://inductotherm.com/resources/faqs/general/>.
- IRENA. 2019. "Innovation Landscape Brief: Flexibility in Conventional Power Plants." IRENA.
- James Temple. 2020. "Tony Pan." MIT Technology Review. June 2020. <https://www.technologyreview.com/innovator/tony-pan/>.
- Jason Deign. 2019. "Germany Looks to Put Thermal Storage Into Coal Plants." Greentech Media. March 18, 2019. <https://www.greentechmedia.com/articles/read/germany-thermal-storage-into-coal-plants>.
- Jeff St. John. 2015. "SustainX to Merge With General Compression, Abandon Above-Ground CAES Ambitions." Greentech Media. March 31, 2015. <https://www.greentechmedia.com/articles/read/sustainx-to-merge-with-general-compression-abandon-above-ground-caes-ambiti>.
- Jiao, Jianmeng, Bettina Grorud, Caroline Sindland, Jafar Safarian, Kai Tang, Kathrine Sellevoll, and Merete Tangstad. 2019. "The Use of Eutectic Fe-Si-B Alloy as a Phase Change Material in Thermal Energy Storage Systems." *Materials* 12 (14). <https://doi.org/10.3390/ma12142312>.
- John, Jeff St. 2017. "Inside GE and SoCal Edison's First-of-a-Kind Hybrid Peaker Plant With Batteries and Gas Turbines." Greentech Media. April 18, 2017. <https://www.greentechmedia.com/articles/read/inside-ge-and-socal-edisons-battery-integrated-gas-fired-peaker-plants>.
- John Parnell. 2020. "How Siemens Gamesa Could Give Coal Plants a Second Life." February 20, 2020. <https://www.greentechmedia.com/articles/read/how-siemens-gamesa-could-give-coal-plants-a-second-life>.
- Kanthal. 2018. "Resistance Heating Alloys and Systems for Industrial Furnaces."
- Kasseris, Emmanuel, Naga Srujana Goteti, Sapna Kumari, Bentley Clinton, Seiji Engelkemier, Sarah Torkamani, Tevita Akau, and Emre Gençer. 2020. "Highlighting and Overcoming Data Barriers: Creating Open Data for Retrospective Analysis of US Electric Power Systems by Consolidating

- Publicly Available Sources." *Environmental Research Communications* 2 (11): 115001. <https://doi.org/10.1088/2515-7620/abc86d>.
- Kavlak, Goksin, James McNerney, and Jessika E. Trancik. 2018. "Evaluating the Causes of Cost Reduction in Photovoltaic Modules." *Energy Policy* 123 (December): 700–710. <https://doi.org/10.1016/j.enpol.2018.08.015>.
- Kelsall, Colin C., Kyle Buznitsky, and Asegun Henry. 2021. "Technoeconomic Analysis of Thermal Energy Grid Storage Using Graphite and Tin." *ArXiv:2106.07624 [Physics]*, June. <http://arxiv.org/abs/2106.07624>.
- Kevin Moriarty. 2019. "Technology & Commercial Review Update." 1414 Degrees. <https://1414degrees.com.au/wp-content/uploads/2020/06/Technology-Commercial-Review-Update-1.pdf>.
- King, Marcus, Anjali Jain, Rohit Bhakar, Jyotirmay Mathur, and Jihong Wang. 2021. "Overview of Current Compressed Air Energy Storage Projects and Analysis of the Potential Underground Storage Capacity in India and the UK." *Renewable and Sustainable Energy Reviews* 139 (April): 110705. <https://doi.org/10.1016/j.rser.2021.110705>.
- LaPotin, Alina, Kevin L. Schulte, Myles A. Steiner, Kyle Buznitsky, Colin C. Kelsall, Daniel J. Friedman, Eric J. Tervo, et al. 2021. "Thermophotovoltaic Efficiency of 40%." *ArXiv:2108.09613 [Physics]*, August. <http://arxiv.org/abs/2108.09613>.
- Laughlin, Robert B. 2017. "Pumped Thermal Grid Storage with Heat Exchange." *Journal of Renewable and Sustainable Energy* 9 (4): 044103. <https://doi.org/10.1063/1.4994054>.
- Lee, Seok Woo, Yuan Yang, Hyun-Wook Lee, Hadi Ghasemi, Daniel Kraemer, Gang Chen, and Yi Cui. 2014. "An Electrochemical System for Efficiently Harvesting Low-Grade Heat Energy." *Nature Communications* 5 (1): 1–6. <https://doi.org/10.1038/ncomms4942>.
- Limia, Alexander, Jong Min Ha, Peter Kottke, Andrey Gunawan, Andrei G. Fedorov, Seung Woo Lee, and Shannon K. Yee. 2017. "A Dual-Stage Sodium Thermal Electrochemical Converter (Na-TEC)." *Journal of Power Sources* 371 (December): 217–24. <https://doi.org/10.1016/j.jpowsour.2017.10.022>.
- Lin, Yaxue, Yuting Jia, Guruprasad Alva, and Guiyin Fang. 2018. "Review on Thermal Conductivity Enhancement, Thermal Properties and Applications of Phase Change Materials in Thermal Energy Storage." *Renewable and Sustainable Energy Reviews* 82 (February): 2730–42. <https://doi.org/10.1016/j.rser.2017.10.002>.
- Linford, Patrick A., Lin Xu, Botao Huang, Yang Shao-Horn, and Carl V. Thompson. 2018. "Multi-Cell Thermogalvanic Systems for Harvesting Energy from Cyclic Temperature Changes." *Journal of Power Sources* 399 (September): 429–35. <https://doi.org/10.1016/j.jpowsour.2018.07.080>.
- Liu, Ming, N.H. Steven Tay, Stuart Bell, Martin Belusko, Rhys Jacob, Geoffrey Will, Wasim Saman, and Frank Bruno. 2016. "Review on Concentrating Solar Power Plants and New Developments in High Temperature Thermal Energy Storage Technologies." *Renewable and Sustainable Energy Reviews* 53 (January): 1411–32. <https://doi.org/10.1016/j.rser.2015.09.026>.
- Ma, Zhiwen, Patrick Davenport, and Ruichong Zhang. 2020. "Design Analysis of a Particle-Based Thermal Energy Storage System for Concentrating Solar Power or Grid Energy Storage." *Journal of Energy Storage* 29 (June): 101382. <https://doi.org/10.1016/j.est.2020.101382>.
- Ma, Zhiwen, Ruichong Zhang, and Fadi Sawaged. 2017. "Design of Particle-Based Thermal Energy Storage for a Concentrating Solar Power System." In *ASME 2017 11th International Conference on Energy Sustainability*, V001T05A003. Charlotte, North Carolina, USA: American Society of Mechanical Engineers. <https://doi.org/10.1115/ES2017-3099>.
- McDonald, Colin F. 2012. "Helium Turbomachinery Operating Experience from Gas Turbine Power Plants and Test Facilities." *Applied Thermal Engineering* 44 (November): 108–42. <https://doi.org/10.1016/j.applthermaleng.2012.02.041>.

- McTigue, Joshua, Pau Farres-Antunez, Kevin Ellingwood, Ty Neises, and Alexander White. 2019. "Pumped Thermal Electricity Storage with Supercritical CO₂ Cycles and Solar Heat Input: Preprint." *Renewable Energy*, 14.
- Medeiros, Michael, Robert Booth, James Fairchild, Doug Imperato, Charles Stinson, Mark Ausburn, Mike Tietze, et al. 2018. "Technical Feasibility of Compressed Air Energy Storage (CAES) Utilizing a Porous Rock Reservoir." DOE-PGE--00198-1, 1434251. <https://doi.org/10.2172/1434251>.
- Mehos, Mark, Craig Turchi, Jennie Jorgensen, and Paul Denholm. 2016. "On the Path to SunShot: Advancing Concentrating Solar Power Technology, Performance, and Dispatchability." U.S. Department of Energy.
- Meroueh, Laureen, and Gang Chen. 2019. "Thermal Energy Storage Radiatively Coupled to a Supercritical Rankine Cycle for Electric Grid Support." *Renewable Energy* 145 (June): 604–21. <https://doi.org/10.1016/j.renene.2019.06.036>.
- Mesquita, Lucio, Doug McClenahan, Jeff Thornton, Jarrett Carriere, and Bill Wong. 2017. "Drake Landing Solar Community: 10 Years of Operation." In *Proceedings of SWC2017/SHC2017*, 1–12. Abu Dhabi: International Solar Energy Society. <https://doi.org/10.18086/swc.2017.06.09>.
- MIT Energy Initiative. 2022. "The Future of Energy Storage." MITei. <https://energy.mit.edu/wp-content/uploads/2022/05/The-Future-of-Energy-Storage.pdf>.
- Mohan, Gowtham, Mahesh B. Venkataraman, and Joe Coventry. 2019. "Sensible Energy Storage Options for Concentrating Solar Power Plants Operating above 600 °C." *Renewable and Sustainable Energy Reviews* 107 (June): 319–37. <https://doi.org/10.1016/j.rser.2019.01.062>.
- Myers, Philip D., and D. Yogi Goswami. 2016. "Thermal Energy Storage Using Chloride Salts and Their Eutectics." *Applied Thermal Engineering*, Special Issue: Solar Energy Research Institute for India and the United States (SERIUS) – Concentrated Solar Power, 109 (October): 889–900. <https://doi.org/10.1016/j.applthermaleng.2016.07.046>.
- Nakhmkin, Michael. 2010. Retrofit Of Simple Cycle Gas Turbine For Compressed Air Energy Storage Application Having Expander For Additional Power Generation. United States US20100083660A1, filed December 8, 2009, and issued April 8, 2010. <https://patents.google.com/patent/US20100083660A1/en?q=US20100083660>.
- Nishioka, Koki, Naoyuki Suura, Ko-ichiro Ohno, Takayuki Maeda, and Masakata Shimizu. 2010. "Development of Fe Base Phase Change Materials for High Temperature Using Solid–Solid Transformation." *ISIJ International* 50 (9): 5.
- NREL. 2018. "News Release: NREL Awarded \$2.8M from ARPA-E to Develop Low-Cost Thermal Energy Storage | News | NREL." NREL. November 2018. <https://www.nrel.gov/news/press/2018/nrel-awarded-28m-from-arpa-e-to-develop-low-cost-thermal-energy-storage.html>.
- NYSERDA. 2009. "Compressed Air Energy Storage Engineering and Economic Study." 10–09. NYSERDA.
- Office of Fossil Energy. 2020. "Areas of Interest: DOE Invests Nearly \$7.6M to Develop Energy Storage Projects." Energy.Gov. December 2020. <https://www.energy.gov/fe/articles/areas-interest-doe-invests-nearly-76m-develop-energy-storage-projects>.
- Olympios, Andreas V., Joshua D. McTigue, Paul Sapin, and Christos N. Markides. 2021. "Pumped-Thermal Electricity Storage Based on Brayton Cycles." In *Reference Module in Earth Systems and Environmental Sciences*, B978012819723300086X. Elsevier. <https://doi.org/10.1016/B978-0-12-819723-3.00086-X>.
- Omair, Zunaid, Gregg Scranton, Luis M. Pazos-Outón, T. Patrick Xiao, Myles A. Steiner, Vidya Ganapati, Per F. Peterson, John Holzrichter, Harry Atwater, and Eli Yablonovitch. 2019. "Ultraefficient Thermophotovoltaic Power Conversion by Band-Edge Spectral Filtering." *Proceedings of the National Academy of Sciences* 116 (31): 15356–61. <https://doi.org/10.1073/pnas.1903001116>.
- Ozarslan, Ahmet. 2012. "Large-Scale Hydrogen Energy Storage in Salt Caverns." *International Journal of Hydrogen Energy*, HYFUSEN, 37 (19): 14265–77. <https://doi.org/10.1016/j.ijhydene.2012.07.111>.

- Palfinger, G nther, Bernd Bitnar, Wilhelm Durisch, Jean-Claude Mayor, Detlev Gr tzmacher, and Jens Gobrecht. 2003. "Cost Estimate of Electricity Produced by TPV." *Semiconductor Science and Technology* 18 (5): S254–61. <https://doi.org/10.1088/0268-1242/18/5/317>.
- Pandya, Shishir, Gabriel Velarde, Lei Zhang, Joshua D. Wilbur, Andrew Smith, Brendan Hanrahan, Chris Dames, and Lane W. Martin. 2019. "New Approach to Waste-Heat Energy Harvesting: Pyroelectric Energy Conversion." *NPG Asia Materials* 11 (1): 1–5. <https://doi.org/10.1038/s41427-019-0125-y>.
- Patel, Sonal. 2021. "Breakthrough: NET Power's Allam Cycle Test Facility Delivers First Power to ERCOT Grid." *POWER Magazine* (blog). November 18, 2021. <https://www.powermag.com/breakthrough-net-powers-allam-cycle-test-facility-delivers-first-power-to-ercot-grid/>.
- Poletayev, Andrey D., Ian S. McKay, William C. Chueh, and Arun Majumdar. 2018. "Continuous Electrochemical Heat Engines." *Energy & Environmental Science* 11 (10): 2964–71. <https://doi.org/10.1039/C8EE01137K>.
- Power Engineering. 2018. "GE-Powered Plant Awarded World Record Efficiency by Guinness." Power Engineering. March 27, 2018. <https://www.power-eng.com/2018/03/27/ge-powered-plant-awarded-world-record-efficiency-by-guinness/>.
- Power Technology. 2019. "1414 Degrees Begins Operations of Biogas Energy Storage System." Power Technology. May 2, 2019. <https://www.power-technology.com/news/1414-degrees-energy-storage/>.
- Quoilin, Sylvain, Martijn Van Den Broek, Sébastien Declaye, Pierre Dewallef, and Vincent Lemort. 2013. "Techno-Economic Survey of Organic Rankine Cycle (ORC) Systems." *Renewable and Sustainable Energy Reviews* 22 (June): 168–86. <https://doi.org/10.1016/j.rser.2013.01.028>.
- Reed, Samuel, Heber Sugo, Erich Kisi, and Peter Richardson. 2019. "Extended Thermal Cycling of Miscibility Gap Alloy High Temperature Thermal Storage Materials." *Solar Energy* 185 (June): 333–40. <https://doi.org/10.1016/j.solener.2019.04.075>.
- Robinson, Adam. 2018. "Ultra-High Temperature Thermal Energy Storage. Part 2: Engineering and Operation." *Journal of Energy Storage* 18 (August): 333–39. <https://doi.org/10.1016/j.est.2018.03.013>.
- Samir Succar and Robert H. Williams. 2008. "Compressed Air Energy Storage: Theory, Resources, And Applications For Wind Power." https://acee.princeton.edu/wp-content/uploads/2016/10/SuccarWilliams_PEI_CAES_2008April8.pdf.
- Sargent & Lundy. 2020. "Capital Costs and Performance Characteristics for Utility Scale Power Generating Technologies." EIA.
- Schmalensee, Richard, Cristian Junge, and Dharik Mallapragada. 2020. "Energy Storage Investment and Operation in Efficient Electric Power Systems." *SSRN Electronic Journal*. <https://doi.org/10.2139/ssrn.3752324>.
- Schmidt, O., A. Hawkes, A. Gambhir, and I. Staffell. 2017. "The Future Cost of Electrical Energy Storage Based on Experience Rates." *Nature Energy* 2 (8): 1–8. <https://doi.org/10.1038/nenergy.2017.110>.
- Schmidt, Oliver, Sylvain Melchior, Adam Hawkes, and Iain Staffell. 2019. "Projecting the Future Levelized Cost of Electricity Storage Technologies." *Joule* 3 (1): 81–100. <https://doi.org/10.1016/j.joule.2018.12.008>.
- Seetenky, Alexander. 2007. *English: Maintenance of a Low Pressure Section of a Steam Turbine at the Balakovo Nuclear Power Plant*. CPI BalNpp(The Centre of the Public Information Balakovo NPP). https://commons.wikimedia.org/wiki/File:BalNPP_m_st2.jpg.

- Sepulveda, Nestor A., Jesse D. Jenkins, Aurora Edington, Dharik S. Mallapragada, and Richard K. Lester. 2021. "The Design Space for Long-Duration Energy Storage in Decarbonized Power Systems." *Nature Energy*, March. <https://doi.org/10.1038/s41560-021-00796-8>.
- Seyf, Hamid Reza, and Asegun Henry. 2016. "Thermophotovoltaics: A Potential Pathway to High Efficiency Concentrated Solar Power." *Energy & Environmental Science* 9 (8): 2654–65. <https://doi.org/10.1039/C6EE01372D>.
- Shawn Flake. 2016. "Using Steam Turbine Warming Blankets to Reduce Startup Time and Rotor Stress." *POWER Magazine* (blog). March 1, 2016. <https://www.powermag.com/using-steam-turbine-warming-blankets-reduce-startup-time-rotor-stress/>.
- Siemens Energy. 2021. "Siemens Energy Signs Agreement to Build First-of-Its-Kind Waste He ..." February 12, 2021. <https://press.siemens-energy.com/global/en/pressrelease/siemens-energy-signs-agreement-build-first-its-kind-waste-heat-power-facility-canada>.
- Sioshansi, Ramteen, Paul Denholm, Thomas Jenkin, and Jurgen Weiss. 2009. "Estimating the Value of Electricity Storage in PJM: Arbitrage and Some Welfare Effects." *Energy Economics* 31 (2): 269–77. <https://doi.org/10.1016/j.eneco.2008.10.005>.
- Soprani, Stefano, Fabrizio Marongiu, Ludvig Christensen, Ole Alm, Kenni Dinesen Petersen, Thomas Ulrich, and Kurt Engelbrecht. 2019. "Design and Testing of a Horizontal Rock Bed for High Temperature Thermal Energy Storage." *Applied Energy* 251 (October): 113345. <https://doi.org/10.1016/j.apenergy.2019.113345>.
- Specialty Grading. 2020. "Rock Excavation Cost In Prescott, AZ (2020 Prices)." *Specialty Grading* (blog). July 16, 2020. <https://www.specialtygrading.com/rock-excavation-cost/>.
- Statista. 2017. "Market Distribution of Photovoltaic Module Manufacturers 2017." 2017. <https://www.statista.com/statistics/269812/global-market-share-of-solar-pv-module-manufacturers/>.
- . 2019. "Global Graphite Price 2018-2019." Statista. June 2019. <https://www.statista.com/statistics/1075217/graphite-price-worldwide/>.
- Strefler, Jessica, Thorben Amann, Nico Bauer, Elmar Kriegler, and Jens Hartmann. 2018. "Potential and Costs of Carbon Dioxide Removal by Enhanced Weathering of Rocks." *Environmental Research Letters* 13 (3): 034010. <https://doi.org/10.1088/1748-9326/aaa9c4>.
- Sugo, Heber, Erich Kisi, and Dylan Cuskelly. 2013. "Miscibility Gap Alloys with Inverse Microstructures and High Thermal Conductivity for High Energy Density Thermal Storage Applications." *Applied Thermal Engineering* 51 (1–2): 1345–50. <https://doi.org/10.1016/j.applthermaleng.2012.11.029>.
- Thiel, Gregory P., and Addison K. Stark. 2021. "To Decarbonize Industry, We Must Decarbonize Heat." *Joule* 5 (3): 531–50. <https://doi.org/10.1016/j.joule.2020.12.007>.
- Thomas McCafferty. 1980. "Compressed Air Energy Storage: Preliminary Design and Site Development Program in an Aquifer. Final Draft, Task 1." EPRI. <https://doi.org/10.2172/6743232>.
- Thompson, Amy. 2016. "DOE/EPRI Electricity Storage Handbook in Collaboration with NRECA," 450.
- Timmer, Michael A. G., Kees de Blok, and Theo H. van der Meer. 2018. "Review on the Conversion of Thermoacoustic Power into Electricity." *The Journal of the Acoustical Society of America* 143 (2): 841–57. <https://doi.org/10.1121/1.5023395>.
- Tong, Zheming, Zhewu Cheng, and Shuiguang Tong. 2021. "A Review on the Development of Compressed Air Energy Storage in China: Technical and Economic Challenges to Commercialization." *Renewable and Sustainable Energy Reviews* 135 (January): 110178. <https://doi.org/10.1016/j.rser.2020.110178>.
- Trading Economics. 2021. "Aluminum | 1989-2021 Data | 2022-2023 Forecast | Price | Quote | Chart | Historical." 2021. <https://tradingeconomics.com/commodity/aluminum>.
- Turchi, Craig S., Zhiwen Ma, and John Dyreby. 2012. "Supercritical Carbon Dioxide Power Cycle Configurations for Use in Concentrating Solar Power Systems." In *Volume 5: Manufacturing*

- Materials and Metallurgy; Marine; Microturbines and Small Turbomachinery; Supercritical CO₂ Power Cycles*, 967–73. Copenhagen, Denmark: American Society of Mechanical Engineers. <https://doi.org/10.1115/GT2012-68932>.
- US EPA, OAR. 2016. “Global Greenhouse Gas Emissions Data.” Overviews and Factsheets. January 12, 2016. <https://www.epa.gov/ghgemissions/global-greenhouse-gas-emissions-data>.
- . 2017. “Inventory of U.S. Greenhouse Gas Emissions and Sinks.” Reports and Assessments. February 8, 2017. <https://www.epa.gov/ghgemissions/inventory-us-greenhouse-gas-emissions-and-sinks>.
- U.S. Geological Survey. 2021. “Mineral Commodity Summaries 2021.” <https://doi.org/10.3133/mcs2021>.
- Wickramaratne, Chatura, Jaspreet S. Dhau, Rajeev Kamal, Philip Myers, D. Y. Goswami, and E. Stefanakos. 2018. “Macro-Encapsulation and Characterization of Chloride Based Inorganic Phase Change Materials for High Temperature Thermal Energy Storage Systems.” *Applied Energy* 221 (July): 587–96. <https://doi.org/10.1016/j.apenergy.2018.03.146>.
- Yu, Haoshui, Seiji Engelkemier, and Emre Gençer. 2022. “Process Improvements and Multi-Objective Optimization of Compressed Air Energy Storage (CAES) System.” *Journal of Cleaner Production* 335 (February): 130081. <https://doi.org/10.1016/j.jclepro.2021.130081>.
- Zeynalian, Mirhadi, Amir Hossein Hajjalirezaei, Amir Reza Razmi, and M. Torabi. 2020. “Carbon Dioxide Capture from Compressed Air Energy Storage System.” *Applied Thermal Engineering* 178 (September): 115593. <https://doi.org/10.1016/j.applthermaleng.2020.115593>.
- Zhang, Qihao, Jincheng Liao, Yunshan Tang, Ming Gu, Chen Ming, Pengfei Qiu, Shengqiang Bai, Xun Shi, Ctirad Uher, and Lidong Chen. 2017. “Realizing a Thermoelectric Conversion Efficiency of 12% in Bismuth Telluride/Skutterudite Segmented Modules through Full-Parameter Optimization and Energy-Loss Minimized Integration.” *Energy & Environmental Science* 10 (4): 956–63. <https://doi.org/10.1039/C7EE00447H>.
- Zhang, Xiang, Hadi Keramati, Martinus Arie, Farah Singer, Ratnesh Tiwari, Amir Shoostari, and Michael Ohadi. 2018. “Recent Developments In High Temperature Heat Exchangers: A Review.” *Frontiers in Heat and Mass Transfer* 11 (July). <https://doi.org/10.5098/hmt.11.18>.
- Ziegler, Micah S., Joshua M. Mueller, Gonçalo D. Pereira, Juhyun Song, Marco Ferrara, Yet-Ming Chiang, and Jessika E. Trancik. 2019a. “Storage Requirements and Costs of Shaping Renewable Energy Toward Grid Decarbonization.” *Joule*, August. <https://doi.org/10.1016/j.joule.2019.06.012>.
- . 2019b. “Storage Requirements and Costs of Shaping Renewable Energy Toward Grid Decarbonization.” *Joule*, August. <https://doi.org/10.1016/j.joule.2019.06.012>.
- Zivar, Davood, Sunil Kumar, and Jalal Foroozesh. 2020. “Underground Hydrogen Storage: A Comprehensive Review.” *International Journal of Hydrogen Energy*, September, S0360319920331426. <https://doi.org/10.1016/j.ijhydene.2020.08.138>.